NEGATIVE IMPEDANCE CONVERTER AND ITS APPLICATION IN ELECTRICALLY SMALL ANTENNAS

THESIS SUBMITTED IN PARTIAL FULFILLMENT OF THE REQUIREMENT FOR THE DEGREE OF

MASTER OF
ELECTRONICS AND TELE-COMMUNICATION ENGINEERING

THESIS SUBMITTED BY

ABHISHEK CHATTERJEE

University Registration No: 137387 of 2016-2017

Exam Roll No: M4ETC19022

Class Roll No: 001710702020

UNDER THE SUPERVISION OF

DR. SAYAN CHATTERJEE

DEPARTMENT OF ELECTRONICS AND TELE-COMMUNICATION ENGINEERING

JADAVPUR UNIVERSITY

KOLKATA – 700032

INDIA

MAY 2019

FACULTY OF ENGINEERING AND TECHNOLOGY
ELECTRONICS AND TELECOMMUNICATION ENGINEERING
JADAVPUR UNIVERSITY

CERTIFICATE OF RECOMMENDATION

This is to certify that the thesis entitled "NEGATIVE IMPEDANCE CONVERTER AND ITS APPLICATION IN ELECTRICALLY SMALL ANTENNAS" has been carried out by **ABHISHEK CHATTERJEE** (***University Registration No: 137387 of 2016-2017***) under my guidance and supervision and be accepted in partial fulfillment of the requirement for awarding the degree of "**MASTER OF ELECTRONICS and TELE COMMUNICATION ENGINEERING**". The research results presented in this thesis have not been included in any other paper submitted for the award of any degree to any other Institute or University.

DR. SAYAN CHATTERJEE

THESIS SUPERVISOR

DEPT. OF ELECTRONICS AND TELECOMMUNICATION ENGINEERING
JADAVPUR UNIVERSITY
KOLKATA 700032

PROF. SHELI SINHA CHAUDHURI

HEAD OF THE DEPARTMENT

DEPT. OF ELECTRONICS AND TELECOMMUNICATION ENGINEERING

JADAVPUR UNIVERSITY
KOLKATA 700032

PROF. CHIRANJIB BHATTACHARJEE

DEAN

FACULTY OF ENGINEERING AND TECHNOLOGY

JADAVPUR UNIVERSITY
KOLKATA 700032

FACULTY OF ENGINEERING AND TECHNOLOGY
ELECTRONICS AND TELECOMMUNICATION ENGINEERING
JADAVPUR UNIVERSITY

CERTIFICATE OF APPROVAL#

The foregoing THESIS is hereby approved as a creditable study of an Engineering Subject carried out and presented in a manner of satisfactory to warrant its acceptance as a pre-requisite to the DEGREE for which it has been submitted. It is to be understood that by this approval, the undersigned do not necessarily endorse or approve any statement made, opinion expressed or conclusion drawn therein but approve the THESIS only for the purpose for which it has been submitted.

Committee on final examination for the evaluation of the Thesis

_____
(Signature of the Supervisor)

_____
(Signature of the Examiner1)

_____
(Signature of the Examiner2)

only in case the thesis is approved.

FACULTY OF ENGINEERING AND TECHNOLOGY
ELECTRONICS AND TELECOMMUNICATION ENGINEERING
JADAVPUR UNIVERSITY

DECLARATION OF ORIGINALITY AND COMPLIANCE OF ACADEMIC ETHICS

I hereby declare that this thesis contains literature survey and original research work done by the undersigned candidate, as a part of his degree of "**MASTER OF ELECTRONICS AND TELE-COMMUNICATION ENGINEERING".** All information in this document has been obtained and presented in accordance with academic rules and ethical conduct. I also declare that as required by these rules and conduct, I have fully cited and referenced all materials and results that are not original to this work.

Thesis Title

NEGATIVE IMPEDANCE CONVERTER AND ITS APPLICATION IN ELECTRICALLY SMALL ANTENNAS

ABHISHEK CHATTERJEE

University Registration No: 137387 of 2016-2017

Exam Roll No: M4ETC19022

Class Roll No: 001710702020

DEPT. OF ELECTRONICS AND TELECOMMUNICATION ENGINEERING

JADAVPUR UNIVERSITY

KOLKATA – 700032

INDIA

Date: _____ _____

(ABHISHEK CHATTERJEE)

ACKNOWLEDGEMENT

Firstly, I wish to take this opportunity to thank my Master's supervisor Dr. Sayan Chatterjee and acknowledge the deep impact he has had in cultivating within me the interest and curiosity that I have developed towards the theory and applications of Electromagnetism of which Microwave Engineering is but a small part. His patience, the immense knowledge he shares with us and the relationship he has with all his students clearly brings out the best in them. I am very thankful that I have been able to do my Master's thesis under the guidance of such an able and well established professor.

I would like to thank Prof. Bhaskar Gupta for all his comments and discussions which have very often helped clear many of my doubts and helped me look at things from a different perspective. I also wish to express my gratitude to the previous head of the department, Prof. Palaniandavar Venkateswaran and the current head of the department Prof. Sheli Sinha Chaudhuri for always extending a helping hand whenever needed.

This thesis would not have been complete without the help and co operation of all my seniors of JU Microwave Lab who took the time and effort to help me immensely with all my fabrications and indulge in very knowledgeable discourse which helped me learn a plethora of things regarding my subject that I was previously unaware of. I would also like to thank Mr. Sukhendu Bhanja, senior scientist, SAMEER Kolkata center for sharing his knowledge and clearing my doubts whenever required.

Lastly, but most importantly, I would like to thank my father and mother for encouraging me to pursue the subject I love and for their constant and unwavering faith in my abilities. Without their support, I would definitely not be where I am today.

Date: _____ _____

(ABHISHEK CHATTERJEE)

ABSTRACT

This thesis mainly focuses on the study of negative impedance converters and its application in electrically small antennas. The demand for miniaturized, broadband communication systems has created a need for electrically small, broadband antennas. There are many applications that require small wideband antennas, from mobile phones and devices (which are required to cover larger frequency bands) to cognitive radios that are expected to operate within any frequency band with minimum reconfiguration. However there are fundamental limits on these antennas as studied by Chu-Harrington and Bode-Fano that restrict the available bandwidths obtainable from small antennas. On the other hand, electrically small antennas are characterized by rather low input resistance in combination with high input reactance that significantly complicates matching of the antennas in a wide frequency band. Conventional matching networks that obey Foster's reactance theorem would only provide spot frequency matching. This is because it involves resonating the reactive part of the antenna and this is only possible at spot frequencies. However, Non-Foster matching provides an alternative because it uses negative elements to provide wideband matching. These negative elements are able to cancel out the reactance of the antenna continuously over a wide bandwidth. Since the reactive part of the impedance is reduced over a desired frequency range, the quality factor also reduces which in turn increases the bandwidth.

Non-Foster elements can be realized using Negative impedance converter (NIC) circuits. This thesis presents various design topologies of negative impedance converters and also shows the application of NIC to electrically small antennas through simulations and fabrication. A rectangular microstrip patch antenna is designed and the NIC circuit is applied to it. The antenna characteristics such as return loss, real and imaginary part of input impedance were studied with and without the NIC circuit. It was found that with the application of NIC circuit the antenna characteristics significantly improved in the frequency range where it was electrically small. The NIC circuit was able to cancel a significant portion of the antenna reactance over a broad range of frequency and also improve the low real part of the antenna input impedance over the concerned frequency range. Thus the antenna was better matched to the source and the operating frequency of the antenna was successfully lowered (keeping the antenna dimension same) which provided a degree of miniaturization as well. Also, a NIC circuit was applied to a circular patch antenna and the improvements in its characteristics were studied in the frequency range where it is electrically small. Last but not least, this thesis also provides areas which require improvement and where further works could be carried on in the years to come.

CONTENTS

List of Figures

Chapter 1

Introduction

1.1 Chapter Overview

This chapter provides a detailed background of small antennas. Section 1.2 throws light on RF and Microwave engineering. Section 1.3 provides the basic definition of small antennas and shows that based on different requirements, small antenna can be categorized into various types. Section 1.4 looks into the necessity of small antennas in general. Section 1.5 presents the areas where small antennas have been used previously and also the areas that require the services of small antennas. Section 1.6 deals with the theoretical limitations of small antennas and how they are different from normal free space antennas. Section 1.7 presents various methods of obtaining small antenna. Section 1.8 deals with some of the practical design issues related to small antennas. Section 1.9 mainly focuses on the motivation behind the thesis and section 1.10 contains the organization of the thesis.

1.2 Introduction to RF and Microwave Engineering

The term microwaves, usually referred to the restricted domains of radar engineering, telecommunications and electromagnetism for decades before it evolved to a more generic term radio frequencies(RFs) and millimeter waves (above 30GHz). Microwaves can be defined in terms of frequencies, the full electromagnetic spectrum is provided in Fig. 1.1. According to most of the literatures available, microwaves correspond to frequencies between 300 MHz to 300 GHz, having wavelengths between 1mm to 1m. The range between 30 GHz to 300 GHz is also referred to as millimeter waves as they correspond to wavelengths between 1mm to 10mm. [1]

Microwaves are characterized by high frequencies (small wavelengths) and for that reason standard circuit theory cannot be used directly to solve the related problems. Standard circuit theory is an approximation of the broader electromagnetic theory as described by Maxwell's equations. This is due to the fact that, at high frequencies the size of the circuit components becomes comparable to the wavelength of the operating frequencies and therefore lumped circuit element approximations of circuit theory are not valid at radio frequencies or microwave frequencies. The components associated in the microwave domain often acts as distributed elements, since as the device dimensions are in the order of the electrical wavelength over the concerned frequency ranges, the phase of the voltage or current changes significantly over the physical extent of the device. The use of higher frequencies comes with a number of advantages such as reduced component size (antennas, line sections and circuit elements), wider bandwidth, efficient signal processing, high data transmission speed and higher antenna directivities. However, it raises a few practical

problems like higher atmospheric attenuation of high frequencies, more stringent fabrication tolerance and high fabrication cost.

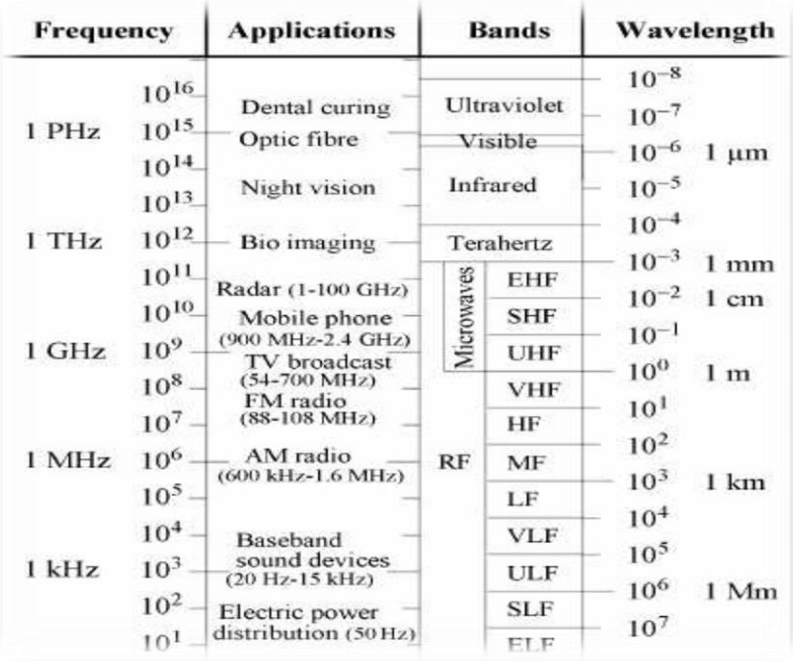

Fig. 1.1: The Electromagnetic Spectrum [1]

1.3 Definition of Small Antenna

Small antennas can be defined with respect to operating wavelength, function and physical dimensions. When an antenna is constructed to have enhanced performance, with the size kept unchanged, the antenna is considered effectively small, since the performance exhibited by the antenna may be that produced by a larger antenna [2]. This type of antenna is defined in regard to the function and named as functionally small antenna (FSA). Other types of antennas made in low-profile or thin structure, the thickness of which is much smaller than the wavelength, can be defined as physically constrained small antenna (PCSA) from a dimensional point of view, as a part of the antenna is constrained to be small. Typical example of PCSA is MSA (microstrip antenna) [2]. Again an antenna having physically small dimensions, but not necessarily small in relation to the wavelength, is defined as physically small antenna (PSA). For example, an antenna that can be put on a human palm can be considered as physically small, even though it could be electrically large. The term electrically small is defined in terms of the operating wavelength or frequency. Thus an electrically small antenna (ESA) is generally defined as an antenna having dimensions much smaller than the wavelength [2]. The classification of small antenna is not unique for an antenna, because one antenna can be included in two or more types of category; for instance, a PCSA can be an ESA, if the whole structure of a low-profile antenna is much smaller than the operating wavelength. ESA is defined from another aspect by taking account of a

dimensionally numerical value, that is, when the whole antenna structure is put into a sphere of the radius a, which satisfies ka<1, where 'k' is the wave number [3]. This sphere is the minimum-sized one that encloses the whole structure of an antenna and is referred to the "Chu sphere." There are many small antennas which are not only electrically small but also functional, defined as FSA and another type, PCSA, when the thickness is very thin.

1.4 Necessity of Small Antenna

With emergence of various wireless systems, including mobile phones, broadband systems, high-rate data transmission systems, radio-frequency identification (RFID) systems, body-centric communication systems, and wearable systems, requirements for small antennas (SAs) are rather urgent, and many SAs have so far been newly developed and practically applied to terminals of wireless systems [2]. Among those wireless systems, the most popular and significant wireless applications are mobile systems that deal with voice, data, and image transmission, radio identification, and wearable systems. Typical voice transmission mobile systems are cellular phones, which have presently advanced to smartphones and data tablets for transmitting information, images (both still and moving), large-quantity data, NFC (near-field communication) systems, and wearable systems including body-centric communication and biomedical systems [2]. The wireless systems, now a day, require small antennas, since the equipment size is generally getting small and the space inside the system is restricted to a limited area to install antennas. In addition, antennas for some mobile terminals not only should be small but should facilitate wideband or multiband capability, because the relentlessly increasing trend in such mobile terminals is to equip them with multiband and other systems such as GPS, WLAN (wireless local area network),Wi-Fi (Wireless Fidelity), etc. as well as telephony. Although multiple operations are required, antennas must still necessarily be small. Furthermore, the wireless world should expect constant development of new systems in the near future, by which effective and flexible use of radio spectrum in wide frequency bands will be made feasible [4]. Thus small antennas play very significant roles in the wireless systems for various situations, as they are always indispensable components.

1.5 Significance of Small Antennas and Applications where they are used

Small antennas are crucial devices and recognized as being indispensable for any wireless systems. This understanding continues up through today since the earliest days of radio communications when ESAs began to be used. The antennas which were used first in communication systems were ESA, however as the operating frequency bands were LF and MF, the antenna dimensions were physically large [2]. The communication range was gradually extended along with the progress in the communication systems from telegraphy to voice transmission. This progress was mainly due to the constant development and

advancement of the antenna technology. Dimensions of antennas had gradually reduced as the frequency allocation progressed to higher bands like HF and VHF, by which long-range communication, even covering worldwide areas, was realized [2]. In those days, antennas practically applied were not only ESA but also other types of small antennas, and though small, their role in communication systems was important. Advancement in antenna technology contributed to progress in communication systems, and in turn communication systems inspired progress in the advancement of antennas. Recent communication systems cover wide ranges of transmission for voice, image, data and radio control, radio identification, sensors, and wideband signal transmissions, including both moving and still images, wearable systems, and so forth. Most of those systems have mobile applications, where equipment is generally small, and antennas to be installed are inevitably small and mostly built into the equipment. At this day and age, the importance of a small antenna is immense in any wireless system. There may be cases, where small antennas would determine the system performance, when the RF front end of the wireless system is designed optimally, and to further improve the performance as is required is almost impossible. The latest mobile systems widely used in public are smartphones, handheld tablets, and wireless broadband systems. Other mobiles are radio sensors, RFID (radio-frequency identification), and wearable systems, including body-centric communications [2]. Types of antennas used for those systems can be any of electrically small, functionally small, physically constrained or physically small. There is growing need for mobile systems that operate multiband or wideband, as systems tend to include more than two subsystems like GPS, WLAN (wireless local area network), Wi-Fi (Wireless Fidelity), etc. that operate in different frequency bands. Recent urgent demand is application of small antennas to the MIMO (Multi-Input Multi-Output) systems [5]. The MIMO system is already employed by WiMAX in order to transmit high data rate to the 4G (4th Generation) mobile systems and other wireless broadband systems where high data rates will be needed will adopt the MIMO system. Small antennas are suitable for small MIMO equipment, where space to install antennas is limited to small areas, and close proximity of antenna elements is unavoidable. The demands for small antennas are not restricted to the domains of physically small, but it also infiltrates to the domains of functional, typically wideband or ultra wideband even multiband operation, or including special characteristics like signal processing capability. Types of antennas required for modern wireless systems are not only ESA, but also PCSA, PSA, and FSA, depending on the system specifications [5]. The major design parameters are the operating frequency, system specifications, dimension of the unit to which the antenna is installed, place and space to install the antenna inside the unit, and so forth. These parameters play a significant role in the selection of type and design of antenna. However, it is important to optimize the antenna design to meet the requirements of the system. Furthermore, some systems require antennas to have functions such as frequency or pattern reconfigurable operation, diversity, and so forth, keeping the antenna size increase as small as possible. In any case, importance of small

antennas does not vary depending upon the system and will continuously grow with further prevalence and advancement of mobile systems.

1.6 Limitations in Small Antenna and difference with normal free space antennas

Small antennas exhibit some specific characteristics that differ from antennas of a size comparable to the wavelength. The input impedance of a small electric (magnetic) dipole antenna is highly capacitive (inductive), while its resistive component is very small [5]. Difficulty in the perfect matching to the load of 50 ohms is mainly due to this impedance characteristic. The radiation pattern of a small antenna, as its size becomes smaller, tends to approach that of the classical elemental vertical dipole which is omnidirectional in the horizontal plane, with a figure-of-eight pattern in the vertical plane, and with a directivity approaching 1.5 [5]. Small antennas, particularly ESAs, need specific design techniques. For an antenna the bandwidth cannot be simply defined as the same way as in circuitry, because in case of antennas there might be factors like change of antenna pattern shape or pattern direction, variation in the impedance characteristics of the antenna, change in the antenna gain which limits the functional bandwidth of an antenna. In general, however, the bandwidth can be defined as a frequency band within which the antenna meets a given set of specifications, typically based on the impedance characteristics. In small antennas, either the antenna input impedance or the power spectra can be taken as the parameter to specify the bandwidth. In small antennas, Quality Factor (Q) or bandwidth that can be attained with a given size is limited. The fundamental limitation of small antennas has so far been discussed by many researchers, first by Wheeler [6] and then Chu [3] and others.

When the size of an antenna is made smaller, the bandwidth tends to grow narrower with reduction of the size [2]. In turn, antenna quality factor (Q) is increased as the antenna size is reduced. As Q becomes large, the bandwidth becomes inversely proportional to Q, implying that the reduction of the antenna size gives rise to increased Q and makes the bandwidth narrower. Now, it should be noticed that increase in the antenna Q with the antenna size reduction is not limitless but bounded by some value [2]. This is the limitation inherently observed in small antennas; that is, the antenna Q or the bandwidth cannot take excess value over the limit value that corresponds to the antenna size. In other words, for a small antenna, a greater bandwidth or a lower Q that violates the limit value depending on the size cannot be achieved. Wheeler [6] first discussed limitations of small antennas in 1947 and showed that Q of a small antenna for the most limiting case was inversely proportional to the third power of ‘ka’ where ‘k’ is the wave number and ‘a’ is the radius of the minimum-sized sphere which encloses the whole structure of an antenna. This indicates Q is inversely proportional to the three dimensional antenna size, and hence the antenna size imposes a fundamental limitation

on the bandwidth B, as when Q > 1, the fractional bandwidth B is considered approximately inversely proportional to the Q. Chu followed Wheeler's work and studied the limitation by using spherical vector wave functions, from which the minimum possible Q for an antenna enclosed in the Chu sphere along with the maximum G/Q (G, gain) was derived [3]. Limitation of the small antenna was studied by many researchers with considerations on the antenna configuration, current distributions, gain, impedance, exciting modes, and polarizations [5]. Nevertheless, if we reduce the radius of the sphere (which translates to a physical reduction in the size of the antenna), the quality factor increases and the gain decreases. Also, as the quality factor of the antenna increases the bandwidth decreases. The quality factor is defined as the ratio of energy stored to energy dissipated. So for an antenna high quality factor means energy stored is more compared to energy radiated and this condition is not desired.

The radiation efficiency η is given by [5]

$$\eta = \frac{R_{rad}}{(R_{rad} + R_{loss})} \qquad 1.1$$

Here R_{loss} denotes the loss resistance. Now, the input impedance of a small electric dipole antenna is characterized by a large capacitive component, so to improve matching, a large conjugate impedance i.e. an inductance is required. When a small dipole, for example, is a short stub of 0.16 λ with radius r of 3.3×10^{-4} λ, R_{rad} is 0.1ohm and X_{rad} (input reactance component) is –2071 ohm. The matching condition requires an inductive component of +2071 ohm [5]. The radiation efficiency η in this case comes out be about 0.005 that is 0.5%. This is because of the much greater loss resistance in the inductive component over the radiation resistance R_{rad}. Practically, a transformer between the low radiation resistance and the load resistance 50ohm is necessary and the loss at that transformer should be taken into consideration [5].

Gain G of an antenna is related to its directivity by accounting for efficiency and two different matching factors [5].

$$G = \eta D M_p \qquad 1.2$$

Here D is directivity, M is the impedance-matching factor, and p is the polarization matching factor. Gain of a very small antenna is determined almost by η and M, because D is around 1.5 independently of the size and p is usually taken as unity, since polarization matching can be good in almost all cases [5]. Now, in the design of practical small antenna, a condition M = 1 will be encountered quite often. The M may take much lower values than unity, as the antenna size tends to be smaller. Gain reduction due to mismatching occurs in many cases with improper design of small antennas, and specific design techniques are needed to avoid degradation of antenna performance due to mismatching [5].

1.7 Principle and Method for Small-Sizing Antennas

The fundamentals of small-sizing an antenna are to lower the resonance frequency, while the size of the antenna is kept much smaller than the operating wavelength. Another aspect is to either improve or enhance the performance of the antenna without varying its size significantly [5]. The former is for producing ESA while the latter is for creating FSA. PCSA can be realized by lowering the profile of an antenna. One of the ways is to thin down the antenna thickness to a value much smaller than the operating wavelength. For PSA it is required to construct an antenna which is physically small, regardless of the operating wavelength.

Following are methods of small-sizing antennas [2]:

(a) Lower the resonance frequency

(b) Increase or extend the current paths on the surface of the antenna element

(c) Occupy antenna space more effectively

(d) Increase number of radiation modes

(e) Make uniform current distributions on the antenna element

These are to be accomplished while the antenna size is kept unchanged.

1.8 Practical design problems with Small Antennas

Design of small antennas, particularly ESA, is to attain an antenna of physically small dimensions, yet having appreciably high performance, even though the dimensions become small. It is rather a challenging issue to realize an ESA, but the practical problem is to achieve a compromise between small-sizing and attaining higher performance in an antenna system [5]. In addition to the physical dimensions, when reducing the size of an antenna there is need to consider various other important parameters such as antenna structure, including type, shape, materials of element, feed system, and environmental conditions, including the platform to install the antenna element, and nearby materials, to list a few. When designing or developing small antennas, one often encounters complicated problems due to environmental conditions that must be met in order to have a practically useful small antenna [5]. When an antenna is to be placed or installed in a complicated or unusual location, one should consider either how to avoid influence of such undesired conditions that may cause degradation of antenna performance, or how to include such conditions in the antenna design to utilize them for enhancing the antenna performance. It may be of almost no use to apply ordinary theory for designing an antenna located in such complicated situations. One of the practical examples is a mobile antenna where mobile terminals are so small that the built-in antenna cannot be isolated electrically from nearby materials, because the antenna is forced to reside in a restrictive area inside the small terminal [5]. Then reduction of coupling between antenna elements is significant for avoiding degradation of antenna performance. This type of

problem is often observed in antennas used for MIMO systems; a typical example is antennas in small mobile WiMAX (Worldwide Interoperability for Microwave Access) terminals. Materials existing near an antenna element give rise to effects on antenna performance that can be either advantageous or disadvantageous, depending on whether they can enhance or improve the antenna performance as a result of acting as a part of the antenna system. In small mobile terminals, the antenna element is usually located in so narrow a space that isolation of the antenna from nearby electronic components, devices, and hardware, including parts like speaker, filter, case, switch, etc. is almost impossible [5]. The main thing to consider here is how to integrate these materials into the antenna system. A ground plane, on which an antenna element is installed, also acts as a part of the antenna system. In this case, the size of the ground plane and the location of the antenna on it should be specified so that integrated design of the antenna and the ground plane can be carried out effectively. The unit's metal case affects radiation too, and it may sometimes be utilized positively as a radiator, as the antenna dimension is essentially extended to the size of the unit. There is a circumstance where the ground plane or the unit case is utilized as one part of a diversity element. When the ground plane or the unit case is used as a part of the radiator, care must be taken for the effect of an operator's hand which can degrade the antenna performance. Since materials existing near an antenna usually yield complicated environmental conditions for the antenna, the antenna design procedure must properly include these materials as part of the antenna system [5]. A similar example is a case where the antenna must be placed in very limited space, such as in a small, thin plastic card or on a tiny dielectric chip. Design of small antennas in these conditions is not very easy and certainly not simple, because matching problems and environmental effects must be taken into account in the antenna design. It is rather usual, in these situations, to aim for either antennas having the maximum obtainable performance, or antennas having the performance attained as a compromise in the complicated situations. Use of computer software is helpful, since modeling of the antenna system, in which even considerably complicated environmental conditions can be included, is made feasible by the appropriately selected software, namely electromagnetic simulators such as MoM (Method of Moments), FDTD, HFSS (High Frequency Simulation Software), IE3D, FEM (Finite Element Method) and so forth [5]. The latest simulation techniques have made remarkable progress and so one can rely on them to obtain reasonably precise results, providing very good approximations that assist in making the antenna design easier and more reliable. Nonetheless, however when one may try to approximate the antenna behavior, some errors is likely to remain, as the modeling cannot be completely perfect.

1.9 Motivation

With emergence of various wireless systems, including mobile phones, broadband systems, high-rate data transmission systems, radio-frequency identification (RFID) systems,

body-centric communication systems, and wearable systems, requirements for small antennas (SAs) are rather urgent, and many SAs have so far been newly developed and practically applied to terminals of wireless systems. Because most wireless systems use small terminals, antennas mounted on such terminals are inevitably SAs. Practically, many small terminals require ESA; however, SAs used so far are not only those having small dimensions but also some functions to implement a variety of performances, including wideband, multiband, reconfigurable operation and other sophisticated operations (FSA). Practical SAs with low-profile structure (PCSA) and having simply physically small dimensions without regarding the operating frequency (PSA) are also significant in small wireless terminals. Each of these four types of SA is appropriately designed and applied to related systems. Design and development of small antennas need special considerations, especially when the dimensions become smaller and designers encounter difficult situations to conquer trade-offs between practical requirements and the fundamental limitation of SA. The challenge is to overcome the limitations and contribute to the continuous development of effective small antennas.

1.10 Organization of the thesis

This chapter mainly emphasizes on the background of small antennas. The areas which are reflected here includes the field of application of small antennas, their significance and how they are different from normal free space antennas and the limitations of small antennas. Chapter 2 presents a systematic literature review of various works on small antennas which include characterization and modeling, application of NIC and noise and stability analysis. Chapter 3 presents a detailed background of Electrically Small Antennas (ESAs) including various mathematical relations and also provides a detailed theory of Negative Impedance Converters (NICs). Chapter 4 is divided into two sections. Section A deals with various NIC circuit designs. Section B highlights the current work on application of negative impedance converter circuit to an electrically small antenna which in this case is a rectangular microstrip patch antenna. The simulated and measured results are shown in this section. Chapter 5 presents the application of NIC circuit to a new design i.e. to a circular patch antenna. Here only simulated results are presented. The concluding comments along with the future scopes of this work are presented in chapter 6 which marks the end of this thesis.

Chapter 2

Literature Review

2.1 Chapter Overview

This chapter deals with a detailed review of various papers, journals and thesis related to the concerned work. Section 2.2 presents a brief history on antennas, antenna evolution over the years and electrically small antennas. Section 2.3 presents a brief study on characterization and modeling of electrically small antennas, limitations of electrically small antennas and how researchers have dealt with those limitations. Section 2.4 presents a brief study on negative impedance converters and how NICs have been used by the researchers along with electrically small antennas to better its performance. Section 2.5 presents a review of various works on noise considerations of NICs and stability analysis of electrically small antennas with negative impedance converters. The previous works that have been mentioned in this chapter are presented in chronological order with proper references.

2.2 A brief history on small antennas

1846 marks the inception of antenna history when J. Henry experimented with spark-gap transmission and reception by using a small loop loaded with an induction coil. After that many pioneers like Edison, Hertz, and Lodge did experiments by using electrically small antennas (ESAs) for radio-wave radiation and reception, although the dimensions of those antennas were physically large, as the frequency bands used were LF and MF. Types of antennas used in those days were thin long wires, monopoles, biconical dipoles, loops, and so forth [7]. By replacement of the early radiotelegraphy spark-gap transmitters, longer-distance communication was promoted, and various antenna technologies such as grounding of one antenna terminal to the earth, resonance by using LC circuits, and impedance matching were developed. [2]

The world's first radio communication accomplished by Marconi in 1901 used also types of ESA, although they were physically quite large; the fan type antenna at the England site was only several tenths of the operating wavelength about 3000 m (820 KHz) but having dimensions of 48-m wide and 68-m high. Since then, radio communications over the Atlantic Ocean spread to be used between ships and coasts in the early 1900s. At that time mostly thin long wires or wired inverted-L types were used as ship antennas. In 1906, the frequency spectrum for the radio communications was restricted to LF and MF bands for ships, long-distance land communications, and military use [2]. Since then, many large, low-frequency antennas were developed. To shorten the long-wire antennas, top-loading technique was invented. Later, by applying the top-loading technique, a new flat-top antenna like an umbrella was developed. Since radiation efficiency of those antennas was very low, multiple

tuning techniques were invented for improving the efficiency [2]. Antenna technology had further advanced to achieve directional radiation by arraying antenna elements. The directional radiation was designed by using another technique, the use of a traveling wave on a long wire placed in parallel to the ground with low height. Other antenna types practically used in those days were (a) T shape, (b) inverted L, (c) harp shape, (d) rhombus, (e) flat top, and so forth [2]; all of those were ESA. In the late 1930s, slot antennas and ferrite antennas were put into practice.

With time and technology improvement, the operating frequencies moved to the higher side, and in the mid-twentieth century, HF band was the major band which was influential for the development of aeronautical radio and marine radio. Remarkable advancement of small antenna technology can be attributed to World War I (1914–1918) and World War II (1939–1945) due to the needs for military communications for airplanes and airships, as well as for land systems. The type of antennas used in such communication systems during World War I was mainly a thin $\lambda/4$ wire monopole, which was installed on the equipment body (metal) that was considered as the ground. Significant progress seen in World War II was mobile systems, particularly for land mobiles used for military force and vehicles. System advancement was accelerated by introduction of higher-frequency bands, VHF, and FM technology [2]. After the war, application of mobile systems was further expanded to various new mobile systems for the public: telephones for personal use and on the airplane. Another notable subject in the 1940s was study of the fundamental limitation of small antennas, initiated by Wheeler in 1947 [6]. The discussion on the limitation has still been active in the present days.

In the 1950s, the UHF band was opened to the public and design concepts of antennas for mobile systems changed. The body of the small radio unit (metal) traditionally considered as the ground was changed to be treated as a part of the radiator, to which the ground was included. This result in turn contributed in improving the performance of the antenna. In 1950s and later, spiral type antennas were designed and applied to various wideband applications. By using spiral structures, design of a small antenna having wideband or UWB (ultra-wideband) characteristics has become feasible [2]. Other antenna types used in those days were newly developed NMHA (normal-mode helical antenna), IFA (inverted-F antenna) and various composite antennas, for instance, combination of a dipole and a loop. In the 1960s, systems underwent changes through time with emergence of various new systems and services, which deployed according to the social needs; they were radar, space communication, TV broadcast, mobile systems, and so forth. Along with advancement of systems, antenna technologies progressed [2]. It should be noted that the design techniques of small antennas changed remarkably to treat an antenna with a comprehensive concept in which wireless system, propagation, and environmental conditions were considered, and so small antennas were treated as a "system." There were some instances where the performance of the antenna, in particular with a small antenna, could finally dominate the system

performance. When the system unit is a handset, influence of the unit operator's hand, head, and body affects antenna design as one of the crucial parameters.

The concept of integrated antennas was introduced in the late 1960s, which contributed to miniaturization of an antenna and to produce functional antennas. These are generally called IASs (integrated antenna systems) [8], since they work as a system, where their structures, being composed of passive or active devices, are dealt in total with systematic concepts. Among them, AIAS (active integrated antenna system) finds its application to small-sizing antennas, particularly in improving the matching of small antennas. Very small antennas exhibit very large reactive components but very small resistive components in their input impedances, making proper matching difficult. An NIC (negative impedance converter) [9], which is one of the representative AIASs, is used for overcoming the matching problem in very small antennas. The NIC can be used at either the antenna load terminals or in the near field of a radiator. The latter is known as space matching [10,5], which is a recently introduced technology. In the 1970s, public mobile phones called cellular phones were first introduced. That technology has progressed to the fourth-generation system from the first systems in the 1980s, and antenna systems used in mobile terminals (handsets) evolved from a wire monopole to planar types such as PIFA, MSA, and parallel plate, and they were at last entirely built into the equipment body. In some phones, functional performances such as diversity, frequency reconfigurable control, and pattern control were required and so facilitated. Those antennas were classified into the type of (Functionally small antenna) FSA [2].

In the 2000s, an increasing demand for access to information anywhere, anytime led to an explosive growth of wireless technologies and accelerated the emergence of various wireless broadband systems, such as Wi-Fi, WiMAX (Worldwide Interoperability for Microwave Access), WLAN, and the advanced mobile system LTE (Long-Term Evolution) evolved from cellular phones, which can deal with high data- rate signals including both still and moving images, large amounts of digital data, and high-quality sounds as well as voice. Antennas for those wireless broadband systems had made remarkable progress along with the newly developed systems, where wideband operation covering wide frequency ranges are needed – several tens of MHz and UWB (ultra-wideband). Most of the latest practical antennas have been no longer simple like just a dipole, a monopole, or a loop but constructed in composite structure with the shape transformed to perform wideband or multiband, integrated types to facilitate function, and combined arrangement of two or more types of antenna to operate adaptive control, even with the small dimensions as ESA [2]. In the integrated antennas, active devices are used as AIAS (active integrated antenna system), which of course contributes to antenna small-sizing. NIC (negative impedance converter) is a representative AIAS. For a very small antenna, which exhibits difficulty in matching because of highly reactive and very small resistive impedance, a NIC can be applied to ease this difficulty, as it can compensate highly reactive components. In the field of antenna

technology, the contribution of electromagnetic materials is notable. Magnetic or dielectric materials have long been applied to antennas for making the dimensions small. In addition, recently introduced metamaterials which exhibit either negative μ (permeability), negative ε (permittivity), or both play an important role for creating such versatile antennas as miniaturized ones; functionalized ones; ones provided with enhanced performances, including reconfigurable control; and so forth [2].

2.3 Characterization, modeling and limitations of ESA

The initial work of studying the fundamental limitation of small antennas was done by Wheeler in 1947 [6]. He assumed that either a lossy capacitor or a lossy inductor could behave as a small antenna, where the dissipated power (loss) stands for only the radiated power. Hence, for his work, he considered a capacitor and an inductor in an equal cylindrical volume to be an electric antenna and a magnetic antenna respectively. The cylindrical volume was intentionally used because it could properly replicate the volume occupied by either the capacitor or the inductor. The electric antenna was represented by a capacitor and the magnetic antenna was represented by a solenoidal inductor. To incorporate practicality in his work he further modeled a capacitor in shunt with a conductor for an electric antenna and an inductor in series with a resistor for a magnetic antenna. This modification was done to account for the losses. Wheeler calculated the capacitance and inductance by using the formulas given in [6]. He also used the formulas mentioned in [6] to obtain the effective area with consideration of the electric field outside the cylinder and the effective length of the magnetic path, considering the external magnetic field of the inductor. Wheeler used the Radiation Power Factor (RPF) rather than the radiation quality factor (Q_{rad}) to account for the ratio of the radiated power to reactive power of the small antenna. Both RPFs were always less than unity for an electrically small size. However, since the most common quantity of a small antenna is the radiation quality factor, the Q_{rad} was derived from the RPF by using the lumped model in [11]. The radiation quality factor was found to be proportional to the reciprocal of the radiation power factor.

Chu's work in 1948 revolved around the theoretical limitations of omni-directional antennas. He used spherical wave functions and applied the recurrence relation of spherical Bessel functions to determine the equivalent lumped element models for the wave impedances of spherical TM and TE modes. Based on these equivalent circuits, theoretical lower bounds for the Q_{rad} of small antennas as a function of 'ka' were developed. The derivation of Chu's is based on [3,12,13]. For $ka<<1$, the Q_{rad} was shown to be proportional to the third power of the reciprocal of 'ka'. Given a small antenna it was also shown that the radiation power factors are proportional to the reciprocal of Q_{rad}. Note that Chu's Q_{rad} does not consider the stored energy inside ($a < r$) of the sphere and there is no mismatch between the antenna and the input port. Later, Mclean [14] improved the lower bound of Chu's Q_{rad}.

For a TM_{10} or TE_{10} mode, the theoretical lower bound for the Q_{rad} was given in [14]. When Qrad is quite large, the fractional half power bandwidth of the antenna can be approximated by the reciprocal of Q_{rad} [15]. From [14] it was deduced that the frequency bandwidth of small antennas was strongly affected with their electrical size.

Harrington in 1959 [16] made a theoretical analysis on the effect of antenna size on parameters such as gain, bandwidth, and efficiency. Both near-zone and far-zone directive gains were considered. It was found that the maximum gain obtainable from a broad-band antenna was approximately equal to that of the uniformly illuminated aperture. If higher gain is desired, the antenna must necessarily be a narrow-band device. In fact, the input impedance becomes frequency sensitive so rapidly that, for large antennas, no significant increase in gain over that of the uniformly illuminated aperture is possible. Also, if the antenna is lossy, the efficiency falls rapidly as the gain is increased over that of the uniformly illuminated aperture. He proposed that to relate the analysis to practical antenna systems, define the radius R of an antenna system to be the radius of the smallest sphere that can contain it [16]. The Q-factor of the ideal lossless antenna must then be less than or equal to the Q-factor of any other loss-free antenna of radius R, since fields r< R can only add to energy storage. In the loss-free case the Q is large. In addition to this, in the lossy case the dissipation is large. In both cases the near-field is characterized by extremely large field intensities. Systems having larger gain than this are called supergain antennas. One cannot obtain a gain higher than that of the uniformly illuminated aperture without resorting to a supergain antenna. A uniformly illuminated and "focused" aperture (phase adjusted so that all elements contribute in-phase at some distance r) has a near-zone gain approximately equal to the far-zone gain of the "unfocused" aperture (uniform phase). Thus, a near-zone gain greater than that obtainable from a focused uniformly illuminated aperture cannot be obtained without resorting to a supergain antenna [16]. Note that for small R, substantial increases in gain can be achieved, but for large R the increase becomes insignificant. Hence, for practical purposes, the uniformly illuminated aperture gives optimum gain. For small antennas, however, a significant increase over normal gain is possible. Perhaps the most common example of a small supergain antenna is the short dipole. The problems of narrow bandwidth and high losses associated with this antenna have been thoroughly treated, since it is one of the few antennas that can be used at very low frequencies [16].

Collin and Rothschild in 1964 improved previously given theory for obtaining Q based on the field rather than the equivalent circuit [17]. They calculated Q for cases where both TE and TM modes are used for excitation, and derived it for the lowest mode. Hansen in 1981 simplified Chu's expression for calculating Q [18]. He stated that when 'ka' is roughly less than unity and only the lowest TM mode propagates, Q is expressed by [18]. Hansen concluded that the value of Q would be halved when TM and TE modes are equally excited.

He illustrated Q with respect to the antenna size 'ka' along with the radiation efficiency η as the parameter.

McLean [14] in 1996 derived an exact method for the calculation of the minimum radiation Q-factor of a general antenna. This expression agrees with the previously published and widely cited approximate expression in the extreme lower limit of electrical size. However, for the upper end of the range of electrical size which is considered electrically small, the exact expression given here is significantly different from the approximate expression. This result has implications on both the bandwidth and efficiency limitations of antennas which fall into this category. For an antenna, the definition for radiation Q that is generally accepted is given in [3,16]. The basis for this definition is that it is implicitly assumed that the antenna will be resonated with an appropriate lossless circuit element to affect purely real input impedance at a specific design frequency. Thus, the definition of the radiation Q of an antenna is similar to the definition of Q for a practical circuit element, which stores predominantly one form of energy while exhibiting some losses. In Chu's theory, the antenna is enclosed by a sphere of radius a, the smallest possible sphere which completely encloses the antenna. The fields of the antenna external to the sphere are represented in terms of a weighted sum of spherical wave functions, the so-called "modes of free space" [12]. It is implicit in Chu's work that these modes exhibit power orthogonality; that is, they carry power independently of one another, just as modes in a uniform metallic waveguide. From the spherical wave-function expansion, the radiation Q is calculated in terms of the time-average, non propagating energy external to the sphere and the radiated power. According to Chu's work, the calculated radiation Q will be the minimum of all the possible radiation Q for any antenna which completely fits in the sphere; any energy stored within the sphere could only increase the Q. However, the calculation of this radiation Q is not straightforward because the total time-average stored energy outside the sphere is infinite just as it is for any propagating wave or combination of propagating waves and non propagating fields [3]. Some technique for separating the non propagating energy from the total energy is required. It is not possible to calculate the non propagating stored energy using simply the near-field electric and magnetic-field components because energy is a nonlinear quantity [3]. Instead of working directly with the electric and magnetic fields, Chu derived an equivalent ladder network for each spherical waveguide mode using a technique based on the recurrence relations for the spherical Bessel functions and a continued fraction expansion. The total non propagating energy and the radiation Q can be calculated from the equivalent circuit, by summing up the magnetic and electric energies stored in the inductances and the capacitances. However, as Chu pointed out in his paper, this would be quite tedious for all but the lowest order modes. Therefore, Chu derived an equivalent second-order series RLC circuit and calculated the Q from this equivalent circuit, assuming it behaved as a lumped second order network over some limited range of frequency. From Chu's calculations, it has been shown that an antenna which excites either TE_{0l} or TM_{01} external to the sphere (and

stores no energy in the sphere) has the minimum of all the possible radiation Q of any linearly polarized antenna. An approximate analytical expression for this Q has been given in [2] but appears to be incorrect. An exact calculation of the radiation Q associated with the TM_{01} and TE_{01} spherical modes, and hence, the minimum attainable radiation Q of a linearly polarized antenna has been given. The exact expression however differs from the previously proposed approximate expression. For small values of 'ka', this radiation Q is approximately given by [14] and thus is in agreement with Chu's [3] theory and Wheeler's [6] theory for this range of 'ka'. However, for values of 'ka' near one (but still less than one), the expressions differ significantly. From the exact expression given here, it would appear that the lowest achievable radiation Q of an antenna of this electrical size is actually somewhat larger than previously thought. As has been previously noted [18,3] the relation between the radiation Q and the maximum achievable bandwidth is not straight forward. However, a larger radiation Q would still suggest that the maximum achievable bandwidth of the system is still narrow. Therefore, the restriction on bandwidth for an electrically small linearly polarized antenna is actually somewhat more restrictive than is implied by Chu's approximate theory.

2.4 Review of various works on non foster impedance matching networks for electrically small antennas

Initial work on negative impedance converter was done by J Linvill in 1953 [19]. Linvill proposed a transistor based open circuit stable type and short circuit stable type negative impedance converter. The property of open-circuit stability holds for transistor converters in which the input terminals are the emitter terminals, independent of the nature of the load or the cross-coupling networks, as long as these are passive. For converters in which the input terminals are the collectors of the transistors, the property of short-circuit stability from the input terminals holds, independent of the nature of the passive cross-coupling network [19].

The earliest work among successfully fabricated Non-Foster impedance matching networks for electrically small antennas was achieved by A. D. Harris et al. in 1968 [20]. Their test antennas were a $2\frac{1}{2}''$ monopole with a $2\frac{1}{2}''$ diameter top hat and a $10''$ monopole with a $10''$ diameter top hat. The improvement of the measured antenna gains with negative capacitors with respect to a 16 foot untuned whip antenna over 0.5MHz-10MHz was shown in [20]. Given a small monopole antenna, the equivalent lumped circuit for the input impedance of the antenna can be modeled as a capacitance connected in parallel to a conductance. To cancel out the capacitance, a corresponding negative capacitance was connected in shunt with the input port of the antenna. Based on a conceptually ideal voltage inversion NIC with a voltage gain (Av) of 2, a negative capacitor was realized by using

multiple amplifiers [20]. However, the performance of this NIC is limited at high frequencies because of the finite input and output impedances [20]. The gain of the amplifier with the factor of two cannot be sustained at higher frequencies. Although the noise of the antenna with a negative capacitor was not measured, the performance was restricted by external noise rather than that of the negative capacitor in the measured frequency range (0.5MHz-10MHz). Harris also discussed the dynamic range of Non-Foster impedances, and measured the non-linear performance of a Non-Foster impedance. For the measurement setup, two transmitter antennas operating at different frequencies (200 kHz and 230 kHz) were placed nearby the test antenna with a Non-Foster impedance. Received signals were measured for three different cases of transmitting power levels: (1) two large signals, (2) large and small signals, (3) two small signals. As larger power was received at the antenna with a Non-Foster impedance, the non-linear effects of the active circuit become severe [20]. Although the non-linear effects of a Non-Foster impedance were identified through measured results, there were not enough cases to determine the dynamic range of the input power for the Non-Foster impedance.

Perry in 1973 elaborated the topic of Non-Foster impedance matching for small receiver antennas further in [21]. He used the term conjugate impedance matching rather than Non-Foster impedance matching to emphasize the partial realization of complex conjugate matching by means of active circuits. The maximum transfer of power between an antenna and a generator with internal impedance can be achieved when the complex conjugate of the input impedance of the antenna is equal to the internal impedance of the generator. He fabricated a 3″monopole receiver antenna (2″ monopole antenna with a 1×1″ top mounted load) with three different Non-Foster impedance matching networks and showed the improvement of the antenna gain relative to a 12 foot untuned Tricor whip antenna over 0.3MHz-2.5MHz. Like Harris, all negative capacitors were connected in shunt with the antenna. Among three different fabricated active networks, two of them were comprised of operational amplifiers (OP-amps) and the last one was implemented with transistors. Although Perry achieved outstanding improvement of the antenna gain with Non- Foster impedance matching networks, the active networks only worked below 5MHz and no noise measurements was performed [21].

Volakis Et al. in 2009 increased a 6” loop’s bandwidth from 50 MHz to 300 MHz in [22] . The loop was designed at 700 MHz and was matched at 300MHz by a composite matching network consisting of an L circuit with a shunt positive and a series negative inductor to match the antenna resistance, and a series circuit of negative capacitor and inductor to cancel the reactive part of the monopole impedance. The loop had a narrow resonance around 700MHz and the goal was to improve its bandwidth and reduce its size using a non-Foster matching network designed via optimization [23]. A negative matching

circuit was given previously for a monopole [24]. Monopole has a square variance in its resistance and linear increase in reactance before its first resonance. Thus to counter this a negative network consisting of an L circuit with a shunt positive and a series negative inductor was selected to match the antenna resistance, and a series circuit of negative capacitor and inductor to cancel the reactive part of the monopole impedance was used. However, the loop impedance has quite different impedance behavior. Below the 700MHz resonance, its resistance slightly decreases (not in quadratic form) until 400MHz and then it rapidly increase. Its reactance is linearly decreasing until 600MHz and then it follows a rather quadratic decrease. Hence, a circuit consisting of a shunt positive inductor and an additional optimized non-Foster network was used. The four element non-Foster network delivered a 300 MHz return loss bandwidth from 300MHz. Moreover the circuit demonstrated how easily a narrow resonance antenna can be transformed to a smaller broadband antenna.

Sussman-Fort in 2009 proposed a single negative capacitor to cancel the reactance of an electrically small 6" monopole [25]. The signal to noise ratio with non foster matching was up by 9dB at 30MHz. He also proposed a dual negative capacitor network to cancel the reactance of an electrically small 12" dipole. The signal to noise ratio with non foster matching was up by 20 dB. In the most recent publication [25], Sussman-Fort summarized his previous work [26,27,28,29,30,31] on fabricated Non-Foster impedance matching networks for a 6″ monopole and a 12″ dipole antenna. A negative capacitor connected in parallel with a monopole type small antenna, can reduce its net-reactance for low frequencies because the equivalent model for the input impedance of the antenna (a parallel combination of a resistor and a capacitor) is valid for only low frequencies. It is therefore necessary to use a negative capacitor connected to the antenna in series to maintain the improvement of the antenna with the Non-Foster impedance matching network for higher frequencies. In his papers, he used balanced Linvill's open circuit stable NICs in [9] [19], comprised of two bipolar junction transistors for receiver antennas. Sussman-Fort showed improvement of both antenna gain and signal to noise ratio (SNR) from 20MHz to 120MHz, when compared to antennas without matching networks. To assess the SNR of a receiver antenna with a Non-Foster matching network, he introduced and applied the following method [25] [27] .Received signals of the antenna with and without a Non-Foster matching network were first recorded. Then, the difference between received signals with the matching network (S_1) and one without a matching network (S_0) were taken. The difference ($S_1 - S_0$ in dB scale) is the gain improvement of the matching network. For noise measurements one can perform the same procedure while the transmitter antenna is turned off. The difference ($N_1 - N_0$ in dB scale) is the added noise of the matching network, where N_1 and N_0 are received signals with and without the matching network, respectively. Hence, the improved SNR with a matching network is given by $SNR_{imp} = (S_1 - S_0) - (N_1 - N_0)$. In [61], the highest effective frequency range obtained by applying a Non-Foster impedance matching circuit to a 20″ × 2″ lossy

dipole antenna is from 60MHz to 400MHz. It is also shown that there is the improvement of antenna gain; however, the electrically size of the antenna is around $\lambda/2$ at 286MHz.

Sussman-Fort also presented Non-Foster matching networks for transmitter electrically small antennas [25,27,28,31]; however, the Non-Foster matching networks were applied to surrogate antenna models (series connections of a resistor and a capacitor). In these papers, he pointed out that the power efficiency (including DC bias for activating NICs) should be considered in applications of Non-Foster matching networks to transmitter antennas. For the high voltage problem in a transmitter antenna, it was suggested that a negative LC matching could be applied to an electrically small antenna. He also showed a measured data with a surrogated antenna model to prove the concept. It was shown that the resonance of the antenna caused by a negative LC matching forces to transfer the maximum power to the antenna (for a narrow bandwidth) [25,27,28,31]. With this concept, class-B and class -C biased NICs were introduced to improve the power efficiency of transmitter antennas. Note that the linearity of circuits, another important factor in transmitter application, was not considered in his papers. Although measured data of antennas with Non-Foster matching networks were shown in [26,27,28,29,30,31] none of this previous work shows in detail how to design and make the whole network stable.

Fan et al. in 2011 [32] proposed a transistor based negative LC converter for an electrically small half loop antenna. The antenna was electrically small up to 665MHz but the antenna was matched at 200MHz. The half loop antenna was realized on a square FR4 board, the outer radius being 10 mm and the wire radius being 0.2 mm. To achieve the non-Foster matching for the antenna design, a wideband transistor based negative parallel LC converter was proposed. Here, two BFP640 as the RF transistors were used and two 2N2907A as the biasing BJTs, which worked as an operation point fixer. This circuit was fabricated on FR4, with $\varepsilon_r = 4.4$ and h=1.524 mm. Furthermore, they incorporated a positive parallel RLC circuit as the stability control unit in series with the NIC circuit for the measurement. In their experiment, an Agilent PNA5230C network analyzer was employed to measure the input impedance of the NIC. They also calculate the gain of the half-loop antenna at 200MHZ with and without non-Foster matching networks. The gain of the half-loop antenna with non-Foster matching networks was significantly enhanced. However, it should be noted that the gain of the electrically small half-loop antenna with non-Foster impedance matching is still poor which limits its commercial use. The key challenge for the design is that the parasitic effects of the transistor model will come up during the incorporation of non-Foster circuits to the antenna which is a limitation that requires further research [32].

Song in 2011 introduced a systematic methodology to design a Non-Foster matching network for an electrically small receiver antenna [33]. Describing each key step in the

methodology, a stabilized Non-Foster impedance matching network with a negative capacitor was fabricated to compensate the considerably high reactance of a thin 3″ wire monopole antenna on a 3″ × 3″ metal ground plane. The schematic of the negative capacitor shown in this paper could be employed for monopole and dipole-type electrically small antennas after adjusting the values of the stabilization elements and the load of the NIC [33]. Through measured and simulated data, it was sequentially shown that a Non-Foster impedance matching network can reduce the input reactance of an electrically small antenna, making the transducer gain between the antenna and a receiver increased. Consequently, the Non-Foster matching network can enhance the realized gain and SNR of an antenna, comparing to the case without a matching network. Based on measured results, the Non-Foster impedance matching network improves the antenna gain (or SNR) up to 20.9dB (or 20.3dB) with respect to the case without a matching network over the frequency band 100MHz to 550MHz [33]. Measured and simulated data for the reflection coefficient of the antenna with a Non-Foster matching network included was obtained for different input power levels. At high power level (> 4dBm), the non-linear behavior of the Non-Foster matching network was observed. When applying a Non-Foster matching network to transmitter antenna, this non-linear behavior should be considered.

Song also introduced a Non-Foster impedance matching network with a series combination of negative capacitor-inductor for an electrically small monopole antenna to maintain the performance of the Non-Foster matching network for higher frequencies [33]. Based on measured data, it was shown that the antenna with the negative capacitor inductor had an advantage over both the antenna with/without a negative capacitor in terms of antenna gain and SNR. Although both Non-Foster impedance matching networks (a series combination of negative capacitor-inductor and a negative capacitor) relative to the case without a matching network improved the antenna gain and SNR at low frequencies, the antenna with the negative capacitor had a poor antenna gain after 558MHz when comparing the case without a matching network (the improved SNR with the negative capacitor relative to the antenna without a matching network was up to 482.8MHz) [33]. However, the Non-Foster impedance with the negative capacitor-inductor made the antenna gain (or SNR) improved up to 793MHz (or 771.8MHz), comparing to that of the antenna without a matching network. However, there are several dips caused by the coupling between the antenna and the matching network. Although the antenna with the negative capacitor-inductor provided improvement of antenna performance up to higher frequencies than the single negative capacitor, the former resulted in a negative resistance as the frequency becomes higher [33]. Thus, it was proposed to use two different NICs (series capacitor and shunt inductor) rather than a single NIC to prevent negative resistance in the series connection of a negative capacitor and a negative inductor at higher frequencies.

Song in 2011 also introduced fabricated Non-Foster inductor load for an electrically small two port loop antenna to both increase the antenna gain and maintain an omni-direction radiation pattern at higher frequencies [33]. It was the first time that a fabricated Non-Foster impedance loading network was applied to this antenna. The fabricated negative inductor could be employed to enhance the performance of any small loop type antenna. They showed the limitations of a Non-Foster impedance matching network comprised of a single element (either a negative inductor or a negative capacitor) for a small loop antenna. When comparing the measured and simulated input impedances of the antenna with the loading networks, the reactance with the Non-Foster loading was reduced and the first parallel resonant frequency of the antenna with the Non-Foster loading was shifted to a higher frequency [33]. Through both measured and simulated reflection coefficients for different input powers, the Non-linear property of the Non-Foster loading was also shown in this paper. For the radiation patterns, the measured data did not agreed well with the simulated results because of two effects: the model of the Non-Foster inductor in the simulation and common mode currents on the cable. However, based on both measured and simulated antenna gains, it could be confirmed that the antenna gain with the Non-Foster loading was improved. For instance, the Non-Foster inductor loading improved the maximum gain in the azimuth plane up to around 6.97dB over 100MHz to 267MHz, compared to the case with a short loading. It was also demonstrated that the SNR with the Non-Foster loading relative to the case with a short loading could be improved as well. Based on measured SNRs, the improvement with the Non-Foster loading was up to 8.3dB over 100MHz to 277MHz, when compared with the short loading case [33].

Gardner et al. [34] in 2012 proposed a negative capacitor up to 1.5 GHz and used a composite matching network to match a small chassis antenna and lower its quality factor even below the Chu limit. The reason why the NICs have not been realized at higher frequency ranges is because of the stability problems associated with realizing the NIC at these frequencies. In this paper they carried out a stability analysis on the NIC circuit, to predict instability and also how to overcome this challenge and realize NIC working at higher frequencies than currently available. The antenna used in this work was a chassis antenna. The ground plane was 40mm by 100mm, fabricated from copper sheet with thickness 0.5mm. The coupling element was 40mm × 5mm × 7mm and was displaced from the ground plane by 6mm [34]. The coupling element and ground plane were supported by Rohacell^{TM} with dielectric constant of 1.08 within the frequency of operation. The Q of the antenna was found to be 19 (at 900MHz). The matching network consisted of three negative reactive elements, a series negative inductor and capacitor and a shunt negative capacitor. The negative elements were obtained by simulating them using the Linvill's model. The matched antenna return loss showed wideband performance. The matching network provided a better than -6dB return loss between 800MHz and 2.4GHz. This means a reduction in the Q of the antenna considerably beyond the Chu limit. The NIC was built using Linvill's model, as a double

layered structure. The double layered layout was chosen because it provided the shortest route for the feedback. The length of the feedback path is critical in ensuring the stability of the NIC. The structure was 50mm × 50mm with a common ground plane in-between the two layers [34]. The top layer consisted of the transistor, capacitor to invert, stabilizing capacitor and the bias network while the reverse layer had the feedback path and DC blocking capacitors. Vias connected the two layers together. SOT-23 packaged NXP BFS-17 transistors were used and they were biased at 5V, 20mA. The substrate was Taconic TLY-5 with dielectric constant of 2.2, loss tangent of 0.0009 and thickness of 1.57mm. A parameter sweep on the value of the inductor shows that reducing the inductance, which implies reducing the length of the feedback path, moves the frequency of oscillation higher. This gave two ways of achieving higher frequency NIC action: the choice of transistor to get a stable NIC and/or reducing the length of the feedback path .The simulated antenna return loss showed a better than -6dB return loss between 647 - 1500MHz. With a bandwidth of 853MHz, the antenna's Q was reduced to 1.258 from 19. However, further work is needed to be done on noise and intermodulation characterization. The loss in NIC and the restriction on the top frequency caused by the feedback path length can be overcome, in principle, by realizing the NIC in MMIC [34].

Jacob et al. [35]in 2012 proposed a negative inductor in series with an ideal negative capacitor along with a shunt inductor to match a loop antenna and achieve an overall matching bandwidth of 85MHz. The matching network consisted of a series negative inductor and a negative capacitor that served to negate only the reactance of the antenna in the region of matching. The antenna was an electrically small loop antenna with 3 turns, 5 cm radius and a 7 cm pitch length that had a resistance close to 50 ohm in the matching region. The antenna was first matched with ideal non-Foster elements, and then with the NIC version of the negative inductor. The results were then compared. The floating NIC of -525nH was connected in series with an ideal -0.7 pF negative capacitor and the antenna model along with a shunt 70nH at the input. The fractional bandwidth was found to be 0.4. At the center frequency of this improved bandwidth, 'ka' was 0.65. The theoretical minimum quality factor (Q) corresponding to this 'ka' was 5.12. The measured Q of this matching was found to be 1.78 [35]. Thus the decrease in measured Q corresponded to a bandwidth increase that is 2.9 times the theoretical Wheeler-Chu limit for a small antenna of size ka=0.65. However, the thing to observe here is that the real part of the antenna impedance is close to 50 ohm in the matching region. Thus the NIC circuit has no contribution to the real part of the antenna impedance. In most cases the real part of electrically small antennas are very small. Hence this work is not a generalized work [35].

Hashemi et al. in 2013 proposed a non-Foster matching network based on the Linvill negative impedance converter (NIC) for an electrically small monopole antenna placed on a square ground plane at the center frequency of 200 MHz [36]. The input impedance of NIC

was derived in terms of the characteristic parameters of several types of transistors and its load capacitive impedance. It was shown that the non-Foster capacitor significantly decreased the antenna input reactance and increased its bandwidth. The Monopole antenna was placed on an aluminum square ground plane of size 15x15 cm^2 and thickness 2 mm. The antenna was an aluminum cylindrical post of length 7.5 cm and diameter of 6 mm. It was to be used as a receiving antenna at 200 MHz. NE68130 transistors were used at the desirable bias (quiescent operating current I_{CQ}=1.5 mA and voltage V_{CEQ}=9 V) [36]. The input capacitance of the monopole antenna was equal to 3.3 pF as the load of NIC. It is varied to 2.9 pF to obtain an optimum performance. The application of NIC in the antenna input circuit resulted in a wide band performance. The values of S11 were less than unity, which guarantees the stability condition of non-Foster matching network.

Kim's work in 2014 [37] includes an operational amplifier based negative impedance converter to match a resistively loaded vee dipole antenna at the feed. The RVD antenna in this work has been designed as two arms loaded according to the Wu-King profile, which is expressed in terms of the resistance per unit length of the arm in [38] which can be parameterized by the length of the arm of h = 15cm, the included angle of 2α =110°, the width of the pattern of t = 3 mm, and R_0 = 3557Ω m. The antenna is fabricated using the copper pattern printed on a 0.4 mm thick FR-4 substrate. The resistance profile is discretized to ten surface-mount resistors. At the feed point, the antenna was supposed to be matched to the feeding transmission line with a characteristic impedance of 75 ohm. The performance of the designed RVD antenna was simulated using method of moments. The simulated result showed that the antenna had a large negative reactance and positive resistance. Note that the reactance had a considerable amount of variations with respect to frequency, and its behavior was similar to a small capacitance [37]. To investigate the performance of the non-Foster impedance matching of the RVD antenna based on the op-amp, the RVD antenna integrated with the designed NIC-based matching network was implemented and measured. The employed op-amp was THS4304, manufactured by Texas Instruments Inc. In order to transform from the unbalanced transmission line to the balanced matching network input, a 1:1 75 balun from TDK Corporation was employed for the low frequency measurement. The reflection coefficient of the impedance matched RVD antenna was seen to be slightly improved when compared to that of the unmatched RVD antenna. However, the improvement was not extremely significant and also due to the frequency limitations of the opamp the operational frequency range was restricted to about 90 MHz [37].

The work of Yizhu Shen, and Tan-Huat Chio 2014 in [39] includes design of a floating negative capacitor to match an electrically small monopole in the FM band of 88MHz to 108MHz. The NIC circuit employed Linvill's floating structure with two cross-coupled transistors. The NIC was used to match a short monopole of 8 cm, modeled with lumped

circuits. The NIC was fabricated on a two-layer FR4 substrate which facilitated the feedback loop to be located at the bottom layer. The advantage of this configuration is that, it minimizes parasitic by reducing the feedback path length, and therefore enhances the stability. The fabricated NIC circuit was then used to cancel the large input reactance of the short monopole. Measured results demonstrated that, signal-to-noise ratio (SNR) and received power gain directly benefited from the NIC matching circuit. An 8 cm electrically small monopole was fabricated first with a 10 × 10 cm^2 ground, and its self-resonant frequency was 850 MHz. Its input impedance consisted of a small positive resistance and a large negative reactance. The NIC consisted of two cross-coupled NPN bipolar junction transistors (BJT) NE68133 [39]. The two-port NIC circuit was fabricated on a two-layer FR4 substrate, with dielectric constant of 4.4 and size of 73 × 50 × 1.6 mm^3. The positive feedback loops were located at the bottom layer of substrate, and they were connected to the top microstrip lines with plated-through-via. Other parts of the bottom layer were used as ground. The two-port NIC circuit was connected with the 8 cm small monopole and tested using spectrum analyzer first. Then the input impedance was tested with vector network analyzer (VNA). Results showed that the input reactance of the conventional short monopole has been largely compensated by the designed NIC. Moreover, the non-Foster matched monopole when used as receiver in transmitting-receiving system, achieved 3 dB antenna gain increment and up to 12.5 dB SNR improvement, compared with the case of monopole itself. Here, a more compact NIC circuit was developed but the frequency range of operation was still limited to the FM band [39].

Palma et al. in 2015 summarized the difficulty in achieving a good design of an ESA matched to a 50 ohm system. We know that there exists a limit on the bandwidth of the impedance matching network [40]. In general, there are two limits for the maximum bandwidth that one could achieve through the use of passive matching network in the case of ESA. One is the minimum quality factor limit which is proportional to the maximum bandwidth of the ESA [14] and the other one is the Fano-Bode limit for the passive matching network [41,42]. In the ESA case, we need to match impedance consisting of frequency dependent very small real part (resistance) and very large negative imaginary part (reactance of a capacitor) to 50 ohm. This could be done traditionally using an external L-section of lumped elements or it could be done through the use of distributed elements like stubs. This passive matching network will make the antenna look larger for the transmitter (source). The bandwidth of matching a capacitive load to a resistive load is limited by the Fano-Bode limit [41,42] . The bandwidth of such matching is very small. Also, the assumption that we always make saying that we use lossless matching network is not applicable [40]. The L-section that is added to match an ESA to a 50 ohm system is not lossless so in general one should compensate for these losses when he/she designs the matching network as these losses will affect the matching process. Furthermore, the included losses actually dominate the radiation

resistance and suck most of the input power and turn it into lost heat instead of radiation. In other words, if one uses an L-section to match an ESA to 50 ohm then one should compensate for the losses of the inductor/capacitor used in the matching network because in practice any inductor/capacitor has resistance depending on the Q-factor of it. Based on the previous discussion, we cannot achieve a low quality factor or equivalently wide VSWR matched bandwidth for an ESA if we start with a simple z-directed dipole/monopole antenna. One solution is to make the passive matching network automatically adjustable based on the desired frequency. This means that the bandwidth of the antenna will move along the desired frequencies but every time the center frequency is changed the bandwidth around it will remain the same [40]. Another solution is the use of the non-Foster elements in the matching network. Non-Foster elements are active; an example of such elements is like –L or –C. The use of this kind of elements in the matching network will provide a larger matching bandwidth as it will not be limited by the Fano-Bode limit. The realization of the non-Foster elements could be done using active elements. Another solution is to alter the structure of the ESA to increase the radiation resistance and achieve a self matched antenna to 50 Ω with low quality factor design. Basically, the task is to come up with a design for an ESA such that it is self resonant at the frequency of interest, self-matched to 50 Ω and has low quality factor. In general, there is a fundamental limit (Chu limit) for the lowest quality factor that we can achieve for an ESA. To design an ESA which is self resonant, self-matched to 50 Ω and with quality factor close to the minimum quality factor (Chu limit), one should maximize the effective volume filled by the ESA structure compared to the volume of the imaginary sphere enclosing the maximum dimension of the ESA antenna (this will assure low quality factor because this will minimize the non-propagating stored energy) and at the same time make the input impedance of the ESA to be simply 50 Ω at the frequency of interest [40].

Ivanov et al. in 2016 proposed a negative capacitor and a negative inductor to increase the matching bandwidth of a printed monopole and a printed loop respectively [43]. However, the proposed network used a lumped element transformer to convert the real part of the antenna impedance to 50 ohm, which complicates the network and increases the overall size. The negative capacitance and inductance realized as active circuits using bipolar junction transistor were used to partly compensate the input reactance of the ESAs. The monopole and loop printed antennas under consideration were implemented on 1.016 mm thick Arlon AD 255 ($\varepsilon_r = 2.55$, $\tan(\delta) = 0.0015$) dielectric substrate with 18 um thick copper metallization. According to results of 3D electromagnetic simulations, the first resonant frequency of the monopole was 1100 MHz [43]. The frequency of the series resonance of the loop antenna was 1600 MHz. At the frequency of 200 MHz the length of the monopole did not exceed $\lambda_g/10$ and the perimeter of the loop antenna was about $\lambda_g/8$ where λ_g is the guided wavelength. Hence, both the antennas were considered to be electrically-small at the frequency of interest. In the frequency range 50-400 MHz, the input impedance of the

monopole was presented by an equivalent circuit consisting of resistor R = 1.6 Ohm and capacitance C = 1.5 pF connected in series. In turn, the loop antenna behavior below 300 MHz was modeled by a series connection of resistor R = 1.5 Ohm and inductance L = 115nH [43]. A transformer was needed to convert the antenna input resistance to 50 Ohm. Since the input resistance of ESAs is small enough, a multi-stage transformer was required to provide a sufficient matching bandwidth. Baluns were used to feed properly loop antennas. A simple single-stage lumped element balun was used in the non-Foster matching network for the electrically-small loop antenna. The matching network consisting of the ideal negative inductance of –110nH and the balun obtained a matching bandwidth of 9%. Meanwhile, the conventional matching network using a positive capacitance instead of the negative inductance resulted in a matching bandwidth of about 1%. BFQ 67 bipolar junction transistors by NXP Semiconductors were employed. The resistors were used to set up operation regime of the transistors. The blocking capacitors were used to prevent undesired DC flowing. Within the frequency band of 150-250 MHz the simulated and measured characteristics agreed well to each other and were close to the theoretical performance of the ideal negative inductance [43].

Abbosh et al. in 2017 proposed an active matching network to match an electrically small loop to cover the MICS (Medical Implantable Communication Services) band and extend its bandwidth for being used as an exterior portable reader in biomedical telemetry [44]. However, the radiation resistance was improved to 50 ohm by the application of a lumped element balun. The negative inductance was realized by a transistor-based active circuit and lumped elements balun to properly feed a differential input loop antenna and improve radiation resistance and the bandwidth. Based on the non-Foster impedance matching of the exterior loop antenna, the operating bandwidth increased to 15.7 MHz from 1.6 MHz. The exterior loop antenna at MICS band resonated at one wavelength, for a circular loop printed on 3.2 mm thickness FR4 substrate with (ε_r = 4.3, tan δ = 0.025), and the perimeter of the loop was around λ_g = 360 mm. Since, the exterior reader is expected to have a small size to be integrated into a portable reader, reducing the size of the exterior reader at MICS required a matching network because the size of the loop is small compared to the wavelength [44]. Specifically, the matching network compensated for the intrinsic high reactive part of the input impedance and the low radiation resistance. The transistor-based NIC was accomplished through MRF 949 bipolar junction transistor (BJT). The non-Foster negative inductance of −16nH was realized to compensate the reactance of the input impedance of the loop at MICS band. In addition, the radiation resistance was improved to 50 Ω with the aid of a lumped elements balun to properly feed the differential input of the loop antenna. The lumped elements balun consisted of an LC tank connected to each arm of the loop antenna. The single stage LC tank balun had C = 143 pF and L = 1.1 nH and the NIC

allowed to widen the operating bandwidth compared to a conventional lumped elements matching network using positive capacitors and surface-mount balun (ATB2012-5001) [44].

Buyantuev1 et al. in 2018 studied the frequency characteristics of NICs based on transistors of different kind [45]. Also, various applications of NICs other than broadband matching of antennas were studied. Either bipolar-junction transistors (BJTs) or field-effect transistors (FETs) can be employed to design NICs. The operational frequency band of a NIC is limited by the critical frequency of transistors used. In order to design a negative inductance with a tolerable variation, the transistor critical frequency must be at least four times higher than the upper edge of the desired operational frequency band as it was shown in [46] by results of simulation. In practice, the transistor critical frequency should be even higher due to variation of transistors' parameters etc. From this point of view, the use of NPN-type BJTs is preferable as they have higher critical frequency than the PNP-type ones. Since FETs have higher mobility of charge carriers and consequently higher critical frequency than BJTs, they seem more promising to design NICs for high-frequency applications. FETs are voltage-controlled current sources whereas BJTs are current-controlled current sources. That is why some FET based NICs can transform the input current into a voltage, i.e. transform inductance into capacitance (or vice-versa) besides negation of the load impedance. A typical example of such a FET-based NIC is Kolev-Meunier's circuit [47]. NICs can be also implemented on operational amplifiers [48,49,50,51]. Op-amp-based NICs are simpler than the transistor ones. However, operational frequencies of the op-amps are much lower compared to those of transistors and do not exceed a few GHz. As a result, operational frequencies of NICs based on op-amps are limited to hundreds of MHz. Parasitic effects which take place in real NIC circuits, and transistor packages can influence dramatically the NIC characteristics and should be taken into account [52]. In order to reduce the parasitic effects and increase the transistor critical frequency at the same time, NICs have been recently designed using CMOS integrated circuits technology [53,54,55]. Although this approach has demonstrated promising results, high cost of design and manufacturing limits applications of the non-Foster elements in CMOS implementation. NICs suffer from potential instability due to the positive feedback. Hence, stability analysis is an important issue of non-Foster circuit design. Antenna applications of non-Foster elements are not limited to the broadband matching networks. Transmission lines periodically loaded with non-Foster elements have been used to design the squint-free leaky-wave antennas [56,57]. Another interesting application of non-Foster negative inductance and capacitance is to deal with engineering low-loss broadband metamaterials as shown in [54,58]. Non-Foster elements can be also employed to design broadband microwave devices, e.g. a broadband 180° phase shifter [59]. The use of NIC with a variable capacitor i.e. a varactor diode allows designing a variable negative inductor. A combination of the negative variable inductor and a conventional static inductor can operate as an electrically controlled positive variable

inductor [60]. Such controlling components are of crucial importance to design advanced tunable filters with enhanced tunability.

2.5 Review of various works on noise performance and stability analysis of NIC matched ESAs

Martin et al. in 2011 presented a critical procedure to analyze the stability of NICs. The analysis of the stability of any microwave system requires both the study of a corresponding transfer function and the modeling of the inside active elements [61]. Linear and nonlinear techniques have been proposed as methods to study the stability of NICs. Because of its speed and simplicity, linear modeling of active circuits is preferred. Non-linear modeling requires both a heavier computational cost and accurate non-linear models of the active devices that are not always available. Classical linear methods for NIC analysis can be classified in two groups: those related with the impedance or admittance function at the NIC output and those related to the analysis of the two port open-loop gain in a network. However, at microwave frequencies, it is difficult to obtain the voltage or current transfer functions to later apply the Nyquist criteria. For those reasons, stability methods based on the S parameters have been used. However, although the simplicity of these methods is clear, there is a lack of capability to linearly predict the NIC stability [61]. The normalized determinant function (NDF) was proposed to study the conditions for amplifier stability. The results obtained from that study provided a complete set of conditions to find out at which frequencies and under which load conditions stability problems could arise. For providing accurate methods to analyze the stability and performance of NICs circuits, linear modeling is allowed by the normalized determinant function (NDF). The paper presents how and why classical methods fail on determining the stability of the corresponding NIC identifying the frequencies at which these problems rise. Classic methods to study NIC stability are mainly based on analyzing some network function and seeing its root-loci in order to apply the Nyquist theorem. The first methods are called reference plane methods [61]. They use the impedance Z, admittance Y or reflection coefficient Γ seen in a plane towards the right side (the loaded NIC) and the Z, Y or Γ towards the left side (external Z, Y or Γ). In the approach given in [62], it is studied how the performance in one port should be when the NIC port is loaded with a short circuit or with an open circuit. It has been stated that the necessary conditions for a device to be passive (stable) are that the input impedance or admittance, seen at either port, when the other port is open-circuited or short circuited, should be positive. This implies that there are no poles in the right-hand complex plane. However, there is a problem with this approach since only short circuit or open circuit impedances are defined and not other ones such as ideal inductances or capacitances. This is an important drawback since most loads to be inverted are precisely inductances or capacitances. In addition to the previous concerns it must be also highlighted that the loaded NIC cannot be considered by

itself but in the presence of the external load. In order to have a stable circuit, the impedance function Z cannot have any poles in the right-hand complex plane. The resulting conditions are given in [61]. The equations in[61] states that in order not to have any pole the magnitude of the external impedance has to be lower than the magnitude of input impedance of the NIC under SCS conditions. This also implies that the analysis on the stability performance has to take into account the external loading. In this way, successive considerations can be extracted by changing the ports and the NIC loading. These conditions are summarized in [61]. The condition for a NIC to be stable is that the overall function, Z or Y, does not have any real pole or any pair of conjugate complex poles in the right-hand complex plane.

Stedler et al. in 2014 made a noise analysis of the NIC-element and performed a system comparison between a NIC-matching network and a conventional active system with short monopole antenna for automotive application [63]. It was shown that with equal gain of both systems the NIC-system provided a significant higher output noise voltage resulting from its unfavorable noise impedance and provided a severe degradation of the SNR at the output. This showed that for the efficient design of small active antennas with non-Foster matching networks realized with NICs a careful noise investigation is always to be performed. As the NIC-circuit is an active circuit, consisting of at least two transistors, noise considerations have to be made in the same way as they have to be performed with any other active antenna system. The result has to be compared to the conventional passive system and represents then the effective SNR advantage or disadvantage of the whole antenna system. The noise voltage at the output port of each matching network was calculated. With active antennas for automotive applications the output noise should not exceed -5 dbμV on a 50 Ohm load impedance referred to a bandwidth of 120 kHz [63]. Now a severe difference between the ideal non-Foster element and the network with the active NIC matching network was seen. An ideal non-Foster element and an ideal LC-network provided noise voltages below this level due to mismatch losses. Surprisingly, the output noise voltage of the NIC matching network was far above the ideal noise level. This meant that the NIC matching network significantly provided electronic noise from the inner circuit to the load impedance. To prove these behavior further noise calculations were made and the noise parameters of the NIC circuit were determined. It was seen that the impedance curve totally lied beside the 10 dB noise circle. Thus a noise figure of higher than 10 dB would result from the NIC matching circuit. Main problem for this high noise seemed to be the high value of the real part of the optimum noise impedance of the NIC. The variation of the real part of the source impedance versus noise figure was calculated. The NIC circuit has to be connected close to the antenna port for optimum matching performance and would require high resistive values of the antenna impedance for optimum noise performance [63].

Qi Tang and Hao Xin in 2015 studied the stability of two types of NICs, based on tunneling diode and cross-coupled pair MOSFET [64]. The influence of device capacitances, load impedance, and bias network were discussed. The main purpose of this work was to find an effective method to accurately predict the stability and analyze the influence of parasitics. Two different types of NICs were investigated, including a negative-resistor (tunnel diode) based NIC and a XCP based NIC. A case study of using NIC for broadband matching of a small monopole antenna was conducted. Stability of NIC circuits in the linear regime was analyzed using Normalized Determinant Factor (NDF) method. A parametric study was then conducted to find out the stable design region of the circuit [64]. The effects of device parameters such as various capacitances and other parasitics on the performance of the circuit were also evaluated. NDF method is equivalent to the return ratio method which usually simplifies the complexity of high-order systems and can also be easily implemented with standard commercial simulation tools. The method first calculates the node admittance matrix, Y, of the circuit network by nodal analysis, or equivalently calculates the loop-impedance matrix, Z, by mesh analysis [65]. The zeros of determinant of matrix are referred as the natural frequencies. A network is stable if and only if all of the zeros of NDF are restricted to the left half of the complex frequency s-plane (LHP). To find out the positions of zeros, one can either directly solve the roots for low-order system, or use Nyquist plot for high-order system. Stabilities of two types of NIC configurations were investigated in this paper. For the negative resistor based NIC to match a RLC system, the junction capacitance had a large impact on the stability and matching performance. Furthermore, if the load is a small antenna, an accurate model of the antenna impedance is necessary to achieve meaningful results. For a XCP transistor NIC, the stability is highly dependent on the bias impedance at the sources of transistors [64].

Chapter 3

Theory on Electrically Small Antennas and NIC

3.1 Chapter overview

This chapter contains a theoretical overview of electrically small antennas and negative impedance converters supported by mathematical modeling. In chapter 1 a detailed discussion on small antennas was presented. It included definition of small antennas, characterization and types of small antennas. In this chapter the primary focus is given to electrically small antennas due to its growing demand. Section 3.2 presents the general representation of electrically small antennas along with mathematical expressions and shows how an antenna can be considered to be electrically small. Section 3.3 presents the design challenges of electrically small antennas. Section 3.4 and 3.5 presents a detailed overview of Foster and Non- Foster elements along with their special characteristics. Section 3.6 provides a comparison between Foster and Non-foster elements and section 3.7 presents the advantage of using non foster elements for the current work. From section 3.8 onwards the main emphasis is given to negative impedance converters. Section 3.9 presents a detailed overview of Linvill's NIC. Section 3.10 and 3.11 presents different types of NICs which include grounded and floating type, voltage inversion and current inversion along with their two port representation and corresponding matrices. Section 3.12 shows pictorially how a voltage inversion NIC actually works. Section 3.13 throws light on how NICs can be used with electrically small antenna to overcome its limitations and to reduce the antenna dimension. Section 3.14 provides a detailed study on stability analysis and noise performance of negative impedance converters.

3.2 Electrically Small Antennas (ESAs)

There is an increasing demand for compact and broadband communication systems and the focus is on electrically small broadband antennas. There are many applications which require small broadband antennas, from mobile phones and devices to cognitive radios. At present, the electronic devices continues to diminish in size and the researchers in many fields such as RF and Microwave, biomedical technology and national intelligence can benefit from electrically small antennas.

Wheeler, in 1947, defined a small antenna as one whose maximum dimension is smaller than the radian length, where the radian length is defined as the operating wavelength divided by 2π [6]. Mathematically, it can be related as

$$\frac{2\pi h}{\lambda} \ll 1 \qquad 3.1$$

Here ‘h’ is the maximum dimension of the antenna and ‘λ’ is the operating wavelength. Chu generalized the conditions and provided a mathematical limit on the design of electrically small antennas which is given by the following expression [3]

$$ka < 1 \qquad 3.2$$

Here, ‘k’ is the wave number and is given by $\frac{\lambda}{2\pi}$ and ‘a’ is the radius of a sphere that completely circumscribes the antenna as shown in Fig.3.1.

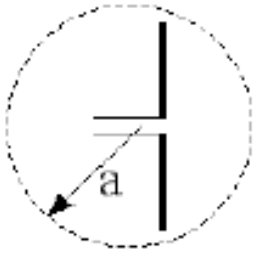

Fig.3.1: Antenna dimensioning using Chu’s Limit [3]

The relationship between antenna size and the realizable bandwidth is defined by the Chu limit. The Chu limit gives the relationship between the radius of the circle that completely circumscribes an antenna and the Q (quality factor) of the antenna. Collin and Rothschild improved previously given theory for obtaining *Q* based on the field rather than the equivalent circuit [17]. They calculated *Q* for cases where both TE and TM modes are used for excitation, and derived it for the lowest mode as

$$Q = \frac{1}{ka} + \frac{1}{(ka)^3} \qquad 3.3$$

Hansen simplified Chu’s expression for calculating Q [18]. He stated that when ka is roughly less than unity and only the lowest TM mode propagates, Q is expressed by

$$Q = \frac{1 + 3(ka^3)}{ka^3(1 + ka^2)} \qquad 3.4$$

However, McLean redefined how the Q of an antenna should be calculated; this is given by equation [14]

$$Q = \frac{1 + 2(ka^3)}{ka^3(1 + ka^2)} \qquad 3.5$$

McLean’s derived his equation from the original Chu Limit. He concluded that when ka is very small, there is not much difference between the previous derivations and his own derivation, and equation (4.7) is an exact expression of the lower bound on Q for a given antenna size. There has also been a lot of research to improve the gain (G) of an antenna

through the use of matching networks but this is also bounded by the Harrington limits on antenna as given by equation [16]

$$G = (ka)^2 + 2ka \qquad 3.6$$

The Chu limit can be related to the antenna bandwidth by rewriting the Q of the antenna as shown in equation [16]

$$Q = \frac{f_c}{\Delta f} = \frac{1}{ka} + \frac{1}{(ka)^3} \qquad 3.7$$

Here f_c is the antenna centre frequency at resonance and Δf is the bandwidth of the antenna.

3.3 Difficulties and design challenges of Electrically Small Antennas (ESAs)

The above equations, under careful examination, give rise to some definite conclusions. If we reduce the radius of the sphere (which translates to a physical reduction in the size of the antenna), the quality factor increases and the gain decreases. Also, as the quality factor of the antenna increases the bandwidth decreases. The quality factor is defined as the ratio of energy stored to energy dissipated. So for an antenna high quality factor means energy stored is more compared to energy radiated and this condition is not desired.

Again experiments showed that for an electrically small antenna most of the input power is stored in the reactive near-field region and little power is radiated in the far-field region. In other words, the input impedance of an electrically small antenna is considerably reactive. Thus, ESAs are characterized by rather low input resistance in combination with high input reactance that significantly complicates matching of the antennas in a wide frequency band.

The return loss at the antenna input terminals is given by equation [36]

$$S_{11}(\mathrm{dB}) = 10\log_{10}\frac{[[Z_0 - R(\omega)]^2 + X^2(\omega)]}{[[Z_0 + R(\omega)]^2 + X^2(\omega)]} \qquad 3.8$$

Where the antenna input impedance Z_{in} is given by equation [36]

$$Z_{in} = R(\omega) + jX(\omega) \qquad 3.9$$

Here $R(\omega)$ is the real part or resistive part and $X(\omega)$ is the imaginary or reactive part of the antenna input impedance. The characteristic impedance of the input line is Z_0. For large values of $X(\omega)$, the scattering parameter S_{11} approaches one and the reflected power at the antenna input increases considerably. Therefore it is crucial to reduce reactance of the antenna and decrease the radiation quality factor in the desire frequency range. Consequently,

various methods should be devised to decrease the reactive part of the antenna input impedance.

3.4 Foster's Reactance Theorem

Foster's reactance theorem is an important theorem in the fields of electrical network analysis and synthesis. The theorem states that the reactance of a passive, lossless two-terminal (one-port) network always strictly monotonically increases with frequency [66]. It is easily seen that the reactance of inductors and capacitors individually increase with frequency.

The reactance of an inductor is given as

$$X_L(\omega) = \omega L \qquad 3.10$$

The reactance of a capacitor is given as

$$X_C(\omega) = -\frac{1}{\omega C} \qquad 3.11$$

The derivative of the reactance is given as

$$\frac{dX_L(\omega)}{d\omega} = L > 0 \qquad 3.12$$

$$\frac{dX_C(\omega)}{d\omega} = \frac{1}{\omega^2 C} > 0 \qquad 3.13$$

Thus the slope of the reactance curve is positive as expected from Foster's theorem.

Now reflection coefficient is given as

$$\Gamma = \frac{1 - jX_F}{1 + jX_F} \qquad 3.14$$

Here 'X_F' denotes the generalized Foster reactance.

Now, the phase of the reflection coefficient is given as

$$\angle\Gamma = -2\tan^{-1} X_F \qquad 3.15$$

Its derivative with frequency is given as

$$\frac{d\angle\Gamma}{d\omega} = -2\,\frac{1}{1 + {X_F}^2}\,\frac{dX_F(\omega)}{d\omega} \qquad 3.16$$

Now since

$$\frac{dX_F(\omega)}{d\omega} > 0 \qquad 3.17$$

It is thus derived that

$$\frac{d\angle\Gamma}{d\omega} < 0 \qquad 3.18$$

It indicates that the loci on the Smith chart move clockwise with increasing frequency as shown in Fig. 3.3.

3.5 Non-Foster elements

An element that violates Foster's reactance theorem by having a reactance which has a negative slope with frequency is therefore called a 'non-Foster' [67] element. It is possible to construct non-Foster networks using active components such as amplifiers. These can generate an impedance equivalent to a negative inductance or capacitance. The negative impedance converter is an example of such a circuit. A Foster network must be passive, so an active network, containing a power source, may not obey Foster's theorem. These are called non-Foster networks. In particular, circuits containing an amplifier with positive feedback can have reactance which declines with frequency.

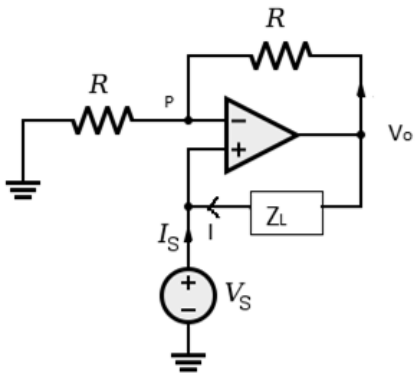

Fig.3.2: Op-amp based NIC showing the generation of non-foster impedance [68]

At first, we have

$$V_+ = V_- = V_S \qquad 3.19$$

If we write KCL at P, we get

$$\frac{V_S}{R} = \frac{V_S - V_0}{R} = 0 \qquad 3.20$$

From here we get

$$V_0 = 2V_S \qquad 3.21$$

Now,

$$I = \frac{V_0 - V_S}{Z_L} = -I_S \qquad 3.22$$

Thus we get

$$\frac{V_S}{I_S} = -Z_L \qquad 3.23$$

From this it can be understood that the input current is the reverse of the current through Z_L, leading to the negative of Z_L, a Non-Foster impedance.

Therefore for the Non – Foster elements

The reactance of an inductor is given as

$$X_L(\omega) = -\omega L \qquad 3.24$$

The reactance of a capacitor is given as

$$X_C(\omega) = \frac{1}{\omega C} \qquad 3.25$$

The derivative of the reactance is given as

$$\frac{dX_L(\omega)}{d\omega} = -L < 0 \qquad 3.26$$

$$\frac{dX_C(\omega)}{d\omega} = -\frac{1}{\omega^2 C} < 0 \qquad 3.27$$

Thus the slope of the reactance curve is negative which violates Foster's theorem.

Now reflection coefficient is given as

$$\Gamma = \frac{1 - jX_{NF}}{1 + jX_{NF}} \qquad 3.28$$

Here "X_{NF}" denotes the generalized Non-Foster reactance.

Now, the phase of the reflection coefficient is given as

$$\angle\Gamma = -2\tan^{-1} X_{NF} \qquad 3.29$$

Its derivative with frequency is given as

$$\frac{d\angle\Gamma}{d\omega} = -2\ \frac{1}{1+\ X_{NF}{}^{2}}\ \frac{dX_{NF}(\omega)}{d\omega} \qquad 3.30$$

Now since

$$\frac{dX_{NF}(\omega)}{d\omega} < 0 \qquad 3.31$$

It is thus derived that

$$\frac{d\angle\Gamma}{d\omega} > 0 \qquad 3.32$$

It indicates that the loci on the Smith chart moves counter- clockwise with increasing frequency as shown in Fig.3.3.

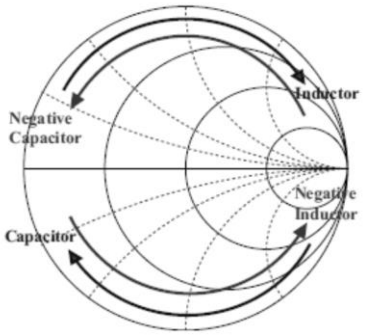

Fig.3.3: Foster and non-Foster elements on a Smith Chart [69]

3.6 Foster vs. Non-Foster

Till now the highlight of the discussion has been the fact that electrically small antennas have very low real part and comparatively high imaginary part of the input impedance. Hence, there is a need to reduce the reactive part of the antenna input impedance. Implementation of foster elements is an alternative. However, complete cancellation of the reactive part of an antenna is only possible over very narrow bandwidth when using passive (Foster) elements. Non-Foster elements provide an attractive alternative because these negative elements are able to cancel out the reactance of the antenna continuously over a wide bandwidth. Fig.3.4 shows how an ideal negative capacitor can cancel a positive capacitance C over all frequencies, as compared to the usual method of resonating C at a single frequency with a positive inductor L [25]. Nevertheless, compensating for both real and imaginary impedance parts of an antenna is difficult. If the antenna resistance follows a simple pattern (like that of a monopole before its first resonance) then known negative topologies can be used. But while it is straightforward to cancel the antenna reactance, it can

get hard to concurrently match the antenna resistance. Impedance transformers can be used but these might be narrowband and add to the antenna size. Alternatively, negative networks can be used within the antenna structure to control both real and imaginary parts of antenna impedance.

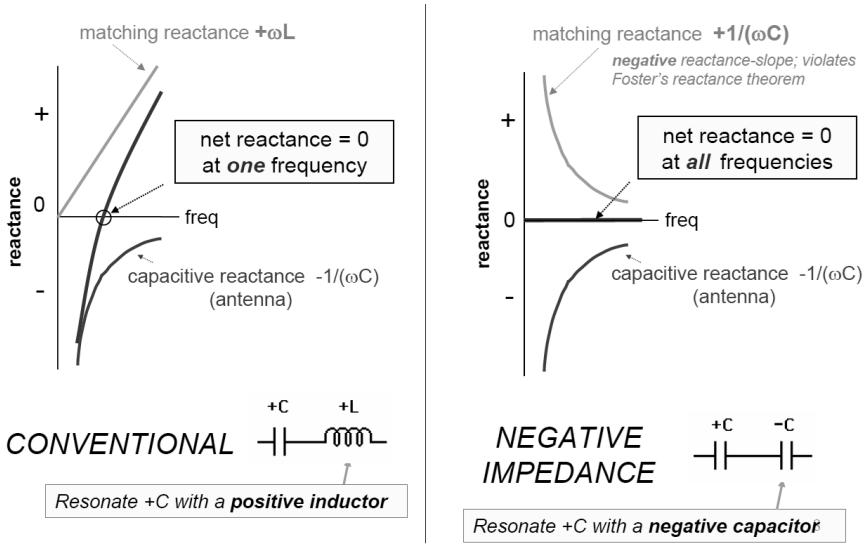

Fig.3.4 Conventional and Non-Foster elements [25]

3.7 Advantages of Non-Foster elements

Non-Foster reactance with a negative frequency slope can be used to completely cancel equivalent Foster reactance with a positive frequency slope. Therefore non- Foster reactance can be used to achieve high bandwidths in impedance matching applications. The counter-clockwise direction of non-Foster elements on the Smith Chart can also be characterized as a 'negative delay'. The reflection phase from non-Foster elements has a positive slope with frequency, which can be used to cancel conventional phase delays with negative slopes, resulting in reduced phase dispersion. In fact, it will be shown later that non-Foster circuits can not only cancel reactance, but can also transform resistance to any required value with specifically designed non-Foster matching networks. This technique of impedance matching with non-Foster elements is especially useful for small antennas, which have a large reactance arising from their intrinsically high Q, leading to a much lower bound on the maximum bandwidth that can be achieved with passive matching.

3.8 NIC background

The circuit by which non foster elements are physically realized is known as a Negative Impedance Converter (NIC). An ideal NIC [9] can be viewed as an active two port network which inverts whatever impedance is connected to its other port.

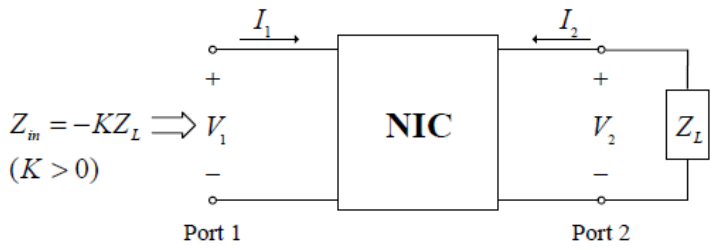

Fig.3.5 An idealized NIC [25]

An ideal two port NIC is shown in Fig.3.5. Z_{in} is the input impedance seen from port 1 and Z_L is the load impedance. The corresponding voltage and current of the two ports are indicated in the Fig.3.5. K is the impedance converter coefficient. Ideally, K is a positive real constant. However, practically, K is not a constant and not always real.

NICs can be realized by the combination of active devices (amplifiers) and lumped elements (resistors, capacitors, inductors). Operational amplifier based negative impedance converters are a good choice to obtain low Q negative resistance due to the significant reactive component of the input impedance. However, the high frequency limitation of non ideal op-amp restricts its use over a broad range of frequency. Transistor based NICs show good performance up to higher frequency range. Transistor based NICs were introduced by Linvill in 1953. Different transistor circuits of grounded as well as floating NICs are known. Either bipolar junction transistors (BJTs) or field effect transistors (FETs) can be employed to design NICs. The critical frequency of transistors limits the operational range of NICs. However, NPN type BJTs is preferred over PNP types because they have comparatively higher critical frequencies. FETs have higher mobility of charge carriers and consequently higher critical frequency than BJTs and they are more promising to design NICs for high frequency applications.

3.9 Linvill's NIC

The Linvill NIC consisted of two transistors connected as shown in Fig.3.6. A feedback connection between the two transistors had been formed. The base of transistor 1 is connected to the collector of transistor 2 and the base of transistor 2 is connected to the collector of transistor 1. The impedance to invert (Z_{load}) is connected between the two collector terminals which in this case are the two 510Ω resistors. When Fig.3.6 is considered, then the voltage from the emitter of transistor 1 is presented at point B via the feedback connection between the two transistors. The same rule applies to the voltage at the emitter of transistor 2 which is presented at point A. Computing the impedance seen across the two

emitter terminals, Z, would give a negative fraction of the impedance connected between the two feedback paths, Z_{load} [19].

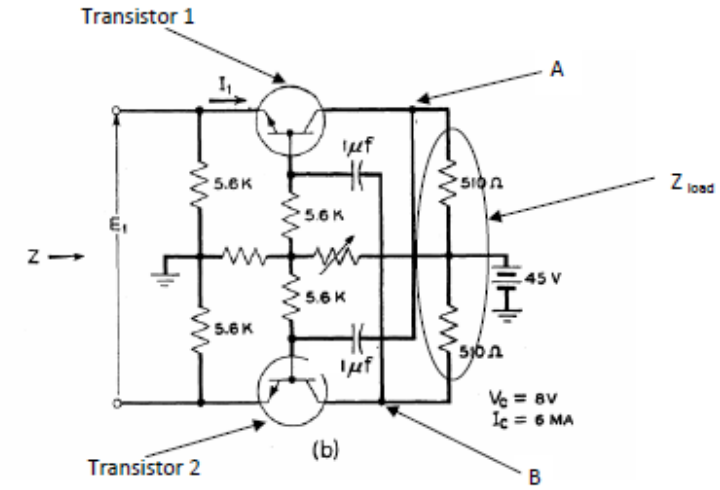

$$Z = -\gamma Z_{load}$$

Fig.3.6: Linvill NIC [19]

3.10 Grounded and Floating point NIC

Negative Impedance converter topology can be of two types depending on the type of application. NICs can be grounded type or floating point type. In grounded type NIC, the impedance to be inverted is connected to ground. It basically functions as a one port network, required in applications which use it as a load, connected with the output port of another component. In floating type NIC, the impedance to be inverted is connected between the collector terminals of the two transistors. Floating type NIC is required in applications which use it as an intermediate or connecting stage between two components.

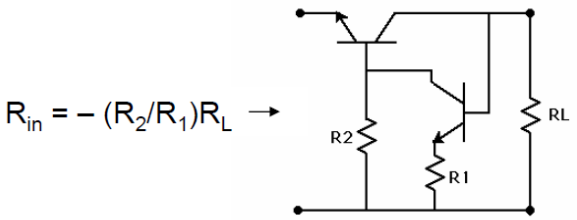

Fig. 3.7: Grounded negative resistance [25]

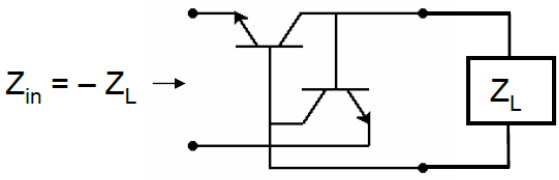

Fig. 3.8: Floating negative impedance [25]

3.11 Voltage inversion and current inversion NIC

An ideal NIC can be expressed in terms of conventional two-port parameters. Herein, the hybrid h-parameters are used to represent ideal NICs [21,70,71]. Fig. 3.9 shows the equivalent model for a general two port h parameter network with an arbitrary passive load Z_L at port 2.

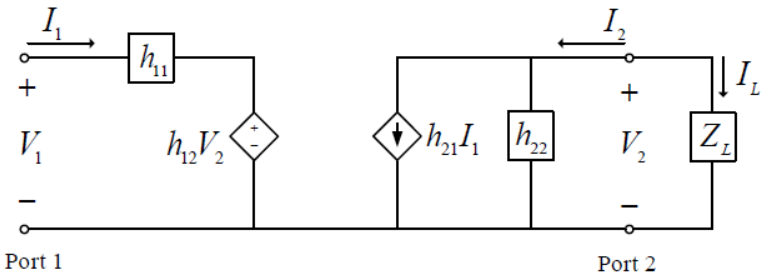

Fig. 3.9: Equivalent two port model [72]

The defining equations for a two port h-parameter model are as follows:

$$V_1 = h_{11}I_1 + h_{12}V_2 \qquad 3.33$$

$$I_2 = h_{21}I_1 + h_{22}V_2 \qquad 3.34$$

Where,

$$h_{11} = \left.\frac{V_1}{I_1}\right|_{V_2=0} \qquad 3.35$$

$$h_{12} = \left.\frac{V_1}{V_2}\right|_{I_1=0} \qquad 3.36$$

$$h_{21} = \left.\frac{I_2}{I_1}\right|_{V_2=0} \qquad 3.37$$

$$h_{22} = \left.\frac{I_2}{V_2}\right|_{I_1=0} \qquad 3.38$$

Given an arbitrary load Z_L, the input impedance at the driving port [21] is Z_{in}.

$$Z_{in} = h_{11} - \frac{h_{12}h_{21}Z_L}{h_{22}Z_L + 1} \qquad 3.39$$

The necessary and sufficient conditions to realize a NIC with the ideal property [73] ($Z_{in} = -KZ_L$) can be obtained from the above equation. For an ideal NIC with impedance converter coefficient K, it should be $h_{11} = 0$, $h_{22} = 0$, and $h_{12}h_{21} = K$. Since the impedance converter coefficient, $h_{12}h_{21} = K$, should be positive to convert a positive impedance into a negative one, both h_{12} and h_{21} can be either positive or negative. Depending on the sign of both h_{12} and h_{21}, the properties of a NIC are different [21]. In the following two subsections, two different types of ideal NICs will be investigated. For simplicity, it is assumed the impedance converter coefficient is unity.

Current Inversion NICs

For current inversion NIC both h_{12} and h_{21} are positive and unity.

Thus $V_1 = V_2$ and $I_1 = I_2$ 3.40

Now, since $I_2 = -I_L$, we have $I_1 = -I_L$ 3.41

Hence, the impedance at port 1 is

$$\frac{V_1}{I_1} = \frac{I_L Z_L}{-I_L} = -Z_L \qquad 3.42$$

From the above voltage and current equation it is observed that the voltage at port 1 is same as the voltage across the load while the direction of current are opposed. Thus, this type of NIC is called a current inversion NIC [33].

For an ideal current inversion NIC, the h parameter matrix is

$$h = \begin{bmatrix} 0 & 1 \\ 1 & 0 \end{bmatrix} \qquad 3.43$$

The ABCD matrix is given by [33]

$$ABCD = \begin{bmatrix} 1 & 0 \\ 0 & -K \end{bmatrix} \qquad 3.44$$

Voltage Inversion NICs

Considering an ideal NIC where both h_{12} and h_{21} are equal to negative unity.

Thus $V_1 = -V_2$ and $I_1 = -I_2$ 3.45

Now, since $I_2 = -I_L$, we have $I_1 = I_L$ 3.46

Voltage at port 1 is $V_1 = -I_L Z_L$ 3.47

Hence, the impedance at port 1 is

$$\frac{V_1}{I_1} = \frac{-I_L Z_L}{I_L} = -Z_L \qquad 3.48$$

From the above voltage and current equation it is observed that the current at the input terminal is same as the current through the load while the voltage across the input port is inverted with respect to that at the load port. Thus, this type of NIC is called a voltage inversion NIC [33].

For an ideal voltage inversion NIC, the h parameter matrix is

$$h = \begin{bmatrix} 0 & -1 \\ -1 & 0 \end{bmatrix} \qquad 3.49$$

The ABCD matrix is given by [33]

$$ABCD = \begin{bmatrix} -K & 0 \\ 0 & 1 \end{bmatrix} \qquad 3.50$$

3.12 How a voltage inversion NIC works

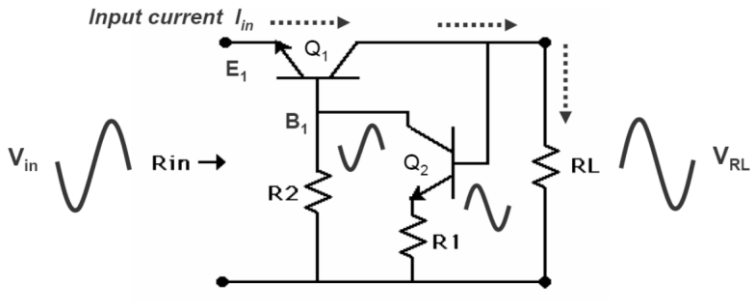

Fig.3.10: Voltage inversion in NIC [25]

Input current flows through Q_1 producing V_{RL} across R_L

• V_{RL} fed back through CE stage Q_2 producing 180° phase inversion at B_1.

• Voltage at E_1, V_{in} appears in phase with voltage at B_1.

• $R_{in} = V_{in} / I_{in}$ seen to be negative of R_L: because current is same, but voltages are inverted.

3.13 How NIC helps in size reduction of antennas

In chapter 1 various ways of reducing the antenna dimension were discussed. Generally size reduction of a resonant antenna signifies one of two things. Either the resonant frequency is lowered keeping the antenna dimension same or reducing the antenna dimension keeping the resonant frequency same. Here the first method is considered. For a resonant antenna, at the frequency of operation the real part of the input impedance is nearly 50 ohm and the imaginary part of the input impedance is close to zero. However, in the remaining region the real and imaginary part of the input impedance varies significantly with frequency. Now, in the frequency range where the antenna is electrically small, the real part of input impedance is found to be very low and the imaginary part of the input impedance is comparatively high. This property makes electrically small antennas difficult to match. The negative impedance converter circuit provides an input reactance which has a negative slope with respect to frequency. This negative reactance is used to cancel the antenna reactance over a broad range of frequency. Now, at a particular frequency the overall input reactance has a zero crossing point. Also, the input impedance of the NIC has some real part which compensates for the otherwise low real part of the antenna impedance. Thus at a particular frequency (lower than the original operating frequency of the antenna) the overall real part of the input impedance becomes close to 50 ohm and the imaginary part of the overall input impedance become close to zero. Thus the antenna becomes matched to the source at a frequency which is somewhat lower than the original operating frequency of the antenna. Thus the resonant frequency of the antenna is lowered keeping the dimension of the antenna fixed. Now if we want to design the antenna at the new resonant frequency the dimension will automatically be large considering the fact that antenna dimension is dependent on frequency. Hence, by using the NIC circuit with the antenna a degree of miniaturization can be achieved.

3.14 Stability analysis of NIC

A stability of NIC can be predicted by the location of poles in the complex s plane of the NIC transfer function. The ratio of the Laplace transforms of the response of a circuit, Y(s), and the input, X(s), is called the transfer function and this is expressed as follows:

$$H(s) = \frac{Y(s)}{X(s)} \qquad 3.51$$

The roots of the numerator of the transfer function are called the zeros of the transfer function and the roots of the denominator are called the poles of the transfer function. The location of the zeros and poles of the transfer function on the complex s- plane determine the stability of a system according to Nyquist. The stability analysis of NIC is done by splitting it into even and odd modes.

Even mode

Fig. 3.11 shows the development of the circuit model. Fig.3.11a shows the Linvill's NIC circuit model without the complete bias network with the required DC blocking capacitors C_{B1} and C_{B2} and the capacitor, C, being inverted. Fig.3.11b shows the circuit with capacitors split into two. In the even mode, the currents that flow out of the transistors into the capacitor C are equal but opposite directions. Hence an open circuit occurs in the middle of this capacitor. This implies that the element to invert, C, does not play a part in this analysis. However, in the feedback paths, the currents out of the transistors are equal and flow in the same (clockwise) direction around the feedback path. Splitting the circuit along its line of symmetry, gives Fig.3.11c. The capacitor to invert has an open circuit on its terminal while the path through the DC blocking capacitors can be combined and closed off because of the symmetric and reciprocal property of the NIC circuit, giving Fig.3.11d. C_1 in the figure is the series combination of $2C_{B1}$ and $2C_{B2}$ [74].

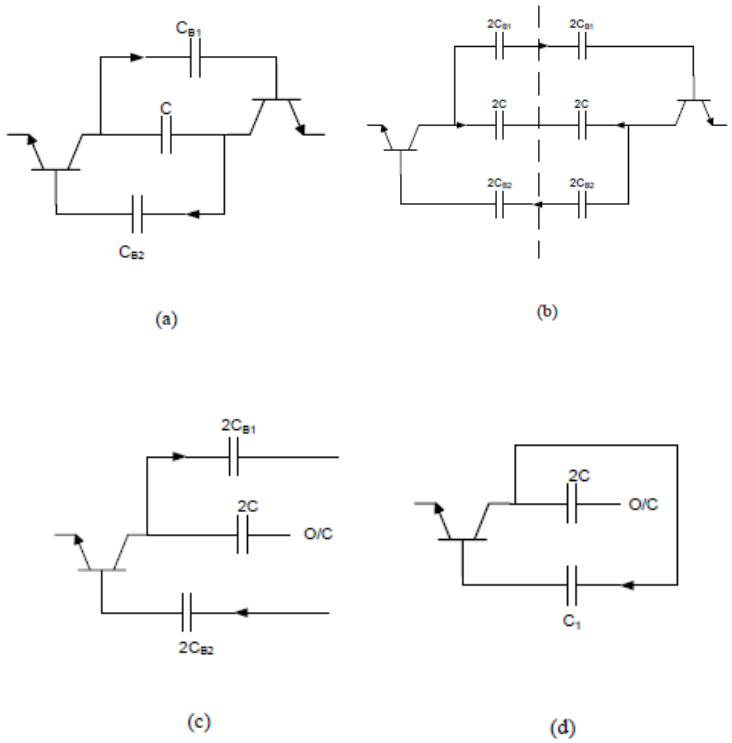

Fig.3.11: Development of the NIC circuit in even mode operation [74]

The equivalent circuit of NIC, with a transistor equivalent circuit, operating in the even mode is shown in Fig.3.12. To the equivalent circuit of the transistor in common emitter mode, capacitor C_1 and an input source voltage V_s and output voltage V_o have been added.

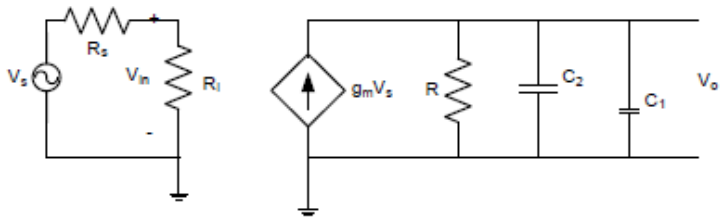

Fig.3.12: Equivalent circuit of the NIC in even mode (C_2 is the collector capacitance) [74]

The transfer function of the circuit in even mode is given as

$$\frac{V_O}{V_S} = \frac{g_m R}{1 + sR(C_1 + C_2)} \qquad 3.52$$

The poles, s, of the transfer function are:

$$s = -\frac{1}{R(C_1 + C_2)} \qquad 3.53$$

The poles are always going to be on the left-hand side of the complex s-plane, indicating unconditional stability, in the Nyquist stability criteria.

Odd mode

An odd mode analysis has also been performed on the circuit. The current out of the two transistors through the feedback path are in the opposite directions around the feedback path, as shown in Fig.3.13a and hence the simplification that was applied in the even mode is not applicable. In the odd mode, the current through the capacitor to invert, C, results in a virtual ground in the middle of that capacitor as shown in the circuit of Fig.3.13b. The capacitor C is split into a series connection of two capacitors of value 2C and a ground is placed between them.

The equivalent circuit of the transistor in the common-emitter mode is shown in Fig.3.13c, with the parallel combination of C_2 and R forming X_T as seen in Fig.3.13d. When the closed circuit formed by the feedback paths and equivalent circuits of the transistor that

make up the NIC in odd mode are analyzed, the NIC equivalent circuit in odd mode is shown in Fig.3.13e is obtained and this forms the basis of the odd mode analysis [74].

The transfer function of the circuit in odd mode is given as

$$\frac{V_O}{V_S} = \frac{2g_m R}{1+sR(4C+C_2)} \qquad 3.54$$

The poles of the transfer function are

$$s = -\frac{1}{R(4C + C_2)} \qquad 3.55$$

The poles are always going to be on the left-hand side of the complex s-plane, indicating unconditional stability, in the Nyquist stability criteria.

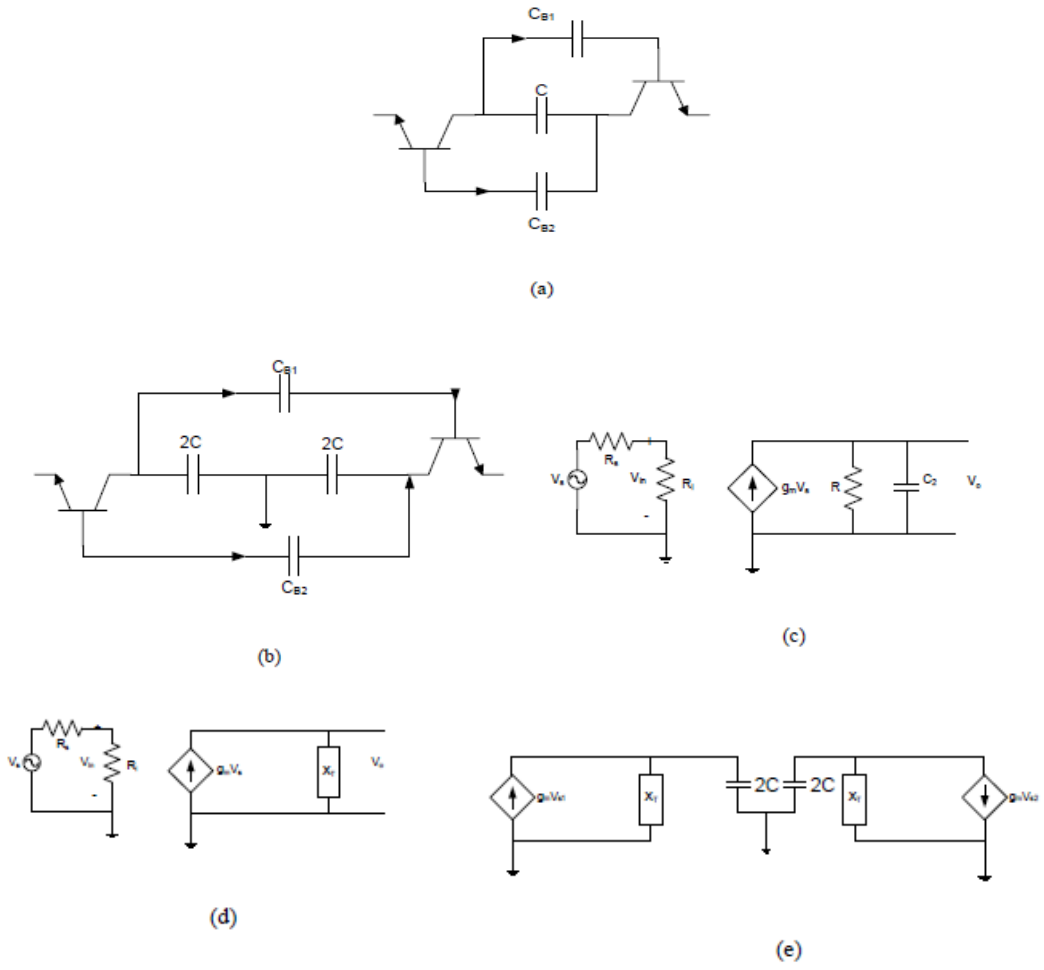

Fig.3.13: Development of the equivalent circuit of the NIC operating in the odd mode [74]

3.15 Summary

This chapter presents a theoretical overview of electrically small antennas and negative impedance converters supported by mathematical modeling. Since the antenna dimension is frequency dependent, an antenna can be considered electrically small only up to a particular range of frequency. The general representation of electrically small antennas along with mathematical expressions is discussed in this chapter. Electrically small antennas posses some design constraints which are discussed in section 3.3. Non-Foster elements are not usual as they do not follow the Foster's reactance theorem. Non-Foster elements have a reactance that decreases with frequency. Negative impedance converter circuits are used to realize these Non-Foster elements. NIC employs active devices. The Non-Foster elements are advantageous as far as antenna matching is concerned. Linvill first proposed the design of NIC circuit based on BJT. Since then, various floating and grounded topologies have been used by researchers in matching of electrically small antennas. However, active devices suffer from instability. Therefore stability analysis is essential before application to antennas.

Chapter 4

Design of NIC and application of NIC to Electrically Small Antennas

4.1 Chapter Overview

This chapter is broadly divided into two sections. Section A covers the design topologies of various negative impedance converter circuits including floating and grounded types. The various subsections of section A presents the circuit model, graphical representation of the real part and imaginary part of its input impedance. Section A also presents a detailed analysis of the NIC circuit that has been used in the current work. Effect of component variation and effect of microstrip lines are also presented with graphical representations. Section B presents the current work. The various subsections of section B presents the problem formulation, problem analysis, the antenna, study of antenna characteristics with passive elements, study of antenna characteristics with NIC circuit, simulated and fabricated results.

Section – A

This section deals with different design topologies of negative impedance converters. Negative Impedance converter topology can be of two types depending on the type of application. NICs can be grounded type or floating point type. In grounded type NIC, the impedance to be inverted is connected to ground. It basically functions as a one port network, required in applications which use it as a load, connected with the output port of another component. In floating type NIC, the impedance to be inverted is connected between the collector terminals of the two transistors. Floating type NIC is required in applications which use it as an intermediate or connecting stage between two components.

4.2 A Grounded Negative Capacitor using BJT

The following circuit represents a one port negative impedance converter. Fig.4.1 shows the circuit schematic. The imaginary part of the input impedance shows the characteristics of a negative capacitor. A load is connected between the base terminal of transistor Q_2 and ground. Fig.4.2 shows the real part (resistive part) of the input impedance and Fig.4.3 shows the imaginary part (reactive part) of the input impedance. The circuit uses two NE856 series NPN, silicon, high frequency transistors. The values of the other elements can be varied to obtain the desired result.

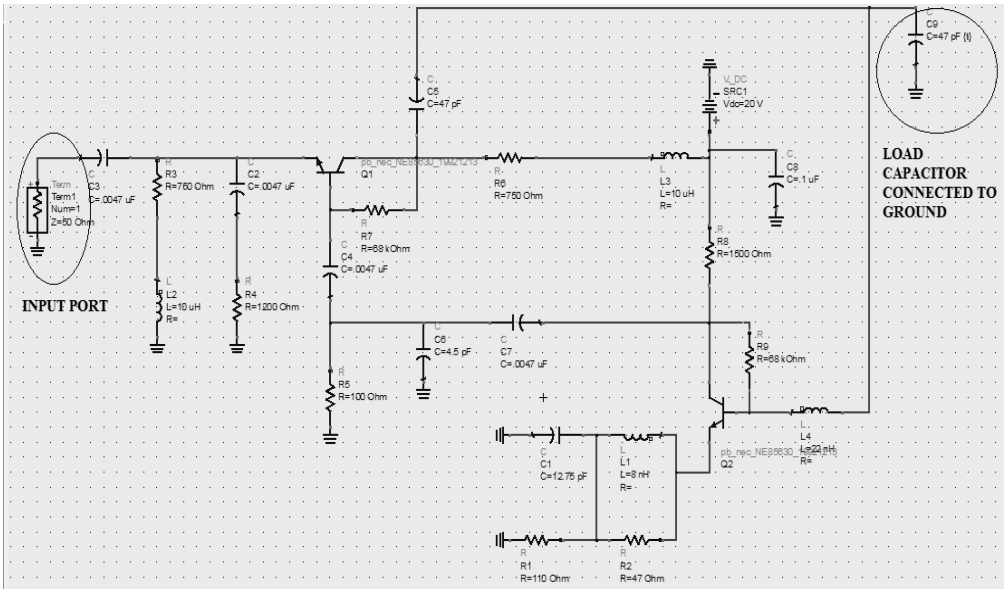

Fig. 4.1: Grounded negative capacitor schematic [25]

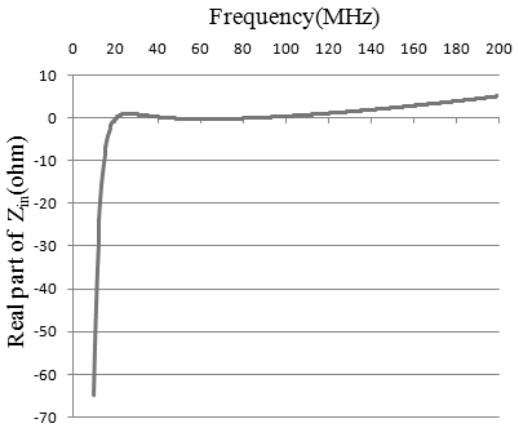

Fig. 4.2: Real part of the input impedance

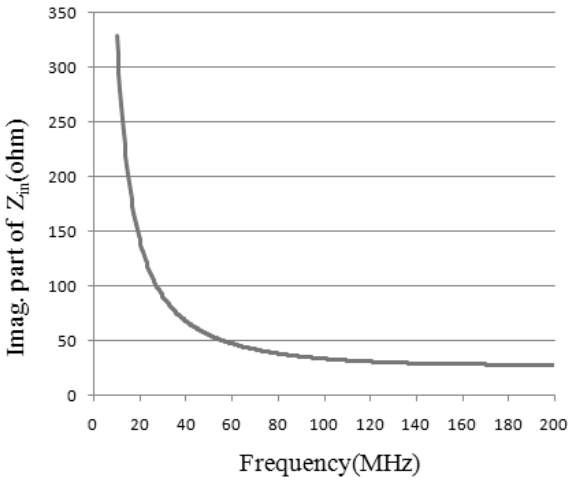

Fig. 4.3: Imaginary part of the input impedance

4.3 A Floating Negative Capacitor using BJT

The following circuit represents a two port negative impedance converter. The imaginary part of the input impedance shows the characteristics of a negative capacitor. A load is connected between the collector terminals of the two transistors Q_1 and Q_2. Fig.4.5 shows the real part (resistive part) of the input impedance and Fig.4.6 shows the imaginary part (reactive part) of the input impedance. The circuit uses two MRF949 series NPN, low noise, silicon, high frequency transistors. The values of the other elements can be varied to obtain the desired result.

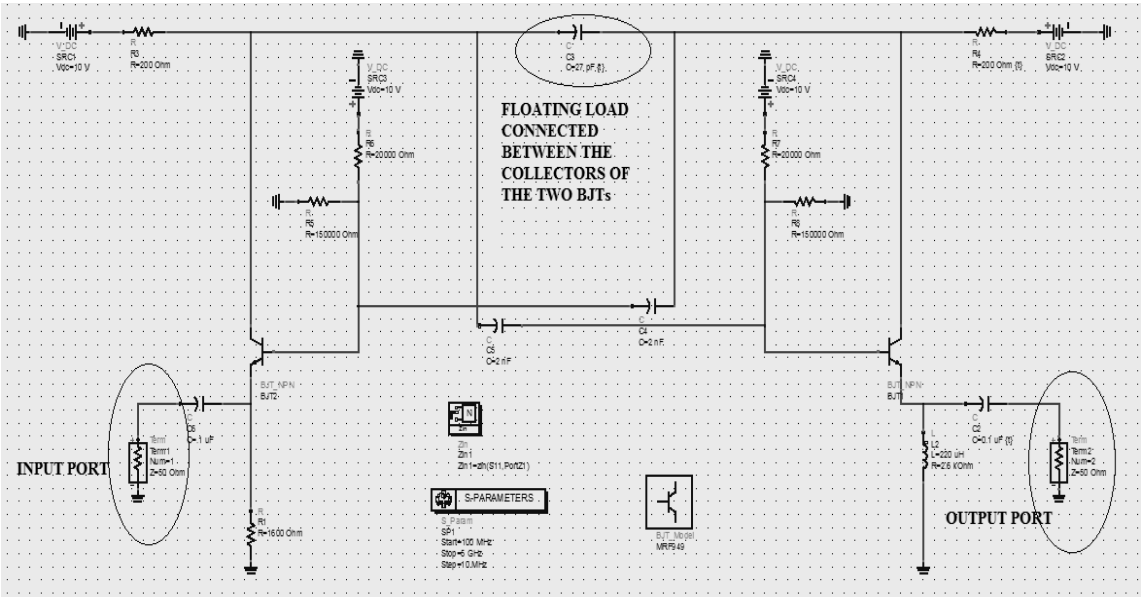

Fig. 4.4: Floating negative capacitor schematic [75]

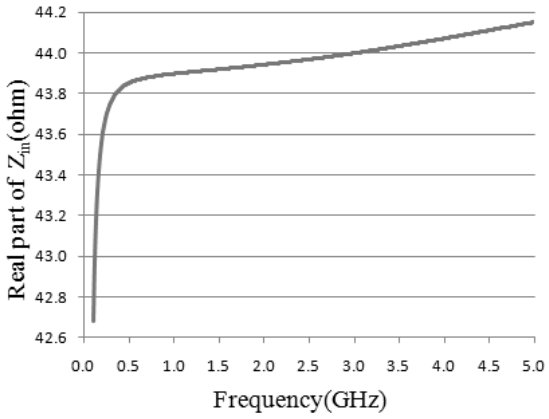

Fig. 4.5: Real part of the input impedance

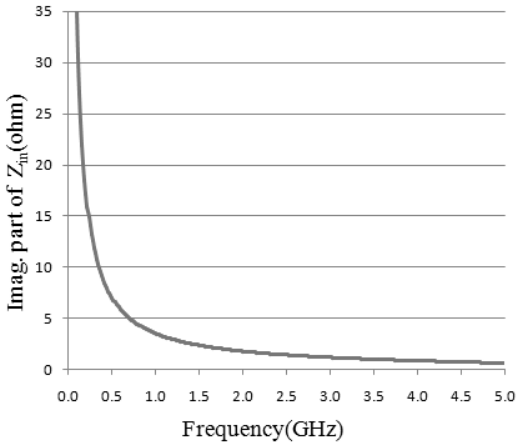

Fig. 4.6: Imaginary part of the input impedance

4.4 A Floating Negative Capacitor using FET

The following circuit represents a two port negative impedance converter using Field Effect Transistors (FETs). The imaginary part of the input impedance shows the characteristics of a negative capacitor. A load is connected between the drain terminals of the two transistors Q_1 and Q_2. Fig.4.8 shows the real part (resistive part) of the input impedance and Fig.4.9 shows the imaginary part (reactive part) of the input impedance. The circuit uses two S8835 series high gain, microwave power GaAs field effect transistors. The values of the other elements can be varied to obtain the desired result.

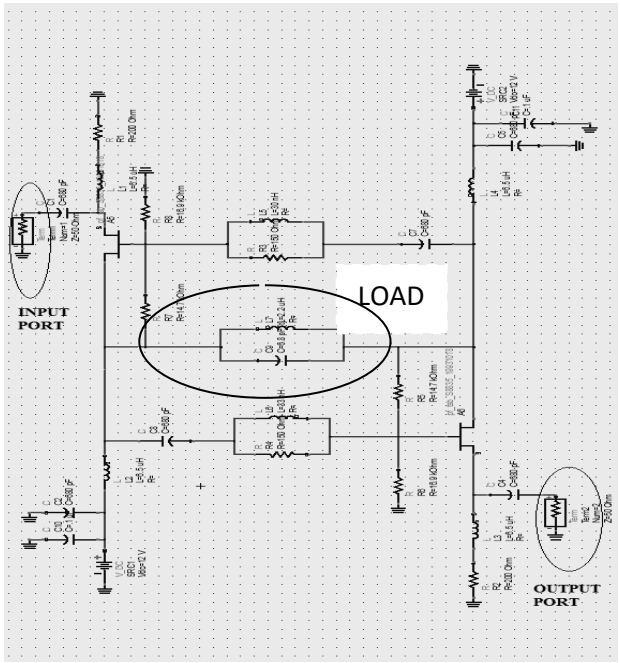

Fig. 4.7: Floating negative capacitor schematic [33]

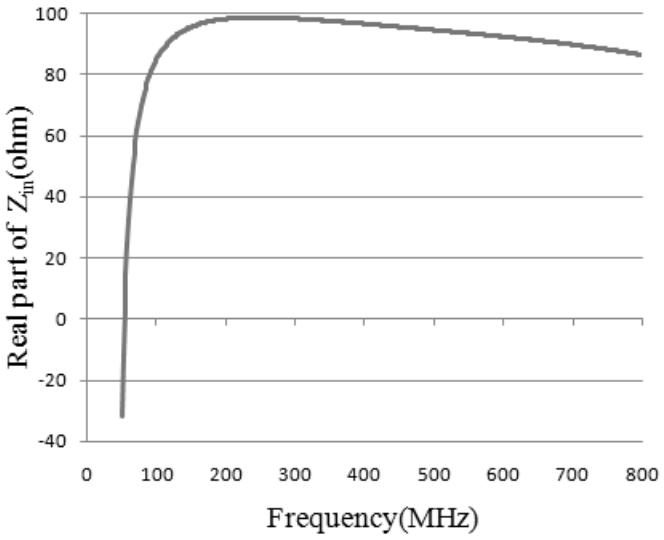

Fig. 4.8: Real part of the input impedance

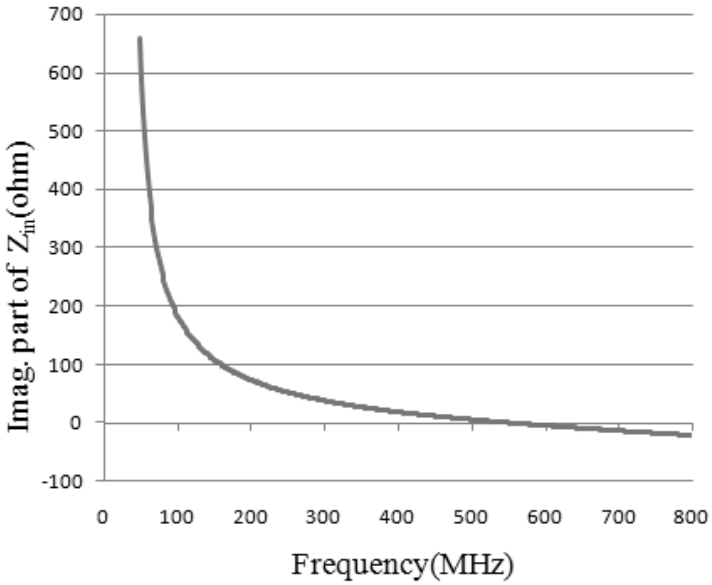

Fig. 4.9: Imaginary part of the input impedance

4.5 A Grounded Negative Inductor using BJT

The following circuit represents a one port negative impedance converter. The imaginary part of the input impedance shows the characteristics of a negative inductor. A load is connected between the base terminal of transistor Q_2 and ground. Fig.4.11 shows the real part (resistive part) of the input impedance and Fig.4.12 shows the imaginary part (reactive part) of the input impedance. The circuit uses two NE856 series NPN, silicon, high frequency transistors. The values of the other elements can be varied to obtain the desired result.

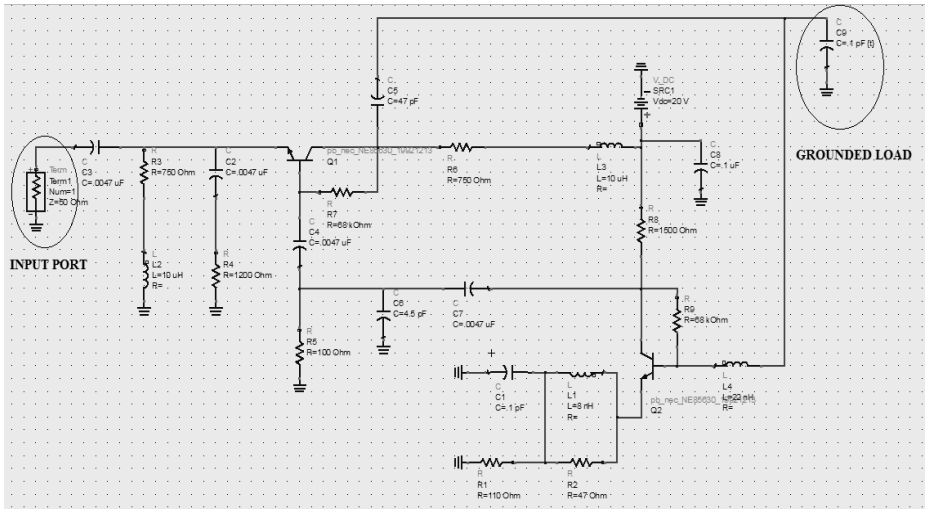

Fig. 4.10: Grounded negative inductor schematic

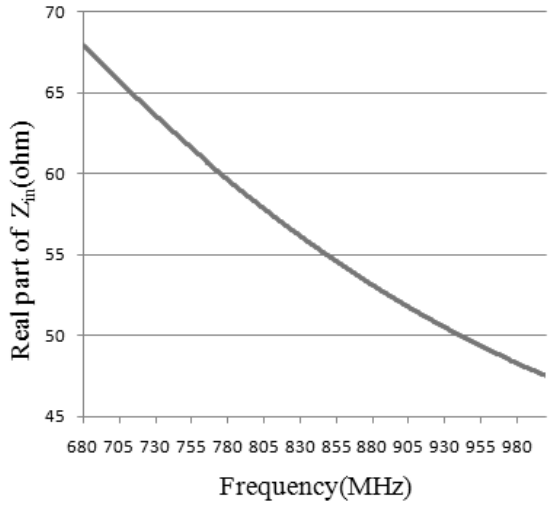

Fig. 4.11: Real part of the input impedance

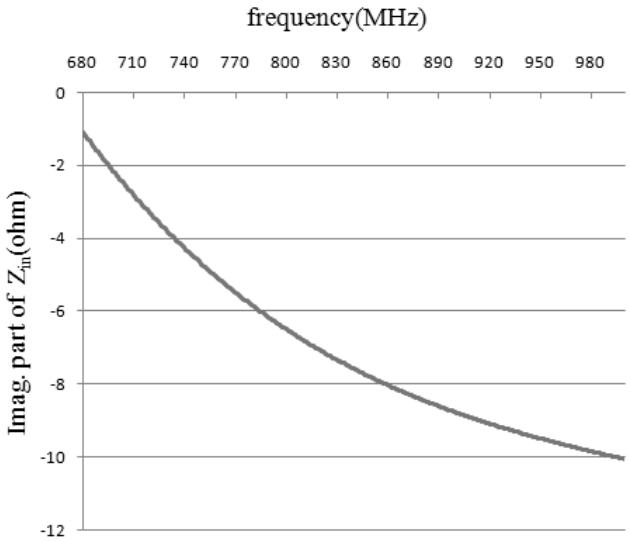

Fig. 4.12: Imaginary part of the input impedance

4.6 A Floating Negative Inductor using FET

The following circuit represents a two port negative impedance converter using Field Effect Transistors (FETs). The imaginary part of the input impedance shows the characteristics of a negative inductor. A load is connected between the drain terminals of the two transistors Q_1 and Q_2. Fig.4.14 shows the real part (resistive part) of the input impedance and Fig.4.15 shows the imaginary part (reactive part) of the input impedance. The circuit uses two S8835 series high gain, microwave power GaAs field effect transistors. The values of the other elements can be varied to obtain the desired result.

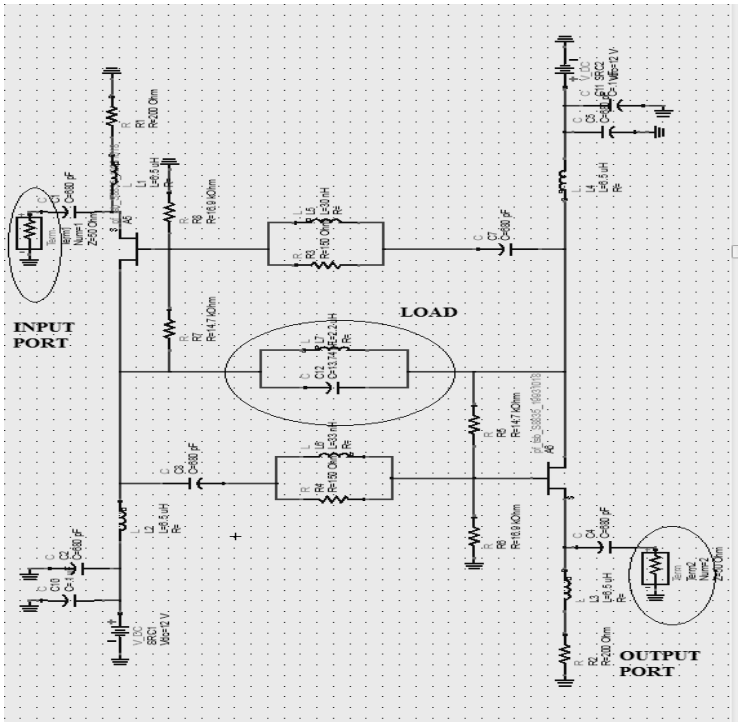

Fig. 4.13: Floating negative inductor schematic

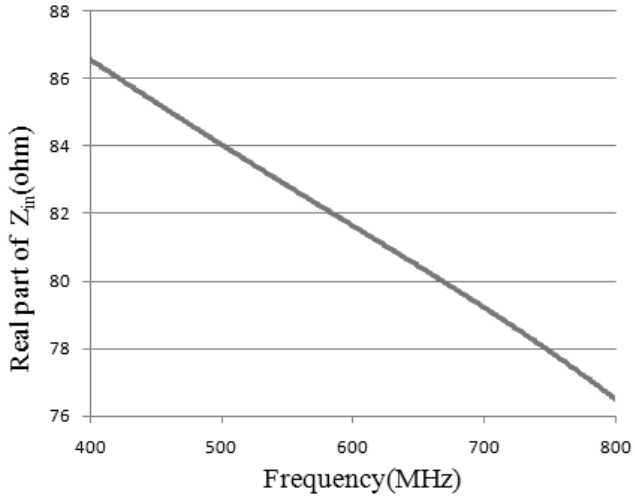

Fig. 4.14: Real part of the input impedance

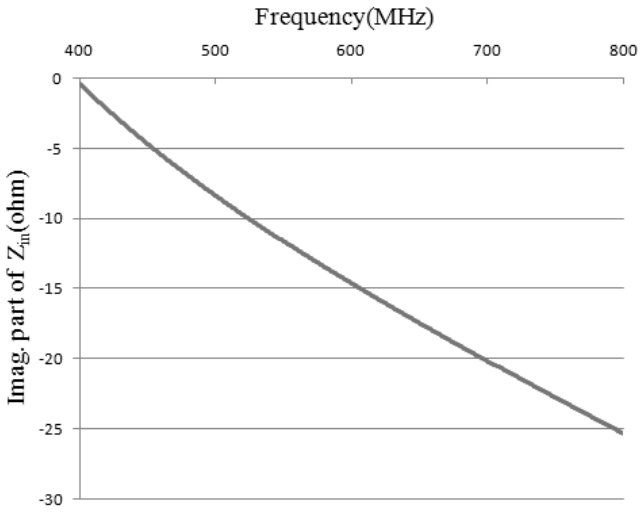

Fig. 4.15: Imaginary part of the input impedance

4.7 A Floating Negative Inductor using BJT

The following circuit represents a two port negative impedance converter. The imaginary part of the input impedance shows the characteristics of a negative inductor. A load is connected between the collector terminals of the two transistors Q_1 and Q_2. Fig.4.17 shows the real part (resistive part) of the input impedance and Fig.4.18 shows the imaginary part (reactive part) of the input impedance. The circuit uses two BFR93A series NPN, low noise, 6 GHz wideband RF transistors. The values of the other elements can be varied to obtain the desired result.

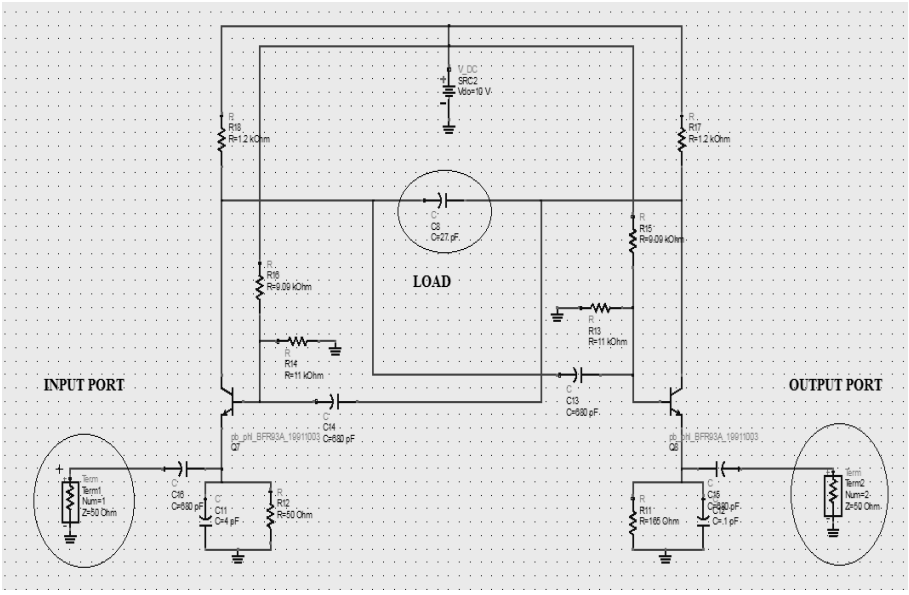

Fig. 4.16: Floating negative inductor schematic [43]

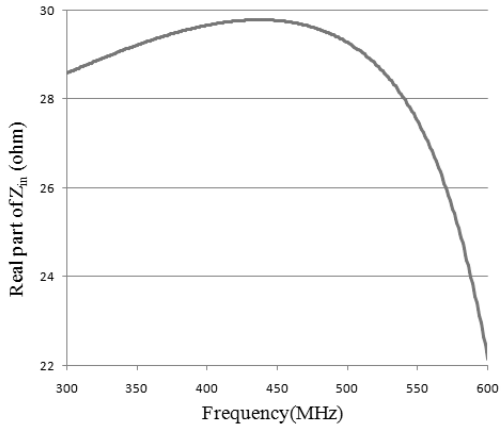

Fig. 4.17: Real part of the input impedance

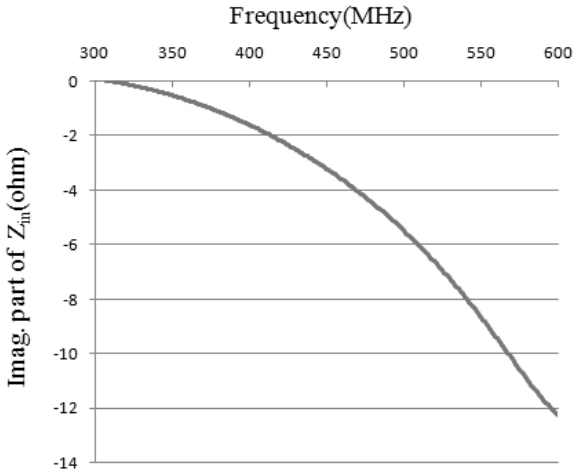

Fig. 4.18: Imaginary part of the input impedance

4.8 Discussion on the NIC model

Fig. 4.16 shows the NIC model that has been used in the current work. It follows the structure of a basic Linvill floating point model consisting of two cross-coupled transistors. The load is connected between the collector terminals of the two transistors. Along with it some other elements has been used to realize the model. The 680pF capacitors acts as dc blocking capacitors as they block the dc signal and bypass the ac signal thereby maintaining proper operation of the circuit. They are also instrumental in stabilizing the circuit at high frequency. The 9.09kohm and 11kohm voltage divider resistive network helps in the proper biasing of the transistors. They serve as voltage divider bias and help in fixing the operating point of the transistors. A 10 volt dc source drives the circuit. The emitter resistors and bypass capacitors are chosen as per the requirement of the work.

The following figure shows the effect of parameter variation in the circuit. Fig.4.19 shows the variation in the imaginary part of the input impedance with respect to emitter bypass

capacitor. Fig.4.20 shows the variation in the imaginary part of the input impedance with respect to emitter resistor. The figures indicate that as we increase the values of the emitter resistor or emitter bypass capacitor, the response becomes more and more reactive.

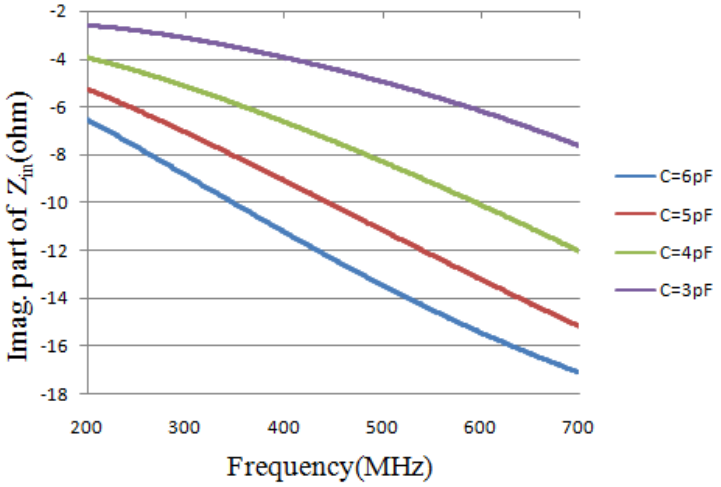

Fig. 4.19: Variation of the imaginary part of the input impedance with respect to emitter by-pass capacitor

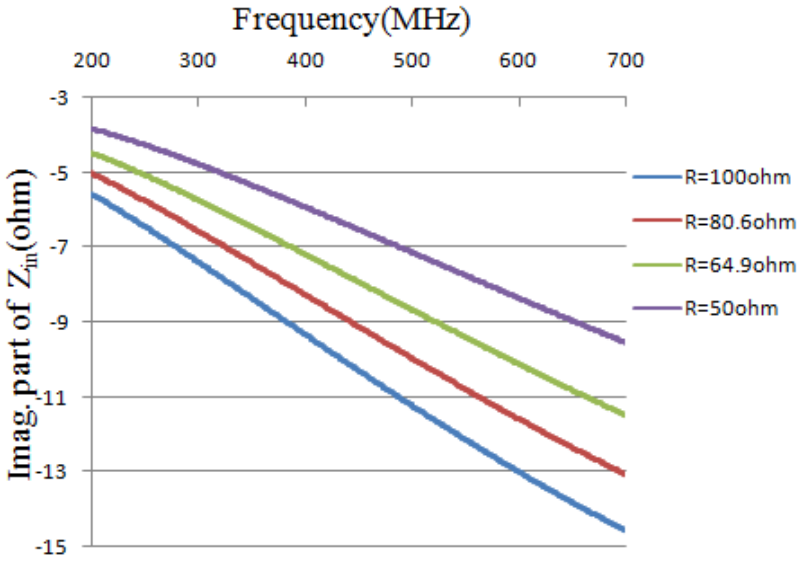

Fig. 4.20: Variation of the imaginary part of the input impedance with respect to emitter resistor

4.9 Effect of microstrip lines

For the fabrication of the designed NIC on a printed circuit board (PCB), at first a layout is to be generated from the schematic. In the layout the connecting wires are replaced by microstrip lines of characteristic impedance of 50 ohm each. The width of the line is an important parameter and it is calculated accordingly. Bends, tee junctions and cross junctions are used as and when required. Fig.4.21 shows the microstrip line equivalent of the NIC schematic. Fig.4.22 shows the variation in the real part of the input impedance with respect to

the inclusion of microstrip lines. Fig.4.23 shows the variation in the imaginary part of the input impedance with respect to the inclusion of microstrip lines. All the other elements are kept fixed.

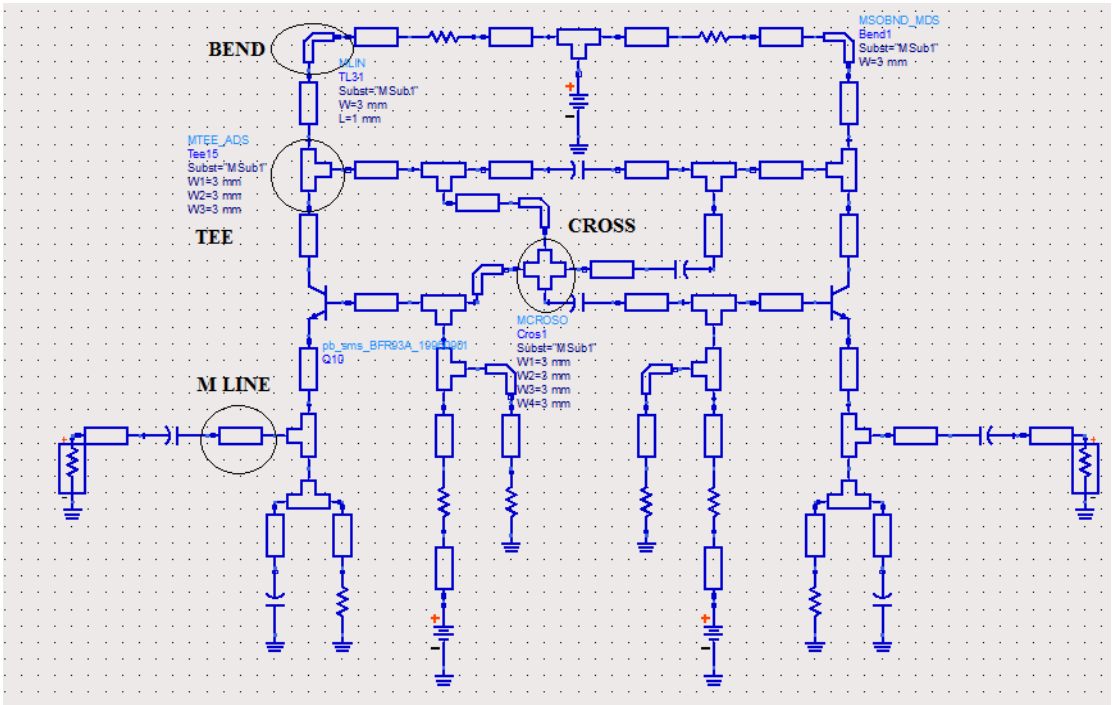

Fig. 4.21: Microstrip line equivalent of the NIC schematic

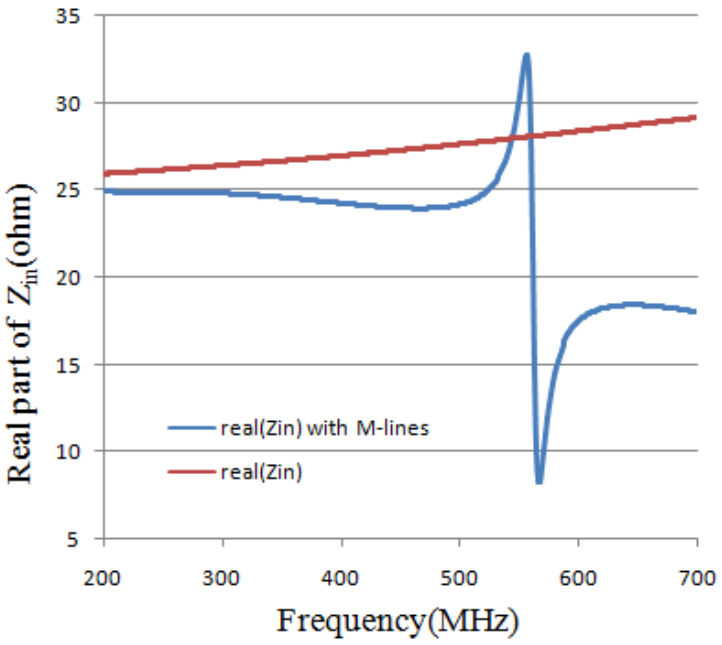

Fig. 4.22: Variation of real part of the input impedance with and without microstrip lines

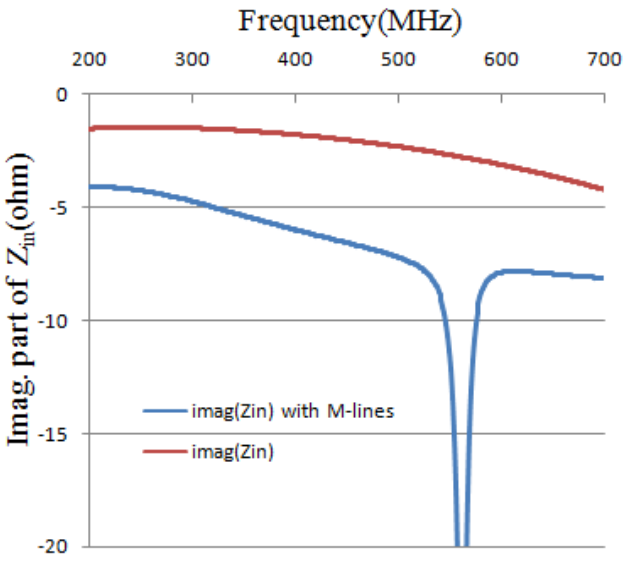

Fig. 4.23: Variation of imaginary part of the input impedance with and without microstrip lines

4.10 Fabricated NIC

The fabricated NIC structure is shown in Fig.4.24, the PCB layout on the left and the overall circuit on the right. The structure is laid on a FR4 substrate having dielectric constant 4.3 and thickness 1.52 mm. The components are soldered into the circuit. The components are properly grounded with via-holes to copper strip situated the back side of the substrate. The transistors are properly biased by providing 10 volt DC from power supply. The back plane conductor of the FR4 board is connected to the power supply ground. The two SMA connectors represent the two ports. Port 1 is considered as the input port where the signal is fed and port 2 is considered as the output port where the antenna is connected.

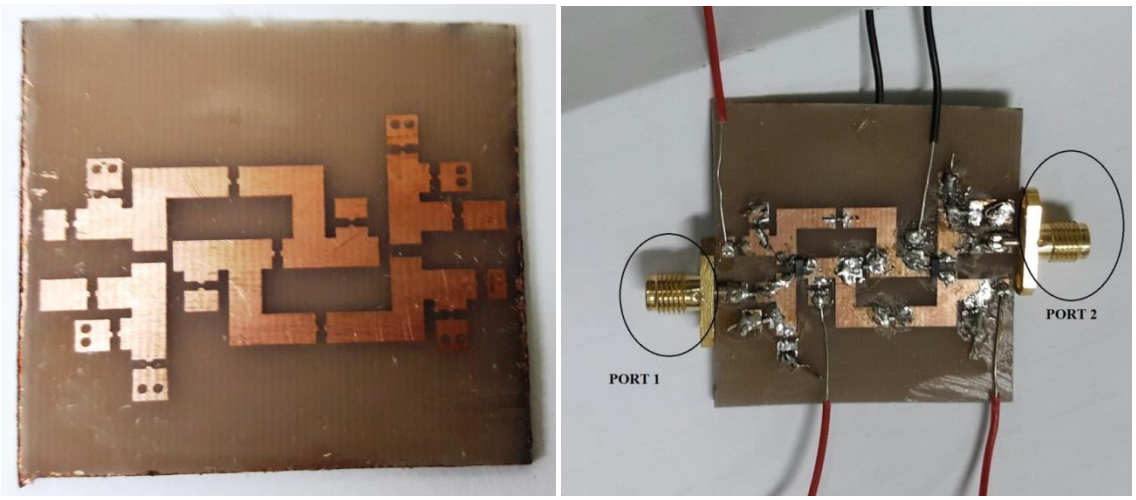

Fig. 4.24: Fabricated NIC circuit

Section - B

In chapter 2, a review of different literatures in this field is presented. The need for negative impedance converters in the domain of electrically small antennas is clearly highlighted in almost every literature. Different ways of interfacing the NIC with the antenna are also highlighted in some papers. However, most of the work discussed in the chapter mainly revolved around complicated matching network and non planar antennas. Planar printed antennas have gained significant attention in recent times. Thus, the main motivation for the current work is to simplify the matching network and implement the concept of negative impedance converters in microstrip antennas. Simplifying the matching network includes removing the bulky transformer network and using the converter itself to adjust the real and imaginary part of the antenna input impedance.

4.11 Problem formulation and analysis

Main focus is given on Microstrip Antennas. The concept of Microstrip Antennas (MSA) was first proposed by Deschamps in 1953 [76]. However, the practical realization of such structure came in the 70s with the works of Munson [77,78] and Howell [79]. The MSA comes with a number of advantages such as its low weight, small size and space requirements and ease of fabrication using printed circuit technology. In its simplest form a microstrip patch antenna consist of a radiating patch on one side of the dielectric substrate and a ground plane on the other. The radiating patch can be circular, rectangular, triangular, square, annular ring-like or any other geometrical shapes that suit the purpose. Radiation from such antennas occurs from the fringing fields between the periphery of the patch and the ground plane.

The main advantages of such structures include their light weight, low profile and smaller space requirements. With the advent of printed circuit fabrication, the commercial production of these components has become easier and cost effective. They offer easy integration with the Integrated Circuits using identical substrates. They can be designed for both linear and circular polarization. They can be used for single, dual, triple and even with intelligent designs, for wideband applications. However, the basic structures come with their inherent disadvantages such as their relatively narrow bandwidth, low gain and low power handling capacity. Also, the input impedance of such antennas are characterized by very low real (resistive) part and comparatively high imaginary (reactive) part over a significant frequency range outside their operating frequency. This feature makes them difficult to impedance match with the feed cable (which is generally of 50ohms) over a broad range of frequency. The test antenna is an inset feed rectangular microstrip patch antenna having the following specification: Substrate: FR4, Dielectric constant: 4, Loss tangent: 0.02, Substrate height:

1.6mm, Length of patch: 93.47 mm, Width of patch: 118.5 mm, Operating frequency: 800MHz.

The schematic is shown in Fig.4.25. The antenna is fed by a 50 ohm source at the input. Fig. 4.26 (a) shows the S_{11} plot of the antenna in dB and Fig.4.26 (b) shows the normalized radiation pattern of the concerned antenna in dB.

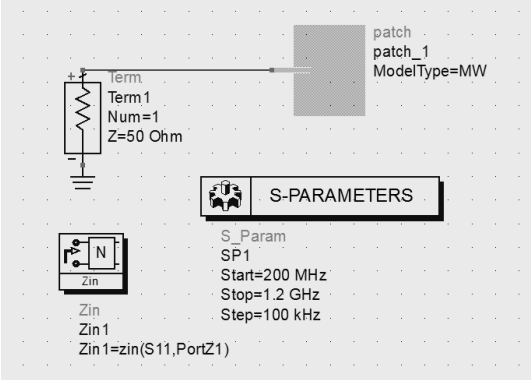

Fig.4.25: Antenna simulation schematic

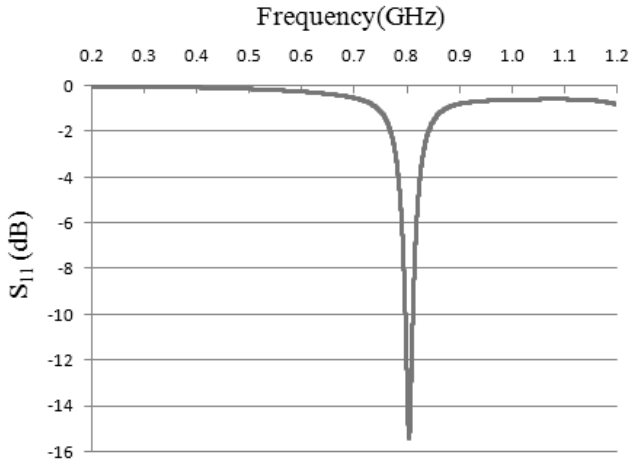

(a)

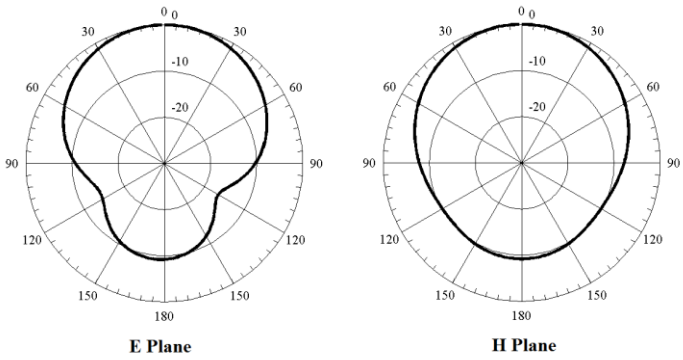

(b)

Fig.4.26: (a) S_{11} (dB) of the antenna (b) Radiation pattern

The real (resistive) part and imaginary (reactive) part of the antenna impedance is shown in Fig.4.27 and Fig.4.28 respectively. Now, as far as antenna dimensioning using Chu's limit is concerned, the test antenna is electrically small (ka<1) up to 600MHz. The real part of the antenna impedance is very low up to 600MHz (for example .2 at 377MHz and 2.2 at 575MHz) whereas the reactive part of the impedance is comparatively high (for example 30.85 at 377MHz and 82.7 at 575MHz) as indicated by the following figures.

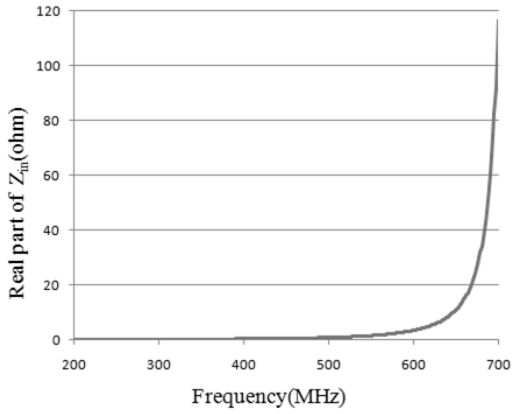

Fig: 4.27: Real part of the antenna impedance up to 700MHz

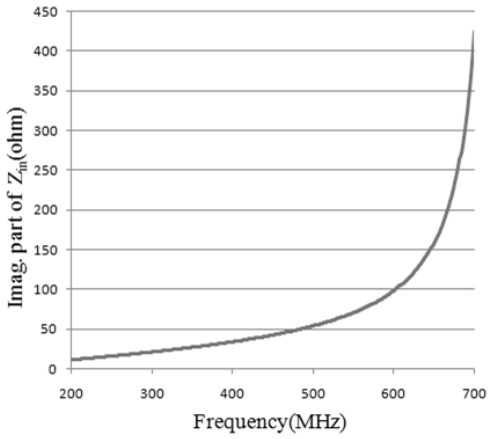

Fig: 4.28: Imaginary part of the antenna impedance up to 700MHz

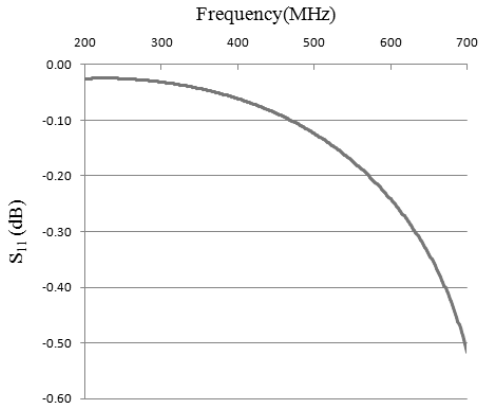

Fig.4.29: S_{11} (dB) of the antenna up to 700MHz

From Fig.4.29 it is clear that the antenna is very poorly matched within the frequency range in which it is electrically small.

In Fig.4.28 we see that the behavior of the imaginary part of the antenna impedance is inductive in nature over the concerned frequency range. Thus one of the obvious techniques to improve the matching would be to cancel the reactive part. Now, in order to cancel the inductive reactance, a capacitive reactance is introduced. A particular frequency of 377MHz is chosen. From Fig.4.28 it is seen that the corresponding reactance is 30.85 ohm. So, a capacitor offering 13.69pF capacitance and a reactance of -30.85ohm is applied before the antenna as shown in Fig.4.30.

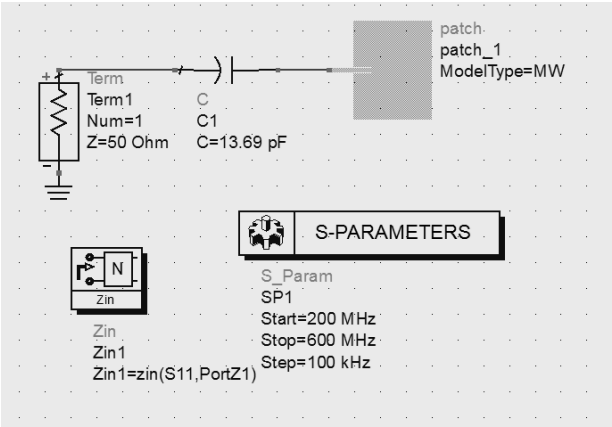

Fig.4.30: Antenna schematic with a 13.69pF capacitor

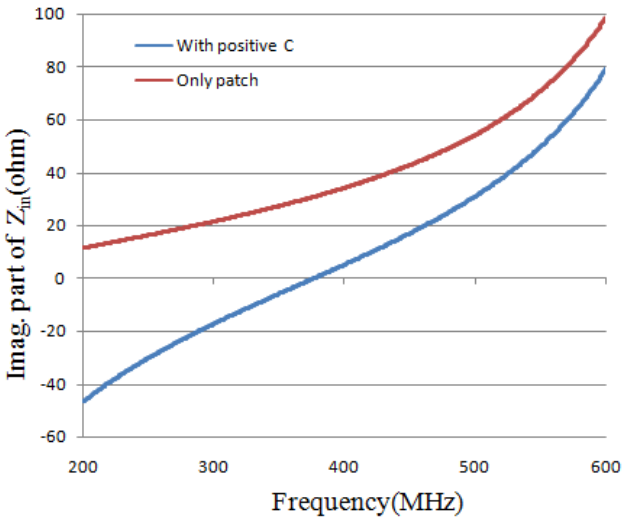

Fig: 4.31: Imaginary part of the input impedance up to 600MHz with and without the application of 13.69pF capacitor

The imaginary part of the input impedance before and after the application of a 13.69pF capacitor is shown in Fig.4.31. It is clearly visible that with the application of the capacitor,

the reactance at 377 MHz has been reduced nearly to zero. Hence, we move to the S_{11} plot of the entire system to see if the matching has improved or not.

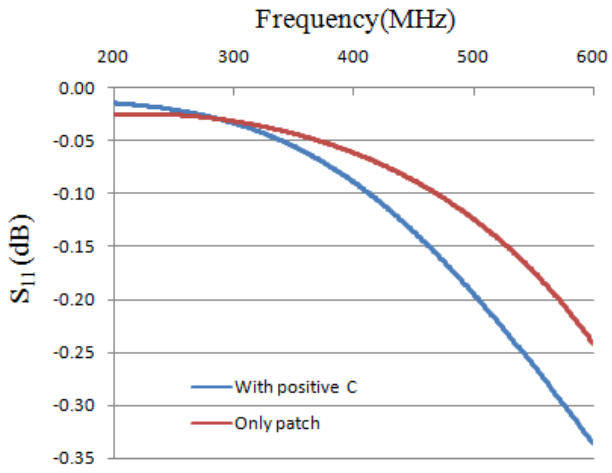

Fig.4.32: S_{11} (dB) of the system up to 600MHz with and without the application of 13.69pF capacitor

The return loss of the antenna up to 600MHz with and without the application of 13.69pF capacitor is shown in Fig.4.32. From the figure it is seen that although the imaginary part of the antenna impedance is nearly zero, the antenna is still poorly matched at 377MHz. This is because the real part of the antenna impedance experiences no change or improvement at all as seen in Fig.4.33. For the antenna to be properly matched at the source the imaginary part of the antenna impedance must be ideally zero and the real part of antenna impedance must be equal to that of the feed line (ideally 50 ohm).

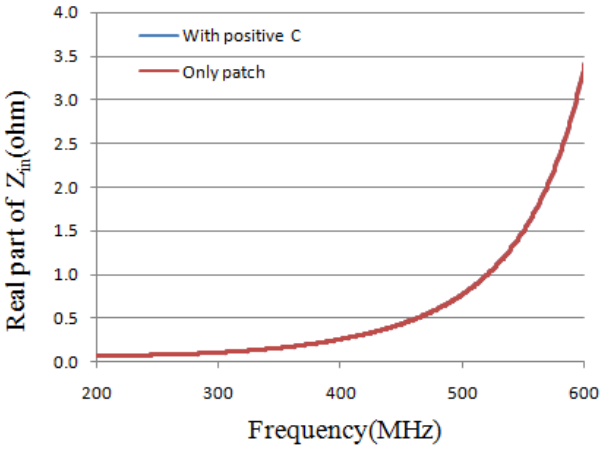

Fig: 4.33: Real part of the input impedance up to 600MHz with and without the application of 13.69pF capacitor

Now, applying the concept of negative impedance an ideal negative inductor is used instead of the capacitor as shown in Fig.4.34. The calculated value of the inductor comes out to be -13.03nH which offers a reactance of -30.85 ohm at 377MHz. The imaginary part of the

input impedance before and after the application of the -13.03nH inductor is shown in Fig.4.35. The variation in the plot with respect to the previously applied 13.69 pF capacitor is also shown in the figure.

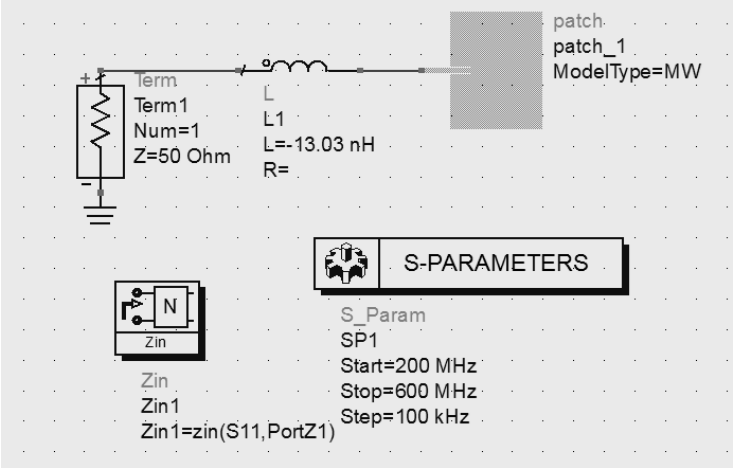

Fig.4.34: Antenna schematic with -13.03nH inductor

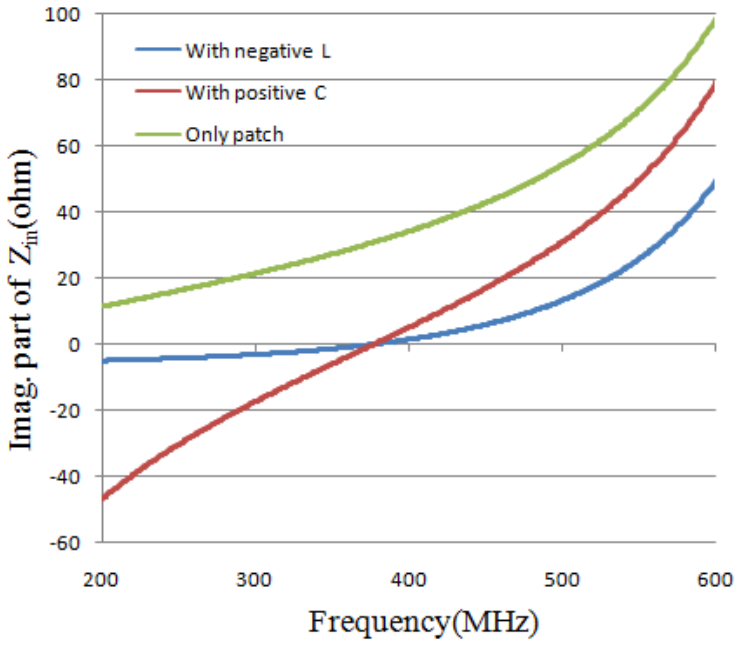

Fig: 4.35: Imaginary part of the input impedance up to 600MHz with and without the application of -13.03nH inductor and 13.69pF capacitor

From Fig.4.35 it is clear that with the application of the ideal negative inductor, the reactive portion of the input impedance has been cancelled over a broad range of frequency compared to the positive capacitor which is effective only at a single frequency. Hence, we again move to the S_{11} plot of the entire system to see if the matching has improved or not. The return loss of the antenna up to 600MHz with and without the application of 13.03nH

inductor (compared with the positive capacitor) is shown in Fig.4.36. From the figure it is seen that although the imaginary part of the antenna impedance is nearly zero over a broad range of frequency, the antenna is still poorly matched at 377MHz. This is because once again the real part of the antenna impedance experiences no change or improvement at all as seen in Fig.4.37.

From the above discussions it is clear that to cancel the reactive part of the antenna input impedance over a broad range of frequency, application of a negative element is essential. However that negative element alone is not able to improve the matching of the antenna to the source. This is because the real part of the input impedance remains unaltered even after the application of the negative impedance.

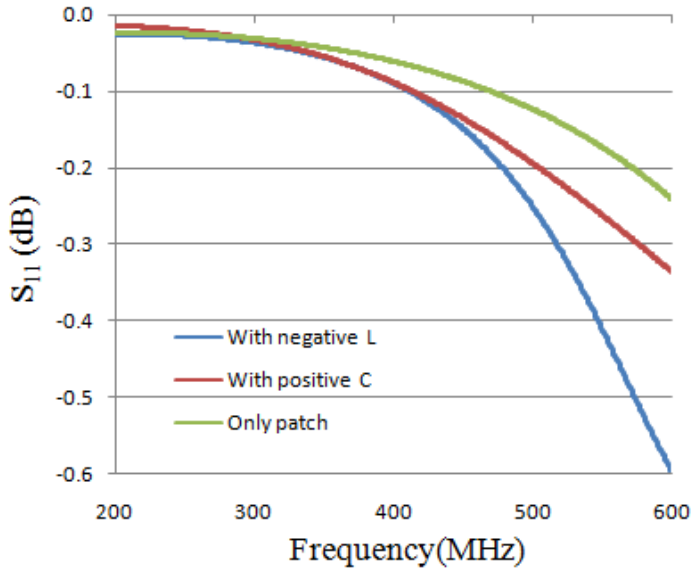

Fig: 4.36: S_{11} of the system up to 600MHz with and without the application of -13.03nH inductor and 13.69pF capacitor

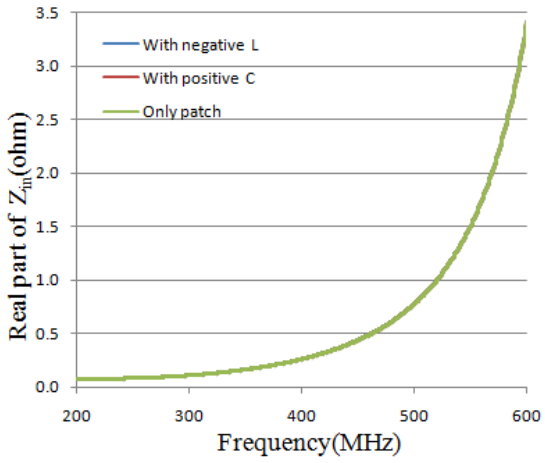

Fig: 4.37: Real part of the input impedance up to 600MHz with and without the application of -13.03nH inductor and 13.69pF capacitor

In this regard, the negative impedance converter finds its requirement. As it is already discussed, the input impedance of NIC circuit has both real part and imaginary part. The imaginary part can be used to cancel the antenna reactance over a broad range of frequency while the real part can be utilized to better the real part of the overall input impedance. Thus the impedance matching is expected to improve at the source. Now, it is difficult to design a NIC circuit in which the imaginary part of the input impedance is the exact value of the reactance to be cancelled (at the desired frequency) while the real part of the input impedance is exactly 50 ohm. Hence, an optimum value should be chosen which satisfies the requirement of the problem.

4.12 Application of the designed NIC to the test antenna

An interesting phenomenon can be observed from Fig.4.27, which represents the real part of the antenna impedance up to 700MHz. Although the antenna is designed at 800MHz, at around 687MHz the real part of the antenna impedance is close to 50 ohm. But the antenna is poorly matched at that frequency (as seen in Fig.4.29) since it has significant reactive part (about 300ohm as seen in Fig.4.28).

Therefore, initial work includes cancellation of the reactive part of the antenna impedance using a NIC circuit in the region where the real part of antenna impedance is 50ohm. Thus the impedance matching at the source is expected to improve over the concerned frequency range. The NIC topology that is used is shown in Fig.4.16. Now as the reactive part of the antenna input impedance is inductive in nature, a NIC based negative inductor is used to cancel the reactive portion. The NIC circuit is tuned to meet the requirements of the problem. Fig.4.38 shows the antenna – NIC co simulation schematic. Here the input is coupled to the antenna through the NIC circuit. Fig.4.39 shows the imaginary part of the input impedance before and after the application of the NIC circuit. From the figure it is clear that a large portion of the reactive part of the antenna impedance has been successfully cancelled over the concerned frequency range. Hence, we move to the S_{11} plot of the entire system to see if the matching has improved or not.

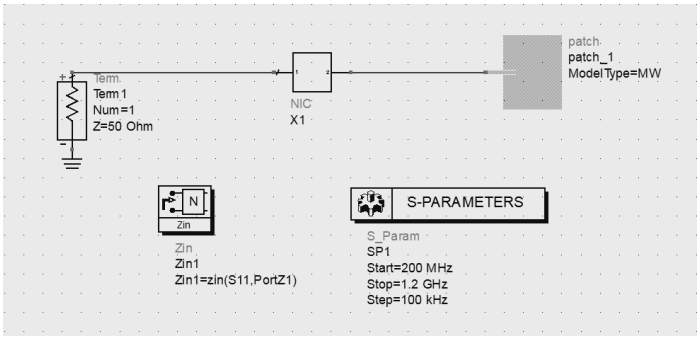

Fig.4.38: Antenna – NIC co simulation

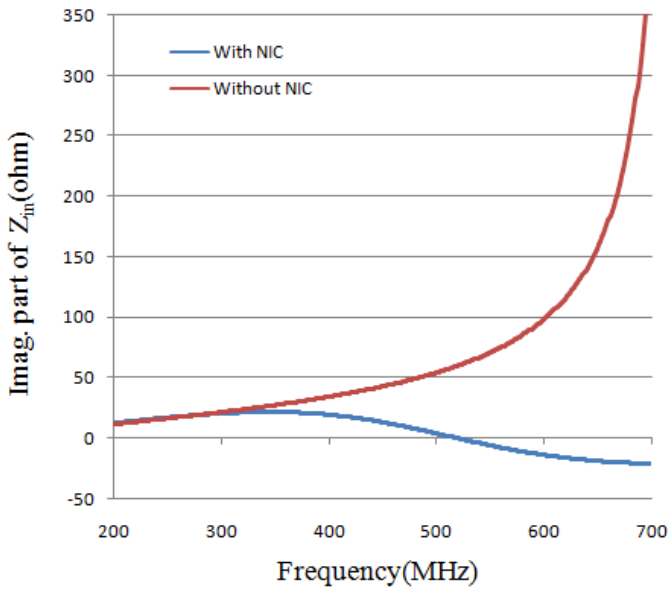

Fig.4.39: Imaginary part of the input impedance with and without the NIC circuit

The return loss of the antenna with and without the application of the NIC circuit is shown in Fig.4.40. Form the plot we can see that the matching of the antenna has significantly improved over the concerned range of frequency including a dip of -45dB at 524.5 MHz and a matching bandwidth of about 327MHz (375MHz to 702MHz). The matching bandwidth also includes the 687MHz frequency where the real part of the antenna impedance is 50ohm.

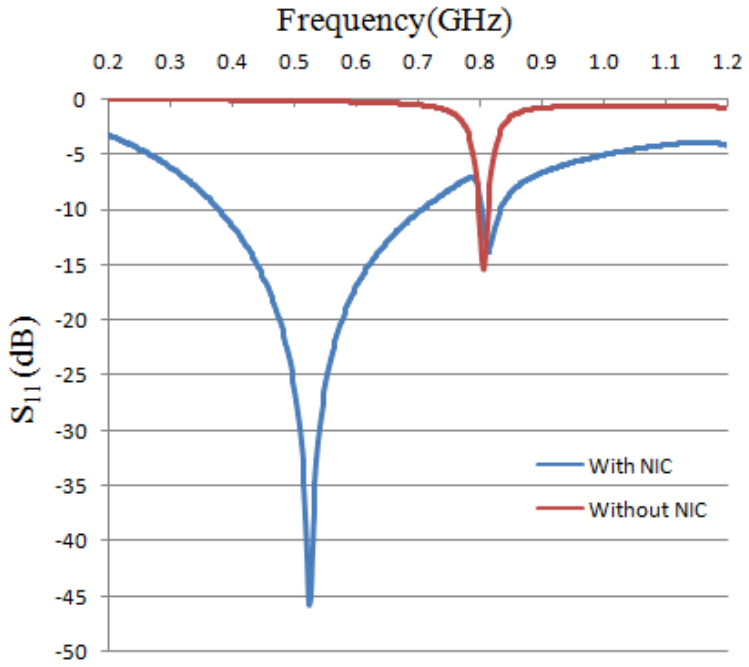

Fig.4.40: S_{11} of the system with and without the NIC circuit

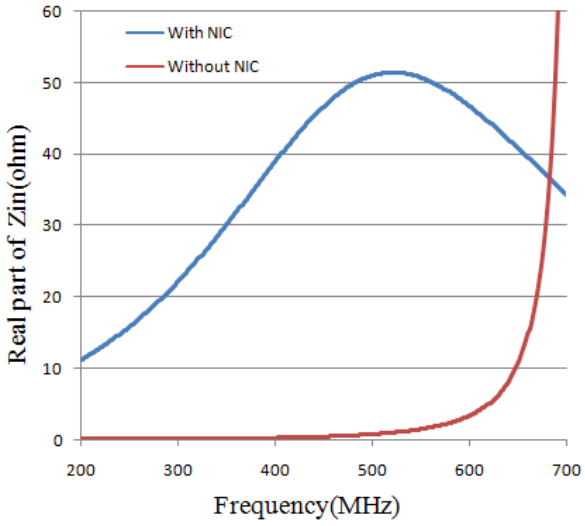

Fig.4.41: Real part of the input impedance with and without the NIC circuit

The real part of the input impedance with and without the application of the NIC circuit is shown in Fig.4.41. From the figure it is clear that the overall real part has significantly improved with the application of the NIC circuit over the concerned range of frequency which plays an important role in improving the matching characteristics of the antenna at the source.

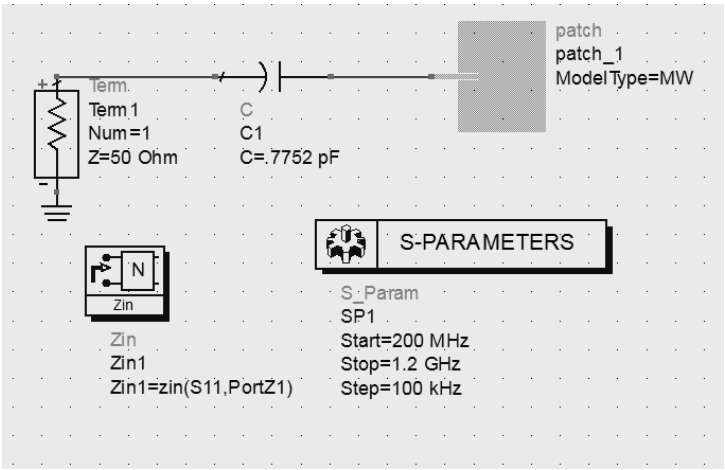

Fig.4.42: Antenna schematic with .7752pF capacitor

As the real part of the antenna impedance is already 50ohm at the concerned frequency, a passive element can also be used to match the antenna at about 687MHZ. In fact, a capacitor having a capacitance of .7752pF and offering a reactance of -299ohm at 687MHz has been used to cancel the inductive reactance of the antenna. The entire scheme is shown in Fig.4.42. However the matching bandwidth obtained is extremely narrow compared to what was obtained by the application of the NIC circuit. Thus use of passive elements does not result in broadband matching. A comparative representation of both active and passive

matching along with the increase in matching bandwidth in active matching scheme is shown in Fig.4.43.

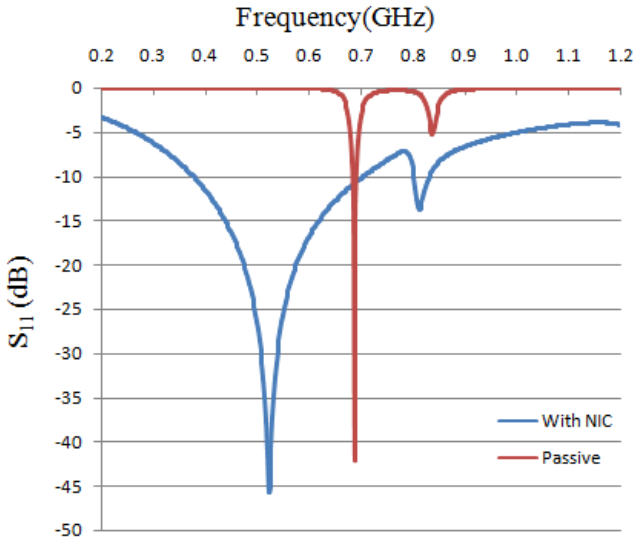

Fig.4.43: Broadband matching using NIC circuit compared to narrowband passive matching

4.13 Application of the designed NIC to the test antenna in the frequency range where it is electrically small

The previous work was based on improving the matching characteristics of the antenna in a region other than its operating frequency where the real part of the input impedance was found to be 50 ohm. However, it was not strictly in the frequency range where the antenna was defined to be electrically small. The following work completely targets the use of NIC circuit to improve the matching characteristics of the test antenna in the frequency range where it is electrically small. From the earlier discussions it is clear that the antenna is electrically small up to 600MHz. The work includes design and simulation of the NIC circuit, design and simulation of the test antenna, application of NIC circuit to the antenna, antenna-NIC co-simulation, observation of results, fabrication of NIC and antenna and validation of results through measurement. The NIC circuit follows the same circuit model as was shown in Fig.4.16. However, some of the component values were adjusted to meet the requirement of the problem. Fig.4.44 shows the antenna – NIC co simulation where the NIC circuit is replaced by its PCB layout. Fig.4.45 shows the imaginary part of the input impedance of the NIC circuit alone. It is seen from the figure that the reactance is that of a negative inductor in the frequency range of 300MHz to 600MHz. It is essential to have a negative inductor because the antenna input reactance follows the behavior of a positive inductor within the concerned frequency range as seen in Fig.4.28.

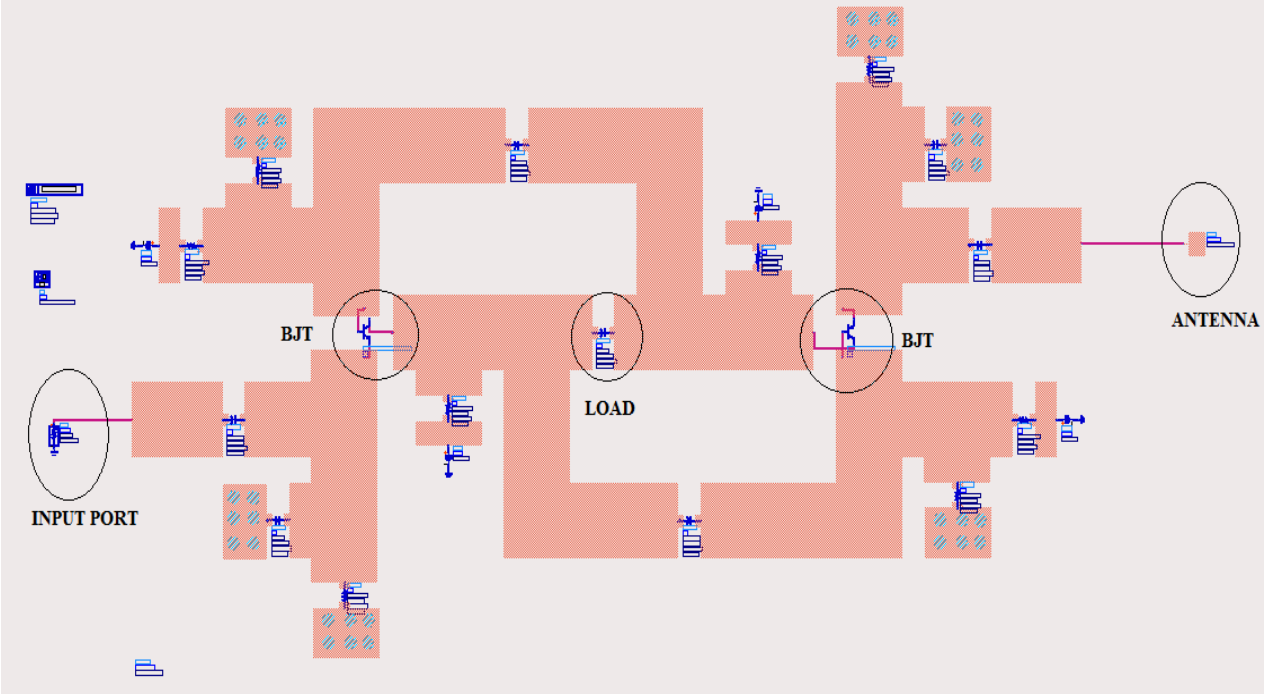

Fig.4.44: Antenna – NIC co simulation

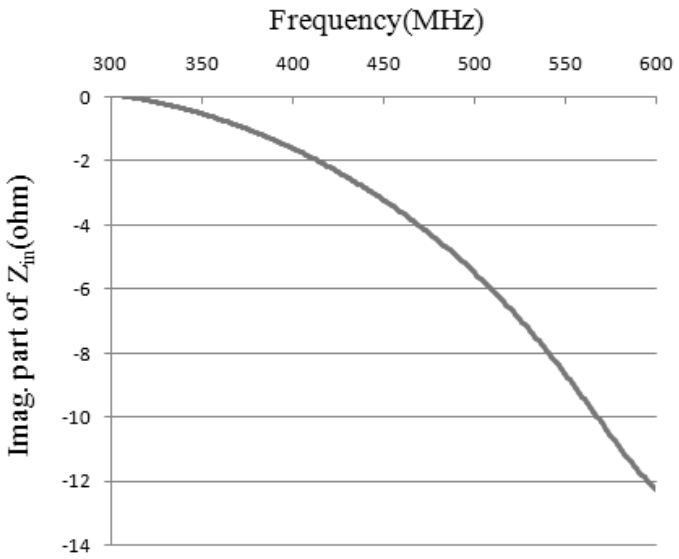

Fig.4.45: Imaginary part of the input impedance of the designed NIC circuit

The real part of the input impedance of the NIC circuit over the concerned frequency range is shown in Fig.4.46.

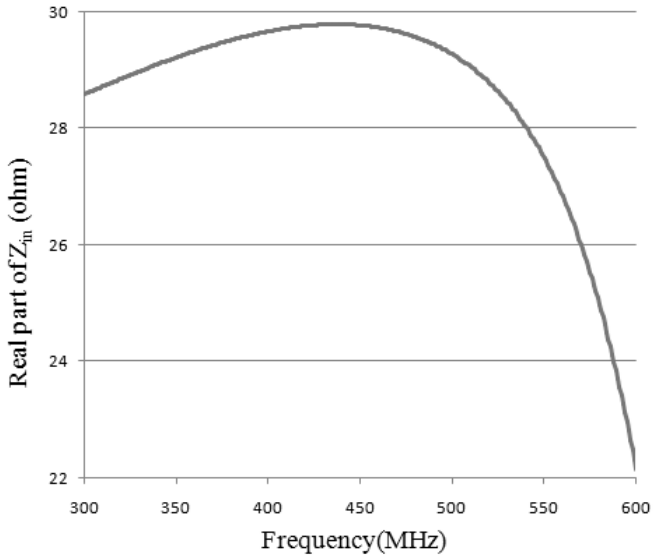

Fig.4.46: Real part of the input impedance of the designed NIC circuit

The imaginary part of the overall input impedance with and without the application of the NIC circuit is shown in Fig.4.47. From the figure it is clearly seen that with the application of the NIC circuit, a significant portion of the reactive part of the antenna impedance has been cancelled over the concerned range of frequency.

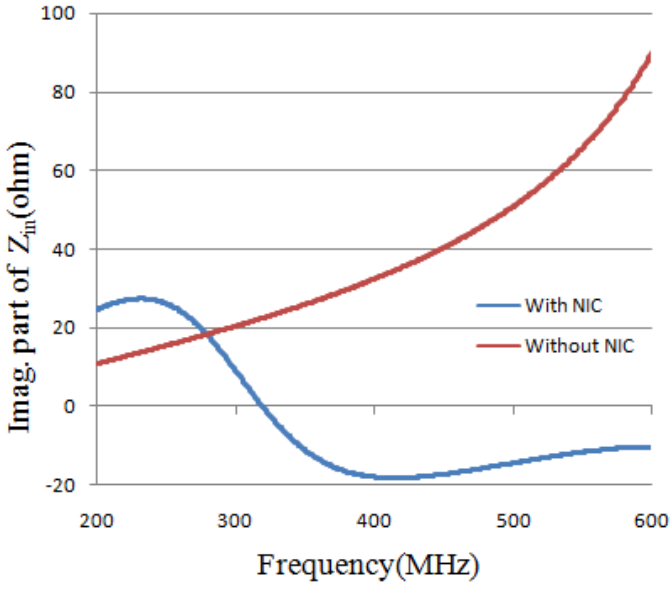

Fig.4.47: Imaginary part of the overall input impedance with and without the NIC circuit

Hence, we move to the S_{11} plot of the entire system to see if the matching has improved or not.

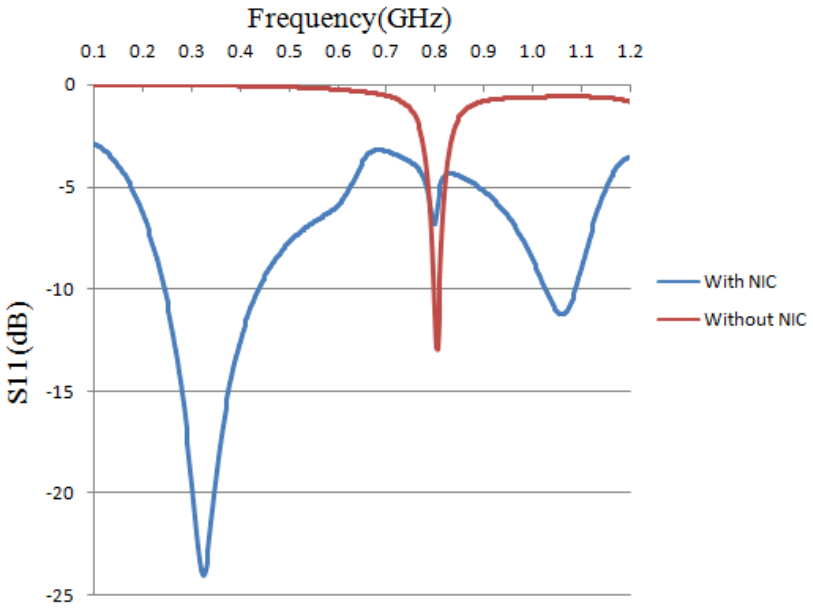

Fig.4.48: S_{11} of the system with and without the NIC circuit

The return loss of the overall system with and without the application of the NIC circuit is shown in Fig.4.48. Form the plot we can see that the matching of the antenna has significantly improved over the frequency range in which the antenna is electrically small including a dip of -24dB at 324.6 MHz and a matching bandwidth of about 200MHz (243MHz to 437MHz). The real part of the input impedance with and without the application of the NIC circuit is shown in Fig.4.49. From the figure it is clear that the overall real part has significantly improved with the application of the NIC circuit over the concerned range of frequency which plays an important role in improving the matching characteristics of the antenna at the source.

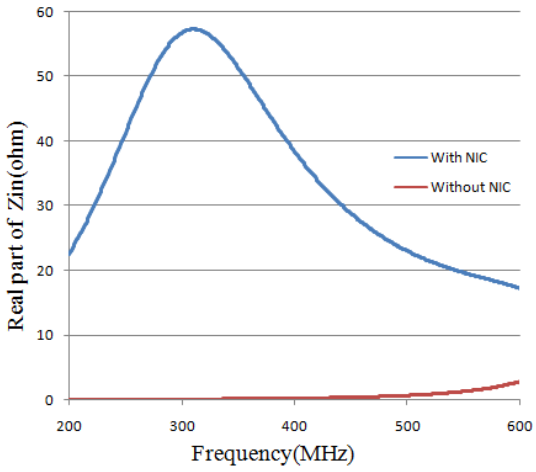

Fig.4.49: Real part of the overall input impedance with and without the NIC circuit

4.14 Fabrication and Testing

The fabricated NIC is shown in Fig.4.24 of Section-A. The antenna is fabricated on the same substrate as the NIC. The complete experimental setup is shown in Fig.4.50. The NIC circuit has been properly biased and grounded. The signal is fed to the antenna through the NIC as seen in the figure. The results are observed on a Vector Network Analyzer (VNA).

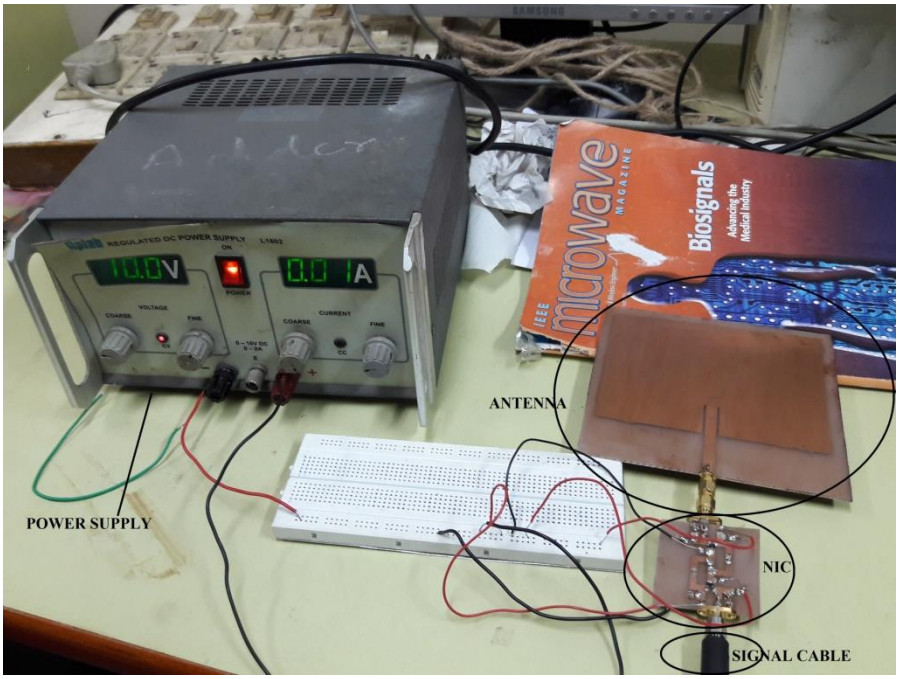

Fig.4.50: Antenna – NIC experimental setup

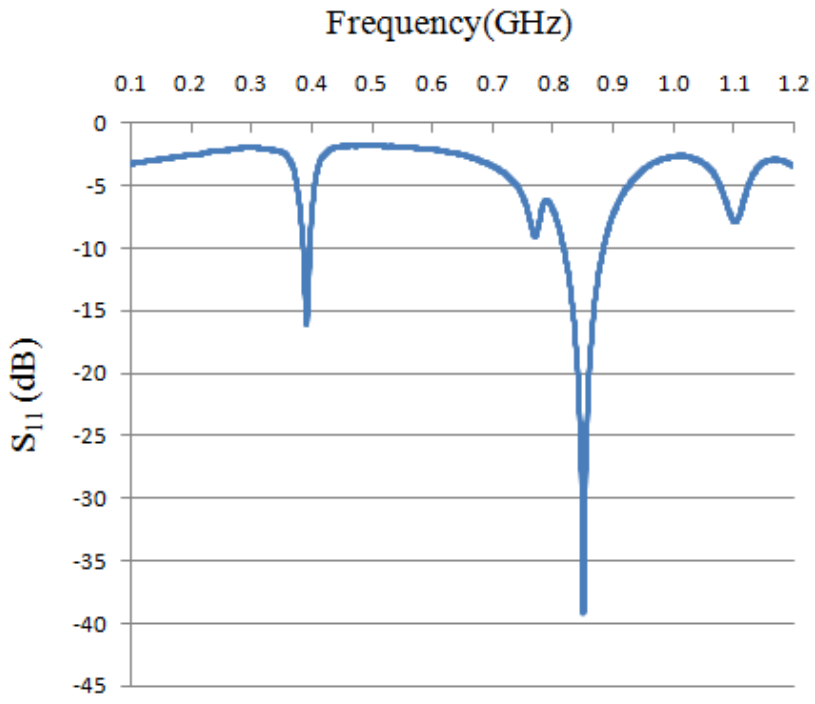

Fig.4.51: Measured S_{11} (dB) from VNA

Fig.4.51 shows the measured S_{11} (dB) plot of the overall system. From the measured results we can see that the matching characteristic has improved in the frequency range where the antenna is electrically small, including a dip of about -16dB at around 393MHz. The measured S_{11} plot of the system with and without the application of the NIC circuit is shown in Fig.4.52. The improvement in the real and imaginary part of the overall input impedance in comparison to that of the antenna is shown in Fig.4.53 and Fig.4.54 respectively.

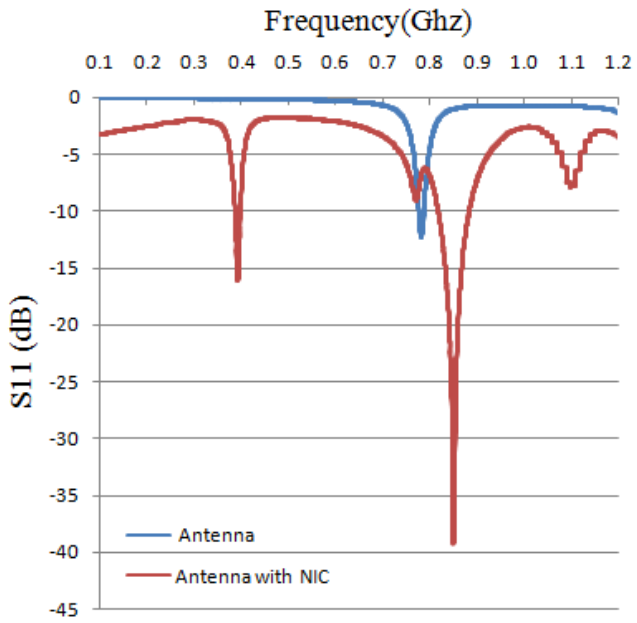

Fig.4.52: Measured S_{11} of the system with and without the NIC circuit

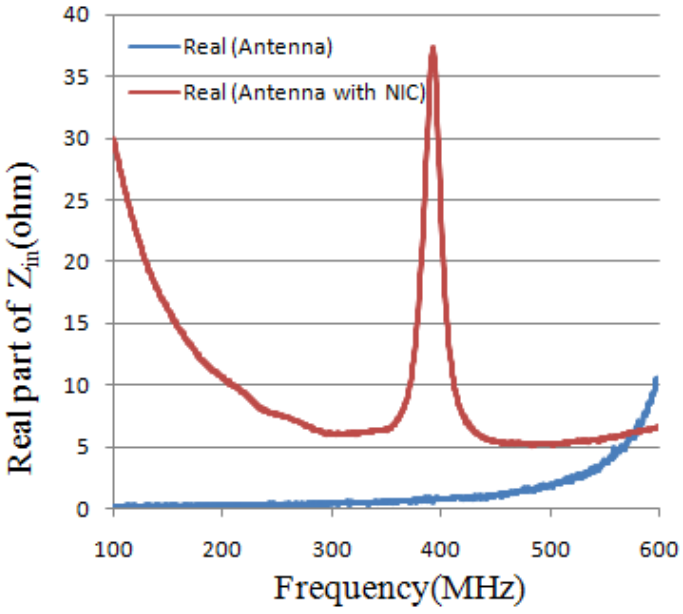

Fig.4.53: Measured real part of the overall input impedance with and without the NIC circuit

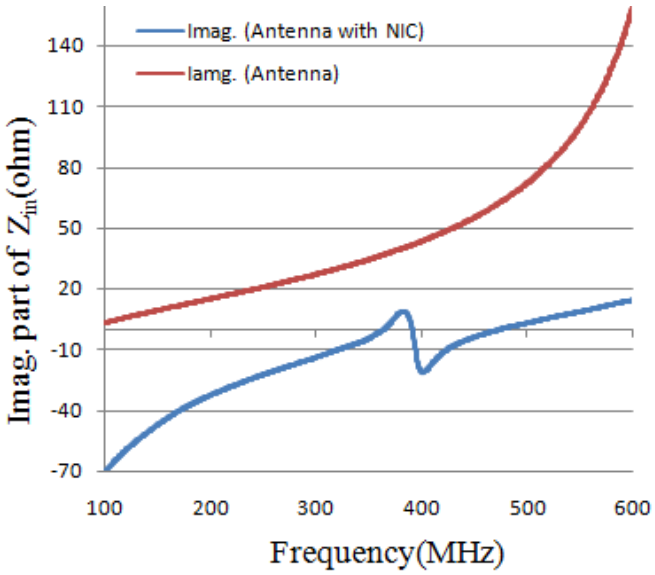

Fig.4.54: Measured imaginary part of the overall input impedance with and without the NIC circuit

4.15 Discussion and comparison of simulated and measured results

The concerned rectangular patch antenna was designed at 800 MHz. The dimension of the patch was found to be 118.5mm X 93.47mm. Hence the area of the patch becomes roughly 11076 square mm. Also, the patch was found to be electrically small up to 600 MHz. Thus the antenna was poorly matched to the source in the frequency range where it is electrically small. The main reason for poor matching was due to the fact that the antenna had very low real part and comparatively high imaginary part of the input impedance. Now, after the application of the negative impedance converter circuit, the overall antenna characteristics were studied. It was found that the real part of the input impedance was significantly improved and the imaginary part of the input impedance was brought down to a considerable value. As a result, the matching characteristic was significantly improved as well over the concerned frequency range. The simulated return loss (S_{11}) plot showed a matching bandwidth of about 200MHz (243MHz to 437MHz) with a dip of -24dB at 324.6 MHz. Now, if the same antenna was to be designed at 324.6 MHz, then the calculated dimension of the patch comes out to be around 293mm X 231mm. The calculated area of the patch comes out to be around 67683 square mm. Thus the test antenna having area 11076 square mm functions like an antenna having area 67683 square mm which corresponds to an area reduction of about 6 times. Thus using negative impedance converter to an electrically small antenna, broadband matching as well as a certain degree of miniaturization is obtained. Now the test antenna and the NIC circuit were fabricated on a FR4 substrate having dielectric constant 4.3 and substrate height of 1.6mm. The fabricated antenna and NIC are shown in previous figures. The entire system is properly tested and measured using a VNA. Fig.4.55 shows a comparison between the simulated and measured S_{11} (dB) plot of the overall system (i.e. antenna with NIC) in the frequency range where the antenna is electrically small. From

the figure we see that the operating frequency has shifted slightly from 324 MHz to 393 MHz and the 200 MHz broadband matching that was obtained in simulation was not obtained after

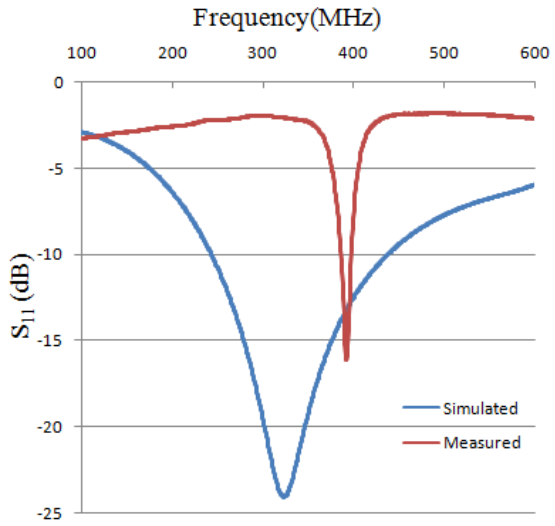

Fig.4.55: Simulated versus measured S_{11} of the overall system up to 600MHz

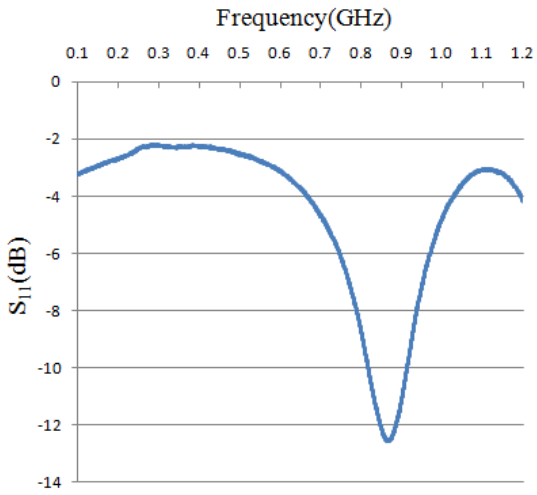

Fig.4.56: Measured S_{11} of the NIC

fabricating and testing the actual system. Now, some of the possible reasons could be the various parasitic effects that arise at high frequencies, frequency dependency of the elements that has been used in the NIC circuitry and mutual coupling between the transmission lines of the NIC and between the antenna and NIC. However both the simulated and measured results does validate the concept of using a NIC circuit to improve the matching characteristic of an electrically small antenna and lowering the operating frequency thereby reducing the dimension of the antenna. Now, from Fig.4.51 we see that the measured overall S_{11} plot shows two dips one at 393 MHz while the other at around 853MHz. Now the dip at 393MHz is expected after the application of the NIC but the dip at 853 MHz is not desired. For that the NIC is studied by applying a broadband load at the output port. The measured S_{11} of the NIC

is given in Fig.4.56. From the figure we see that the NIC itself has a resonance at around 850 MHz and no resonance around the 393MHz region. Also during the experiment it has been observed that by varying the bias voltage, the value in dB of the dip can be brought up or down depending on the increase or decrease of the bias voltage respectively. Thus it may be concluded that the dip at 393 MHz is because of the application of NIC to antenna (as expected) and the dip at 853MHz is a harmonic of the NIC itself.

4.16 Chapter Summary

This chapter is broadly classified into two sections. Section-A mainly focuses on the design of various types of NIC circuits. The NIC circuits can be divided into two based on their nature of application. They can either be grounded type having only one port or they can be of floating type having two ports, one for input and the other for output. In grounded type NIC, the impedance to be inverted is connected to ground. It basically functions as a one port network, required in applications which use it as a load, connected with the output port of another component. In floating type NIC, the impedance to be inverted is connected between the collector terminals of the two transistors. Floating type NIC is required in applications which use it as an intermediate or connecting stage between two components. Thus in Section-A, various topologies of grounded and floating NIC circuits are shown which are used to realize negative inductance and negative capacitance. And not only BJT based implementations but FET based implementations are also presented in a systematic way. The circuit schematics are followed by their respective real (resistive) and imaginary (reactive) part of the input impedance. Next a detailed analysis of the NIC topology that has been used in the current work is presented which includes effect of component variation and microstrip lines for generating a RF layout of the circuit. Also, the fabricated NIC circuit is presented in this section.

Section-B however completely deals with the application of the designed NIC to a test antenna. The test antenna is a rectangular microstrip patch antenna on a FR4 substrate. The antenna is designed at about 800 MHz. The antenna can be treated as electrically small up to 600 MHz. Now the antenna input impedance show very low real part and significantly high imaginary (reactive) part which is inductive in nature. Because of this feature, the antenna is poorly matched in the concerned frequency range. Now, to improve the matching characteristic of the antenna its input reactance is needed to be significantly brought down while compensating for its low input resistance. One of the techniques is to resonate the antenna using passive (Foster) elements, however a detailed study concerning this technique is provided in this chapter which clearly shows that this method fails to produce satisfactory results. Thus Non-Foster element realized by a NIC circuit is employed in this regard. The NIC circuit is appropriately designed and simulated with the antenna. Antenna-NIC co-simulations results show significant improvement in the real part and imaginary part of the

input impedance of the antenna. This improvement resulted in a significant improvement of the matching characteristics of the antenna. The antenna has been matched to the source over a broad range of frequency especially in the range where it is electrically small. Also the operating frequency of the antenna has been brought down (keeping the antenna dimension same) to achieve a degree of miniaturization. The antenna and the NIC circuit were fabricated and tested. Measured and simulated results were compared. The measured results validated and strengthened the concept.

Chapter 5

Application of NIC to new design

5.1 Chapter Overview

This chapter presents a detailed study of application of negative impedance converter on new design. Previously, application of NIC circuit to rectangular microstrip patch antenna was discussed. The corresponding antenna parameters were studied before and after the application of NIC circuit. Finally, the improvement in matching of the antenna with the application of NIC was shown and simulated and measured results were verified after fabrication. In this chapter, focus is primarily on new antenna designs and applying the NIC circuit to see the change in antenna parameters. Therefore, instead of the rectangular patch, a circular patch has been used. Section 5.2 presents a background and design procedure of circular patch in general. Section 5.3 presents the problem formulation and a detailed analysis along with it. Section 5.4 presents a detailed analysis of the antenna with Nic circuit. All the parameters are provided in the form of graphs and results are compared for better understanding. Section 5.5 presents an overall discussion on the work followed by summary.

5.2 Circular patch Antenna

Other than the rectangular patch, the next most popular configuration is the circular patch or disk. It also has received a lot of attention not only as a single element [80,81,82] but also in arrays [83] and [84]. By treating the patch, ground plane, and the material between the two as a circular cavity, the modes supported by the circular patch antenna can be found. As with the rectangular patch, the modes that are supported primarily by a circular microstrip antenna whose substrate height is small ($h \ll \lambda$) are TM_z where z is taken perpendicular to the patch. As far as the dimensions of the patch, there are two degrees of freedom to control (length and width) for the rectangular microstrip antenna. Therefore by changing the relative dimensions of the width and length of the patch (width-to-length ratio), the order of the modes can be changed. However, for the circular patch there is only one degree of freedom to control (radius of the patch, a). Doing this does not change the order of the modes; however, it does change the absolute value of the resonant frequency of each [85]. Other than using full-wave analysis [86,87], the circular patch antenna can only be analyzed conveniently using the cavity model [88,81,89]. This can be accomplished using a procedure similar to that for the rectangular patch but now using cylindrical coordinates [85]. The cavity is composed of two perfect electric conductors at the top and bottom in the form of the patch and the ground plane, and by a cylindrical perfect magnetic conductor around the circular periphery of the cavity. The dielectric material of the substrate is assumed to be truncated beyond the extent of

the patch. Based on the cavity model formulation, a design procedure is outlined which leads to practical designs of circular microstrip antennas for the dominant TM_{z110} mode.

The radius of the patch can be calculated using the following expression [90], here f_r (resonance frequency) is in Hz, and h (substrate height) is in cm

$$a = \frac{F}{\{1 + \frac{2h}{\pi\varepsilon_r F}\left[\ln\left(\frac{\pi F}{2h}\right) + 1.7726\right]\}^{\frac{1}{2}}} \qquad 5.1$$

Where,

$$F = \frac{8.791X\ 10^9}{f_r\sqrt{\varepsilon_r}} \qquad 5.2$$

The resonant frequency in the above equation does not take into account fringing. Fringing makes the patch look electrically larger and it should be taken into account. Thus for the circular patch a correction is introduced by using an effective radius a_e, to replace the actual radius *a*, given by [90]

$$a_e = a\{1 + \frac{2h}{\pi\varepsilon_r a}\left[\ln\left(\frac{\pi a}{2h}\right) + 1.7726\right]\}^{\frac{1}{2}} \qquad 5.3$$

5.3 Problem formulation and Analysis

Main focus is given on Circular Microstrip Patch Antennas. The test antenna is an inset feed circular microstrip patch antenna having the following specification: Substrate: FR4, Dielectric constant: 4, Loss tangent: 0.02, Substrate height: 1.6mm, Radius of patch: 25mm, Operating frequency: 1.74 GHz. The schematic is shown in Fig.5.1. The antenna is fed by a 50 ohm source at the input. Fig. 5.2 shows the S_{11} plot of the antenna in dB.

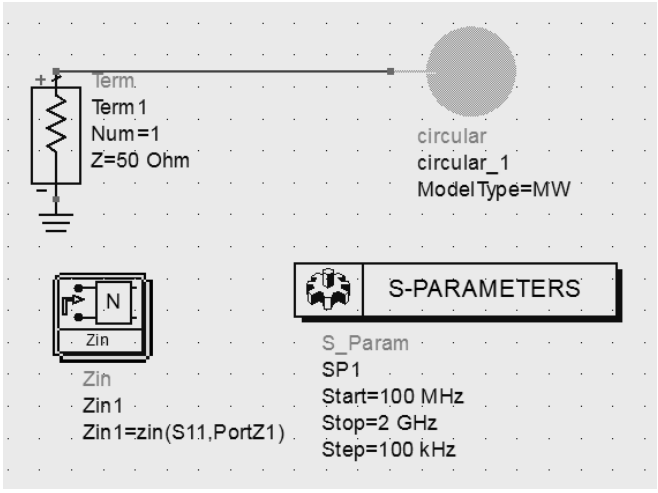

Fig.5.1: Antenna simulation schematic

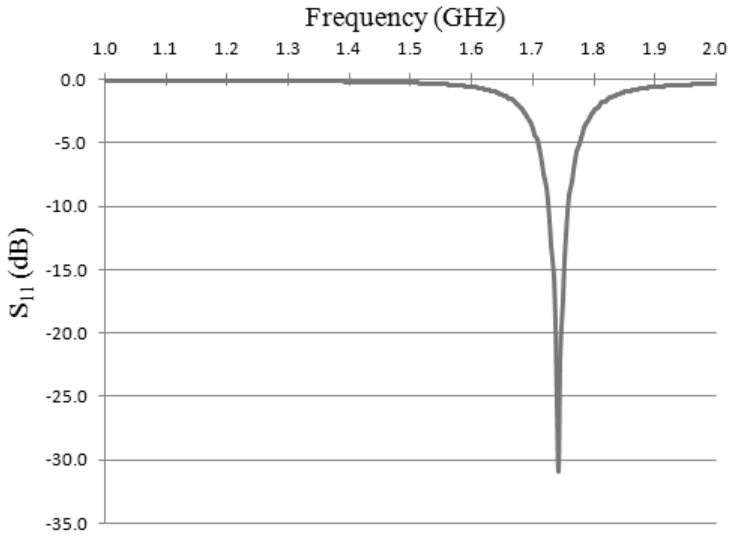

Fig.5.2: S_{11} (dB) of the antenna

The real (resistive) part and imaginary (reactive) part of the antenna impedance is shown in Fig.5.3 and Fig.5.4 respectively. Now, as far as antenna dimensioning using Chu's limit is concerned, the test antenna is electrically small (ka<1) up to 1100MHz. The real part of the antenna impedance is very low up to 1100MHz (for example between .5 ohm to 4.5 ohm between 400MHz to 1200MHz) whereas the reactive part of the impedance is comparatively high (for example between 20 ohm to 200 ohm between 400MHz to 1200MHz) as indicated by the following figures.

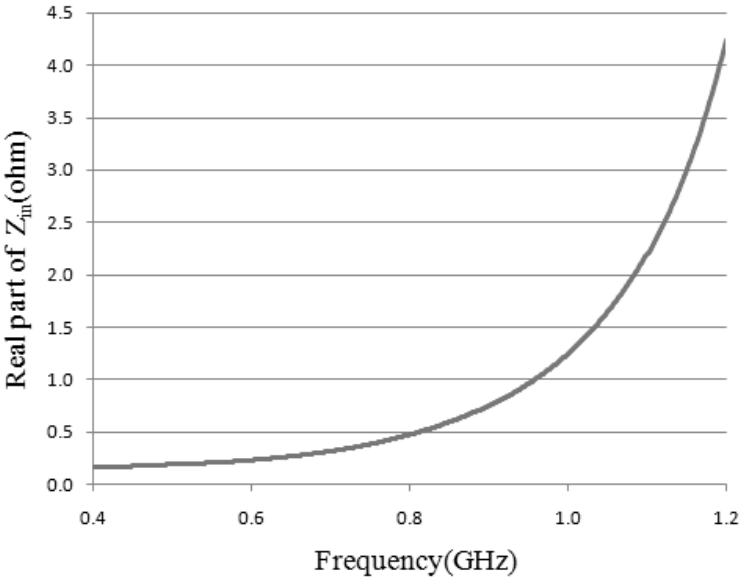

Fig: 5.3: Real part of the antenna impedance up to 1.2GHz

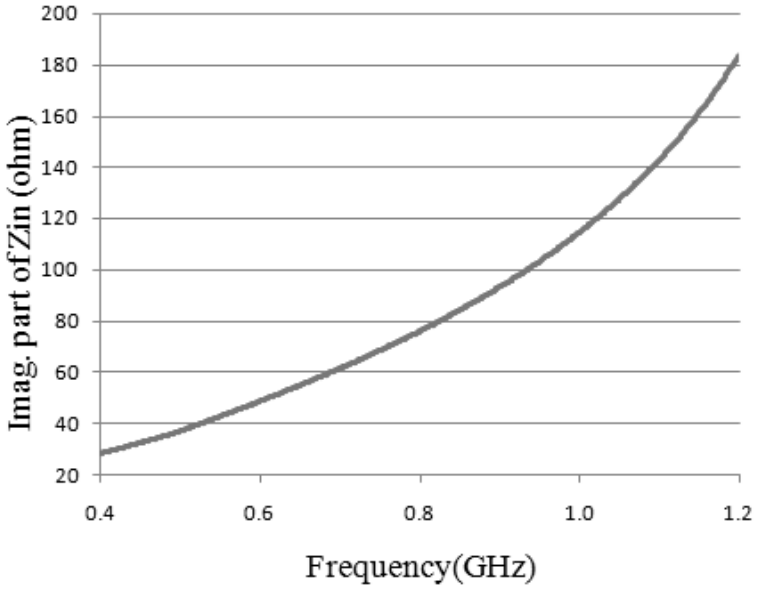

Fig: 5.4: Imaginary part of the antenna impedance up to 1.2GHz

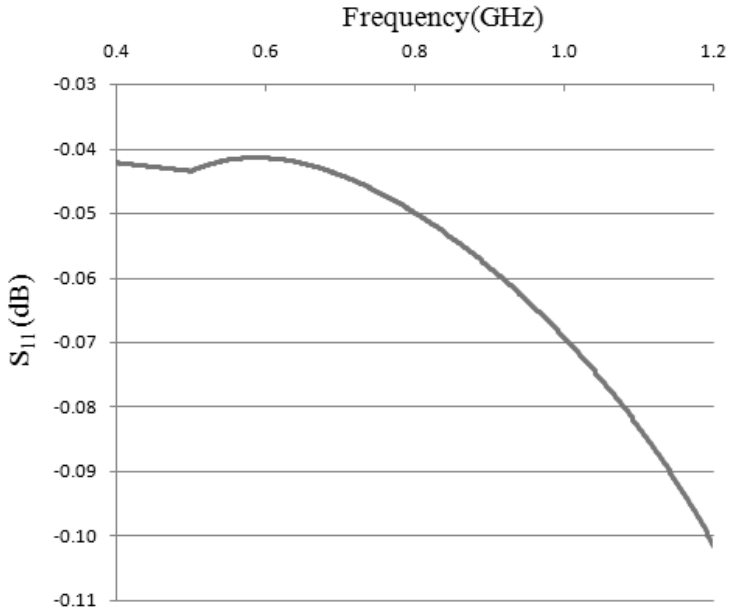

Fig.5.5: S_{11} (dB) of the antenna up to 1.2GHz

From Fig.5.5 it is clear that the antenna is very poorly matched within the frequency range in which it is electrically small. In Fig.5.4 we see that the behavior of the imaginary part of the antenna impedance is inductive in nature over the concerned frequency range. Thus one of the obvious techniques to improve the matching would be to cancel the reactive part. Now, in order to cancel the inductive reactance, a capacitive reactance is introduced. A particular frequency of 800MHz is chosen. From Fig.5.4 it is seen that the corresponding reactance is

76.082 ohm. So, a capacitor offering 2.62pF capacitance and a reactance of -76.028ohm is applied before the antenna as shown in Fig.5.6.

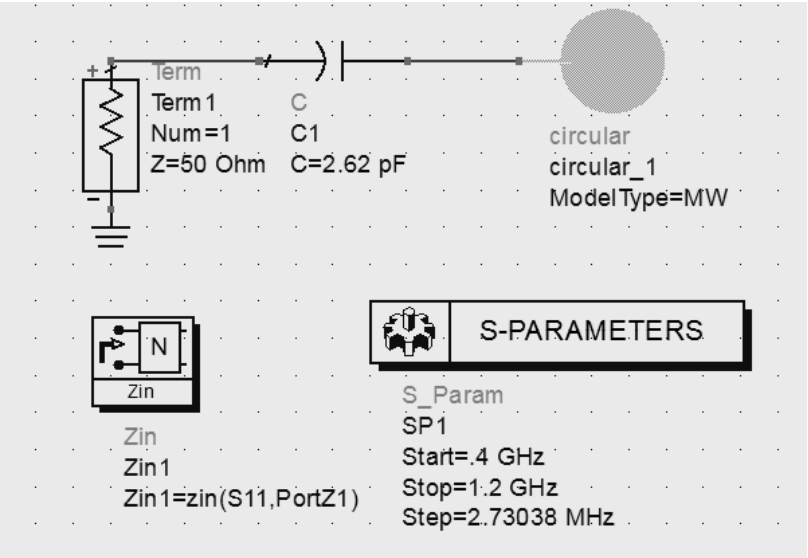

Fig.5.6: Antenna schematic with a 2.62pF capacitor

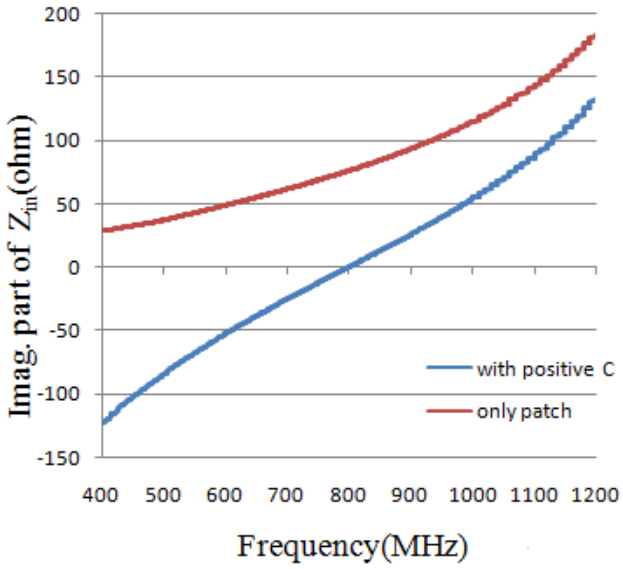

Fig: 5.7: Imaginary part of the input impedance up to 1200MHz with and without the application of 2.62pF capacitor

The imaginary part of the input impedance before and after the application of a 2.62pF capacitor is shown in Fig.5.7. It is clearly visible that with the application of the capacitor, the reactance at 800 MHz has been reduced nearly to zero. Hence, we move to the S_{11} plot of the entire system to see if the matching has improved or not.

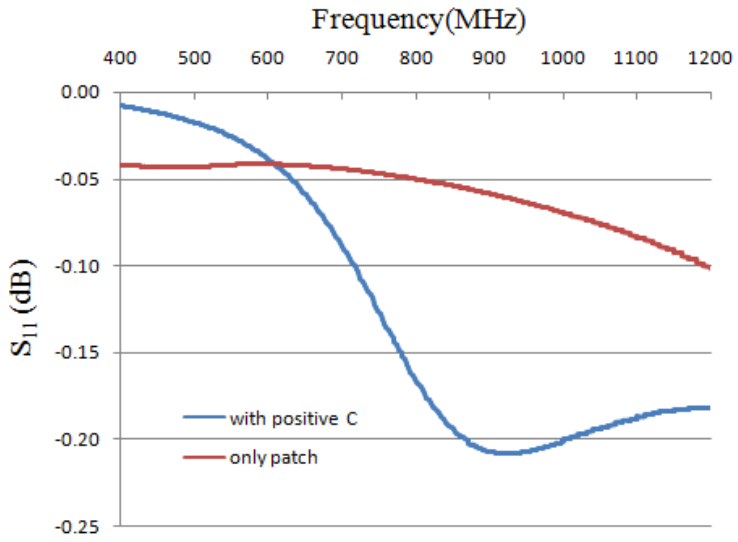

Fig.5.8: S_{11} (dB) of the system up to 1200MHz with and without the application of 2.62pF capacitor

The return loss of the antenna up to 1200MHz with and without the application of 2.62pF capacitor is shown in Fig.5.8. From the figure it is seen that although the imaginary part of the antenna impedance is nearly zero, the antenna is still poorly matched at 800MHz. This is because the real part of the antenna impedance experiences no change or improvement at all as seen in Fig.5.9. For the antenna to be properly matched at the source the imaginary part of the antenna impedance must be ideally zero and the real part of antenna impedance must be equal to that of the feed line (ideally 50 ohm).

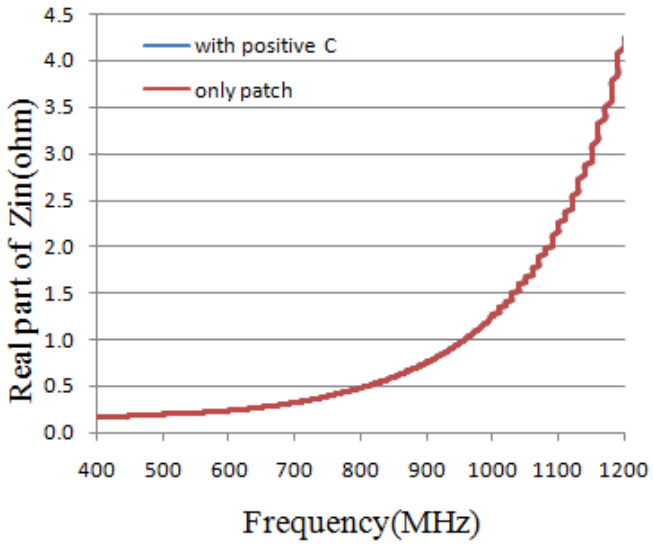

Fig: 5.9: Real part of the input impedance up to 1200MHz with and without the application of 2.62pF capacitor

Now, applying the concept of negative impedance an ideal negative inductor is used instead of the capacitor as shown in Fig.5.10. The calculated value of the inductor comes out to be -

15.1nH which offers a reactance of -76.028 ohm at 800MHz. The imaginary part of the input impedance before and after the application of the -15.1nH inductor is shown in Fig.5.11. The variation in the plot with respect to the previously applied 2.62 pF capacitor is also shown in the figure.

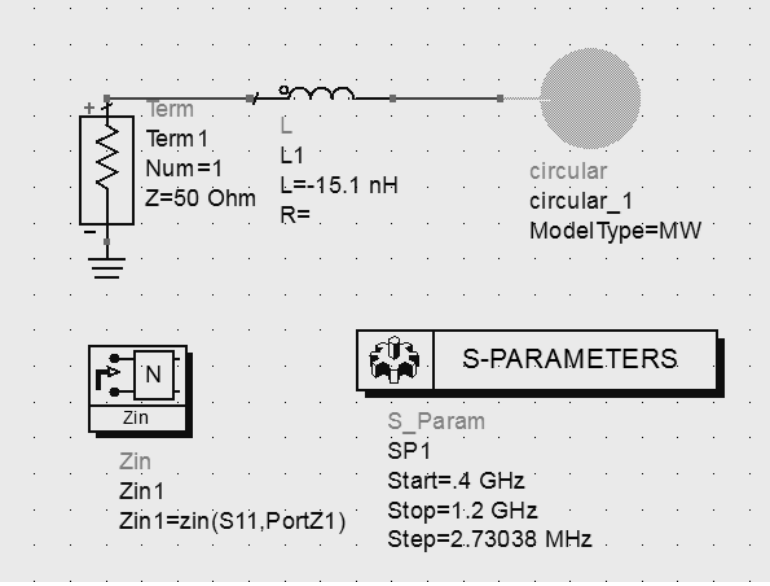

Fig.5.10: Antenna schematic with -15.1nH inductor

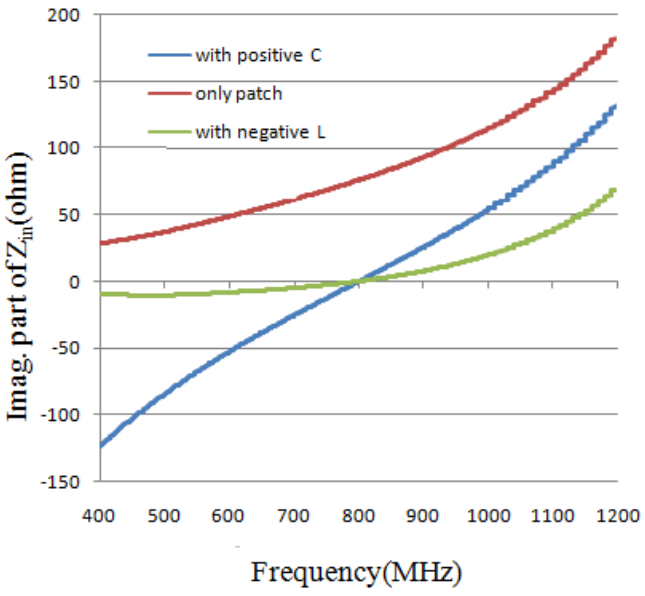

Fig: 5.11: Imaginary part of the input impedance up to 1200MHz with and without the application of -15.1nH inductor and 2.62pF capacitor

From Fig.5.11 it is clear that with the application of the ideal negative inductor, the reactive portion of the input impedance has been cancelled over a broad range of frequency compared to the positive capacitor which is effective only at a single frequency. Hence, we again move to the S_{11} plot of the entire system to see if the matching has improved or not. The return loss

of the antenna up to 1200MHz with and without the application of -15.1nH inductor (compared with the positive capacitor) is shown in Fig.5.12.

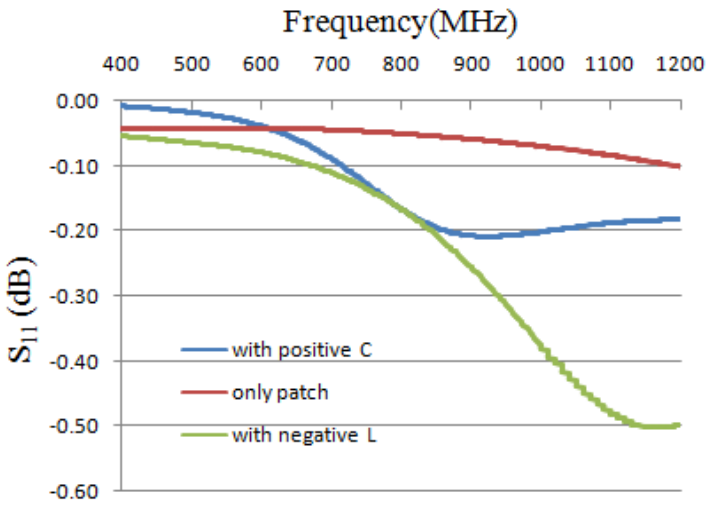

Fig: 5.12: S_{11} of the system up to 1200MHz with and without the application of -15.1nH inductor and 2.62pF capacitor

From the figure it is seen that although the imaginary part of the antenna impedance is nearly zero over a broad range of frequency, the antenna is still poorly matched at 800MHz. This is because once again the real part of the antenna impedance experiences no change or improvement at all as seen in Fig.5.13.

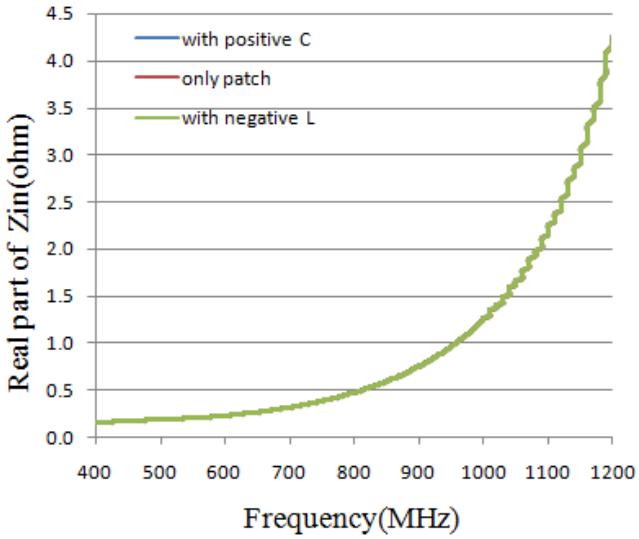

Fig: 5.13: Real part of the input impedance up to 1200MHz with and without the application of -15.1nH inductor and 2.62pF capacitor

From the above discussions it is clear that to cancel the reactive part of the antenna input impedance over a broad range of frequency, application of a negative element is essential. However that negative element alone is not able to improve the matching of the antenna to

the source. This is because the real part of the input impedance remains unaltered even after the application of the negative impedance.

In this regard, the negative impedance converter finds its requirement. As it is already discussed in chapter 4, the input impedance of NIC circuit has both real part and imaginary part. The imaginary part can be used to cancel the antenna reactance over a broad range of frequency while the real part can be utilized to better the real part of the overall input impedance. Thus the impedance matching is expected to improve at the source. Now, it is difficult to design a NIC circuit in which the imaginary part of the input impedance is the exact value of the reactance to be cancelled (at the desired frequency) while the real part of the input impedance is exactly 50 ohm. Hence, an optimum value should be chosen which satisfies the requirement of the problem.

5.4 Application of the designed NIC to the test antenna in the frequency range where it is electrically small

The following work targets the use of NIC circuit to improve the matching characteristics of the test antenna in the frequency range where it is electrically small. From the earlier discussions it is clear that the antenna is electrically small up to 1200MHz. The work includes design and simulation of the NIC circuit, design and simulation of the test antenna, application of NIC circuit to the antenna, antenna-NIC co-simulation, and observation of results. The NIC circuit follows the same circuit model as was shown in Fig.4.16. However, some of the component values were adjusted to meet the requirement of the problem. Fig.5.14 shows the antenna – NIC co simulation.

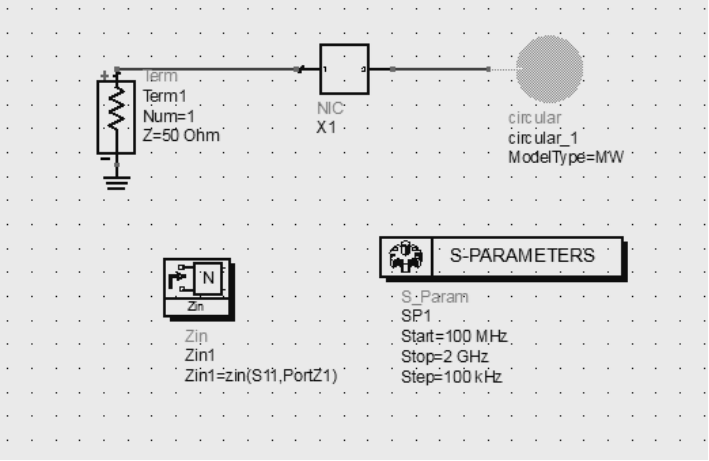

Fig.5.14: Antenna – NIC co simulation

Fig.5.15 shows the imaginary part of the input impedance of the NIC circuit alone. It is seen from the figure that the reactance is that of a negative inductor in the frequency range of

400MHz to 1200MHz. It is essential to have a negative inductor because the antenna input reactance follows the behavior of a positive inductor within the concerned frequency range.

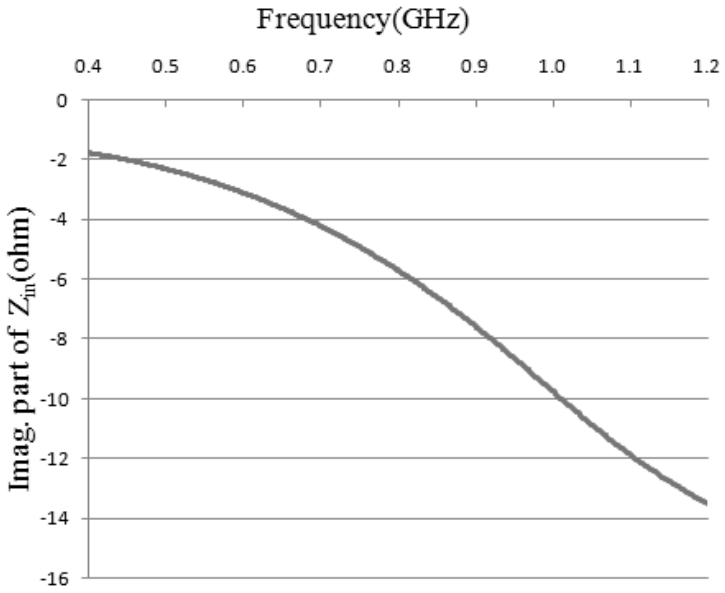

Fig.5.15: Imaginary part of the input impedance of the designed NIC circuit

The real part of the input impedance of the NIC circuit over the concerned frequency range is shown in Fig.5.16.

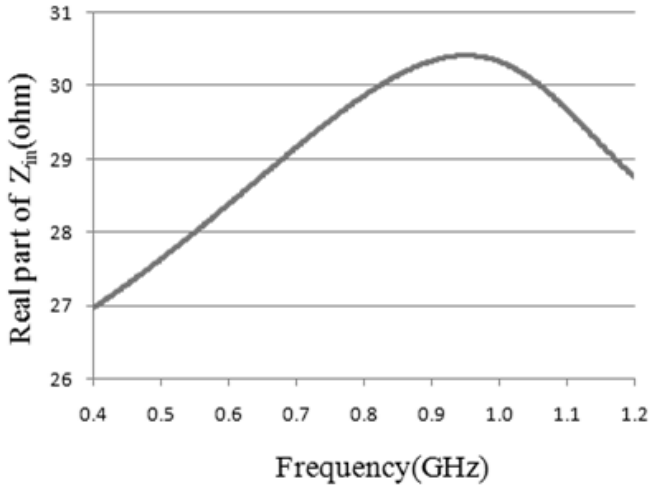

Fig.5.16: Real part of the input impedance of the designed NIC circuit

The imaginary part of the overall input impedance with and without the application of the NIC circuit is shown in Fig.5.17. From the figure it is clearly seen that with the application of the NIC circuit, a significant portion of the reactive part of the antenna impedance has been cancelled over the concerned range of frequency.

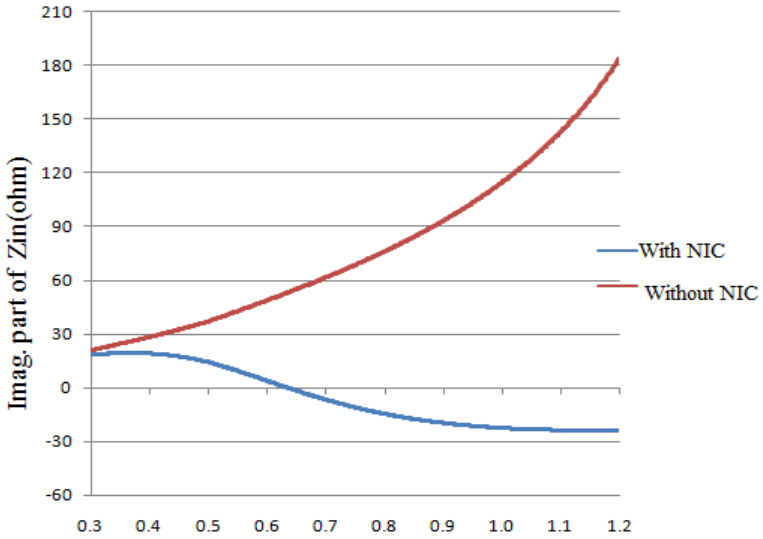

Fig.5.17: Imaginary part of the overall input impedance with and without the NIC circuit

Hence, we move to the S_{11} plot of the entire system to see if the matching has improved or not.

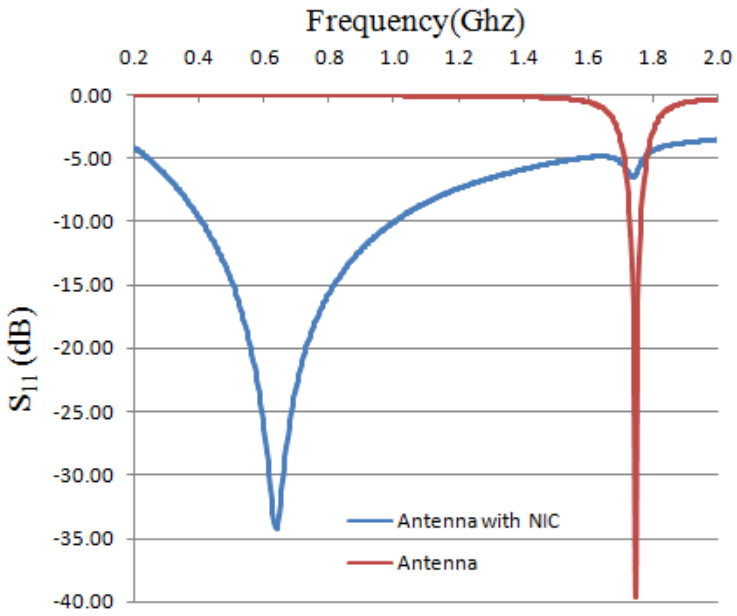

Fig.5.18: S_{11} of the system with and without the NIC circuit

The return loss of the overall system with and without the application of the NIC circuit is shown in Fig.5.18. Form the plot we can see that the matching of the antenna has significantly improved over the frequency range in which the antenna is electrically small including a dip of -34dB at 640 MHz and a matching bandwidth of about 600MHz (400MHz to 1000MHz). The real part of the input impedance with and without the application of the NIC circuit is shown in Fig.5.19. From the figure it is clear that the overall real part has

significantly improved with the application of the NIC circuit over the concerned range of frequency which plays an important role in improving the matching characteristics of the antenna at the source.

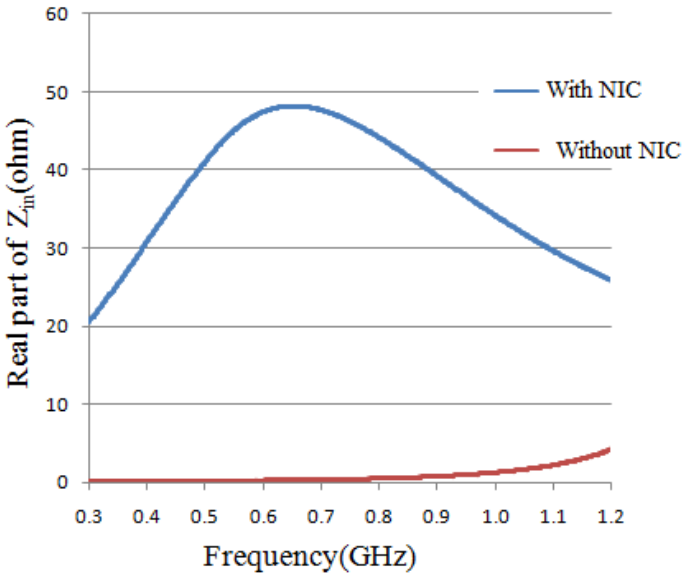

Fig.5.19: Real part of the overall input impedance with and without the NIC circuit

5.5 Discussion

The concerned circular patch antenna was designed at 1.74 GHz. The radius of the patch was found to be 25mm. Hence the area of the patch becomes 1962 square mm. Also, the patch was found to be electrically small up to 1100 MHz. Thus the antenna was poorly matched to the source in the frequency range where it is electrically small. The main reason for poor matching was due to the fact that the antenna had very low real part and comparatively high imaginary part of the input impedance. Now, after the application of the negative impedance converter circuit, the overall antenna characteristics were studied. It was found that the real part of the input impedance was significantly improved and the imaginary part of the input impedance was brought down to a considerable value. As a result, the matching characteristic was significantly improved as well over the concerned frequency range. The return loss (S_{11}) plot showed a matching bandwidth of about 600MHz (400MHz to 1000MHz) with a dip of -34dB at 640 MHz. Now, if the same antenna was to be designed at 640 MHz, then the calculated radius of the patch comes out to be around 66mm. The calculated area of the patch comes out to be around 13678 square mm. Thus the test antenna having area 1962 square mm functions like an antenna having area 13678 square mm which corresponds to an area reduction of about 7 times. Thus using negative impedance converter to an electrically small antenna, broadband matching as well as a certain degree of miniaturization is obtained.

5.6 Chapter Summary

The application of NIC circuit to a circular patch antenna has been studied in this chapter. The problem statement has been clearly formulated in the initial sections. The antenna can be treated as electrically small up to 1.2 GHz. The application of passive elements and their lack of significant contribution in matching have been clearly explained. The negative impedance converter characteristics have been explained through graphs. Then the NIC circuit is applied to the antenna and the changes in its matching characteristics are observed through graphs. Significant improvement in the real part and imaginary part of the input impedance of the antenna is observed. This improvement resulted in a significant improvement of the matching characteristics of the antenna. The antenna has been matched to the source over a broad range of frequency especially in the range where it is electrically small. Last but not least, a degree of miniaturization has been achieved as well.

Chapter 6

Conclusion and Future Work

6.1 Conclusion

This thesis looks into the background of Negative Impedance Converters and specifically deals with the application of NIC in electrically small antennas. The demand for miniaturized, broadband communication systems has created a need for electrically small, broadband antennas. There are many applications that require small wideband antennas, from mobile phones and devices (which are required to cover larger frequency bands) to cognitive radios that are expected to operate within any frequency band with minimum reconfiguration. Chapter 1 presents a detailed overview of small antennas in general. It provides the basic definition of small antennas and shows that based on different requirements, small antenna can be categorized into various types. It looks into the necessity of small antennas in general. It presents the areas where small antennas have been used previously and also the areas that require the services of small antennas. It also deals with the theoretical limitations of small antennas and how they are different from normal free space antennas and presents various methods of obtaining small antenna.

Chapter 2 deals with a detailed review of various papers, journals and thesis related to the concerned work. It presents a brief history on antennas, antenna evolution over the years and electrically small antennas. It also presents a brief study on characterization and modeling of electrically small antennas, limitations of electrically small antennas and how researchers have dealt with those limitations. It throws some light on how NICs have been used by the researchers along with electrically small antennas to better its performance. Finally it presents a review of various works on noise considerations of NICs and stability analysis of electrically small antennas with negative impedance converters.

Chapter 3 presents a theoretical overview of electrically small antennas and negative impedance converters supported by mathematical modeling. Since the antenna dimension is frequency dependent, an antenna can be considered electrically small only up to a particular range of frequency. The general representation of electrically small antennas along with mathematical expressions is discussed in this chapter. Electrically small antennas are characterized by high quality factor which makes them narrow band. Also, their input impedance is highly reactive and less resistive which makes them difficult to match. Conventional networks with elements obeying Foster's reactance theorem, provide only spot frequency matching. However, Non- Foster elements helps to combat this limitation. Non-Foster elements are not usual as they do not follow the Foster's reactance theorem. Non-Foster elements have a reactance that decreases with frequency. Non-Foster elements are

realized using negative impedance converters (NIC). With the help of NICs, it is possible to generate negative reactance which does not obey Foster's reactance theorem. Linvill first proposed the design of NIC circuit based on BJT. Since then, various floating and grounded topologies have been used by researchers in matching of electrically small antennas. However, active devices suffer from instability. Therefore stability analysis is essential before application to antennas. Using these elements it became possible to cancel the reactive part of the input impedance over a broad range of frequency thereby attaining a broadband matching. Also, these elements can also be used within the antenna structure to achieve a controlled resistance at the input. Since the reactive part of the impedance is reduced over a desired frequency range, the quality factor also reduces which in turn increases the bandwidth. Thus, using negative impedance converters broadband matching is achieved and this has significantly contributed to the development of various small antennas.

Chapter 4 is broadly classified into two sections. Section-A mainly focuses on the design of various types of NIC circuits. The NIC circuits can be divided into two based on their nature of application. They can either be grounded type having only one port or they can be of floating type having two ports, one for input and the other for output. In grounded type NIC, the impedance to be inverted is connected to ground. It basically functions as a one port network, required in applications which use it as a load, connected with the output port of another component. In floating type NIC, the impedance to be inverted is connected between the collector terminals of the two transistors. Floating type NIC is required in applications which use it as an intermediate or connecting stage between two components. Thus in Section-A, various topologies of grounded and floating NIC circuits are shown which are used to realize negative inductance and negative capacitance. And not only BJT based implementations but FET based implementations are also presented in a systematic way. The circuit schematics are followed by their respective real (resistive) and imaginary (reactive) part of the input impedance. Next a detailed analysis of the NIC topology that has been used in the current work is presented which includes effect of component variation and microstrip lines for generating a RF layout of the circuit. Also, the fabricated NIC circuit is presented in this section. Section-B of chapter 4 however completely deals with the application of the designed NIC to a test antenna. The test antenna is a rectangular microstrip patch antenna on a FR4 substrate. The antenna is designed at about 800 MHz. The antenna can be treated as electrically small up to 600 MHz. Now the antenna input impedance show very low real part and significantly high imaginary (reactive) part which is inductive in nature. Because of this feature, the antenna is poorly matched in the concerned frequency range. Now, to improve the matching characteristic of the antenna its input reactance is needed to be significantly brought down while compensating for its low input resistance. One of the techniques is to resonate the antenna using passive (Foster) elements, however a detailed study concerning this technique is provided in this chapter which clearly shows that this method fails to

produce satisfactory results. Thus Non-Foster element realized by a NIC circuit is employed in this regard. The NIC circuit is appropriately designed and simulated with the antenna. Antenna-NIC co-simulations results show significant improvement in the real part and imaginary part of the input impedance of the antenna. This improvement resulted in a significant improvement of the matching characteristics of the antenna. The simulated return loss (S_{11}) plot showed a matching bandwidth of about 200MHz (243MHz to 437MHz) with a dip of -24dB at 324.6 MHz. The antenna has been matched to the source over a broad range of frequency especially in the range where it is electrically small. Also the operating frequency of the antenna has been brought down (keeping the antenna dimension same) to achieve a degree of miniaturization. The antenna and the NIC circuit were fabricated and tested. Measured and simulated results were compared. The measured results validated and strengthened the concept.

The application of NIC circuit to a circular patch antenna has been studied in chapter 5. Previously, application of NIC circuit to rectangular microstrip patch antenna was discussed. The corresponding antenna parameters were studied before and after the application of NIC circuit. Finally, the improvement in matching of the antenna with the application of NIC was shown and simulated and measured results were verified after fabrication. In this chapter, focus is primarily on new antenna designs and applying the NIC circuit to see the change in antenna parameters. Therefore, instead of the rectangular patch, a circular patch has been used. The problem statement has been clearly formulated in the initial sections. The antenna can be treated as electrically small up to 1.2 GHz. The application of passive elements and their lack of significant contribution in matching have been clearly explained. The negative impedance converter characteristics have been explained through graphs. Then the NIC circuit is applied to the antenna and the changes in its matching characteristics are observed through graphs. Significant improvement in the real part and imaginary part of the input impedance of the antenna is observed. This improvement resulted in a significant improvement of the matching characteristics of the antenna. The return loss (S_{11}) plot showed a matching bandwidth of about 600MHz (400MHz to 1000MHz) with a dip of -34dB at 640 MHz. The antenna has been matched to the source over a broad range of frequency especially in the range where it is electrically small. Last but not least, a degree of miniaturization was achieved as well.

6.2 Future Work

An important aspect of every thesis is the work that can be done in future from the concepts highlighted and work done in the thesis. This thesis being no exception highlights the areas that need improvement and also presents some interesting areas where the concepts

that have been discussed can be applied in future by the fellow readers. This section particularly highlights some areas where further work can be done in future.

6.2.1 Application of NIC in circularly polarized, dual polarized antennas

Till now almost all works on NIC matched electrically small antennas have been on linearly polarized antennas. The work presented in this thesis is also based on linearly polarized antennas. Compared to linear polarization, circular polarization has less polarization loss. Since circular polarized antennas send and receive in all planes, the signal strength is not lost but is transferred to a different plane and is still utilized. As a result circularly polarized antennas give a higher probability of a successful link. Circularly polarized signals are much better at penetrating and bending around obstructions. Thus it would be interesting to see the effects of NIC in circularly polarized antennas particularly in terms matching, gain, radiation efficiency and axial ratio. Dual polarized antenna can be used of two separate communication purpose. When the available space is limited, the use of a dual polarized antenna is more suitable that two separate antennas. Thus the application of NICs to dual polarized antennas can be treated as future work. Also NICs can be applied to ultra wideband systems for various applications for 5G communication.

6.2.2 Using different feeding methods

The antennas that have been used in this work are all inset fed. However CPW-fed (coplanar waveguide) planar antennas have gained much attention nowadays, due to their promising characteristics showing wider impedance bandwidth, lesser radiation loss, easier fabrication, lower profiles, and better integration performances with RF circuits and systems. In CPW-fed planar antennas ground and signal are both on the top layer making them accessible for wire bonds or other transitions. Thus the application of NIC to CPW-fed antennas can be treated as an interesting research field. The change in the input impedance, matching characteristics, radiation pattern and gain can be studied with and without the application of the NIC circuit.

6.2.3 NIC design constraints for miniature antennas

The antenna dimension considered in this thesis was not comparable to the dimension of the NIC circuit but somewhat larger. But as the antenna operating frequency goes higher, the antenna dimension becomes even smaller. Now, if the antenna dimension becomes comparable with the dimension of the NIC circuit, coupling effects will arise which will degrade the system performance. One of the immediate solutions to this problem would be to reduce the size of the NIC circuit even further. However, in RF layout there are some design constraints which are needed to be followed and hence the dimension of the NIC circuit

cannot be reduced abruptly. Thus one needs to find out the optimum design dimension of the NIC circuit when the size of the antenna becomes comparable to the size of the NIC circuit.

6.2.4 Integrated Non-Foster Impedances

It is well known that active circuits composed of discrete transistors and components have a limitation to operate at high frequencies due to parasitics and the electrically large size of the layout. It would be highly recommended to design and fabricate integrated-version Non-Foster impedances for antenna applications, especially, loading Non-Foster impedances for compact antennas. Therefore, the integrated version of negative impedance converters is feasible solutions to extend the operation of Non-Foster impedances to much higher and wider operating frequencies. Some works were done previously with Non-Foster loaded antennas but to a small extent. Therefore proper design and fabrication of Non-Foster loaded antennas can be considered as an interesting research field. A Non-Foster matched antenna and a Non-Foster loaded antenna can be compared to see which design concept provides better results and a comparative study can be done. Also, Non-Foster loaded antennas can be developed for specialized applications.

6.2.5 Low power Non-Foster Impedances

Unlike passive elements, Non-Foster elements consume DC power because they rely on active devices such as transistors. It can be considered a drawback in using Non- Foster impedances, when comparing to passive elements. It is important to consider low power NICs or NIVs in designing Non-Foster impedances. The easiest way to solve the power issue is to use low power transistors. The solution comes back to the integrated version of NICs or NIVs because lower power is easier to achieve with integrated circuits relative to discrete circuits. Sussman-Fort in [25,31] used a figure of merit for the power efficiency, η, to consider DC power biasing of active circuits in a transmitter application. In [25,31] the efficiency of the Non-Foster impedance was expressed as

$$\eta_{\text{active}} = \frac{P_{\text{ant}}}{P_{\text{Dc-active}}} \qquad 6.1$$

Here, $P_{DC-active}$ = DC power biasing NIC + DC power for a transmitter, and P_{ant} is the power delivered to the antenna. According to [91], equation 6.1 could be overvalued because the RF input power is not considered in this definition. Hence, it could be better to use the power added efficiency instead of the power efficiency defined above. The power added efficiency (PAE) is given by [91]

$$\eta_{\text{PAE}} = \frac{P_{\text{out}} - P_{\text{in}}}{P_{\text{Dc}}} \qquad 6.2$$

When using a Non-Foster impedance in a transmitter antenna, the power added efficiency can be written as

$$\eta_{\mathrm{PAE}} = \frac{\mathrm{P_{ant}} - \mathrm{P_{in}}}{\mathrm{P_{Dc-active}}} \qquad 6.3$$

In a receiver application, the total (overall) efficiency could be used to measure the efficiency of an active circuit. The total (overall) efficiency is given by

$$\eta_{\mathrm{total}} = \frac{\mathrm{P_{out}}}{\mathrm{P_{in}} + \mathrm{P_{Dc-active}}} \qquad 6.4$$

Appendix A

Software Overview

A.1 Introduction to Advanced Design System

Advanced Design System (ADS) has been used to perform all the designs and simulations in this thesis. Advanced design system (ADS) is an electronic design automation software that was produced by Keysight EEsof EDA. It provides an integrated design environment to designers of RF electronic products. Keysight ADS supports every step of the design process - schematic capture, layout, design rule checking, frequency domain and time domain circuit simulation and electromagnetic field simulation. The version used in this thesis is ADS 2009.

A.2 Advanced Design System setup and working

Advanced design system has a very simple user interface. The two main parts of ADS are the schematic window and the layout window. In the schematic the circuit level representation of every component is available. In the layout window a circuit board layout of the component (created in the schematic window) can be developed. First, a new project is to be created to open its corresponding schematic window. The project is specified by its name, location and standard length unit as shown in the Fig.A.1.

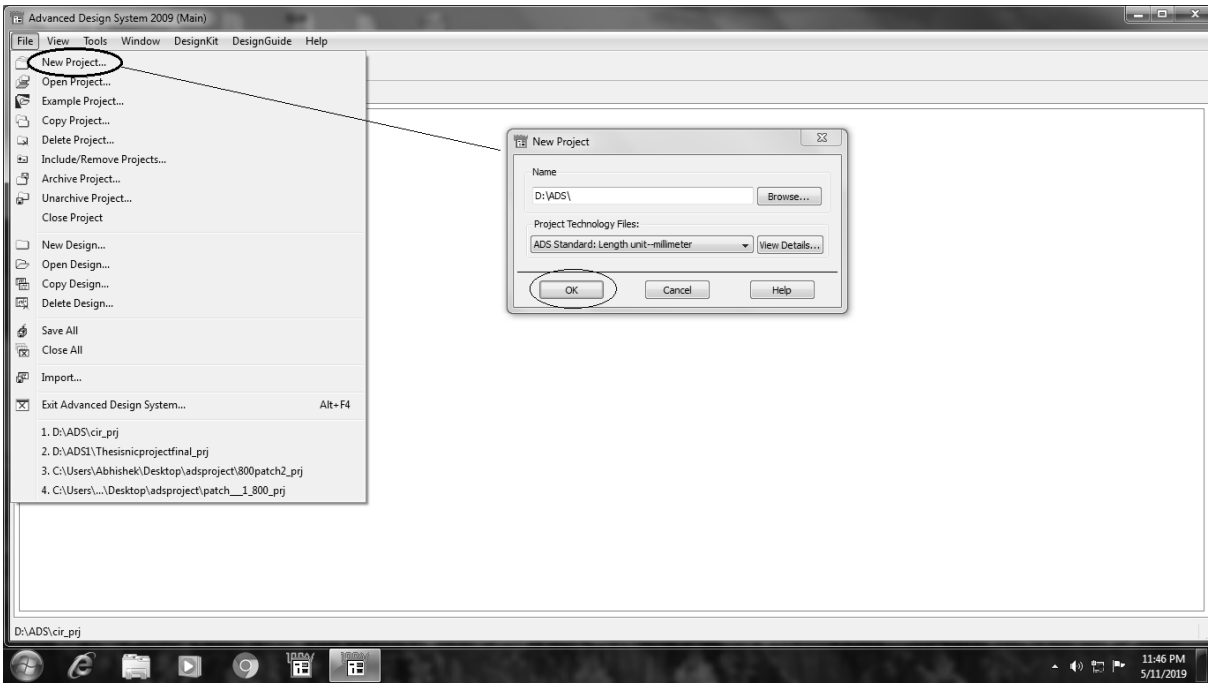

Fig.A.1: New project in ADS

The schematic window in shown in Fig.A.2 showing its various tools like component palette where all the lumped components are available, the simulator tool, tuning and optimizing tool etc. The S-parameter controller and the data display window are shown in Fig.A.3.

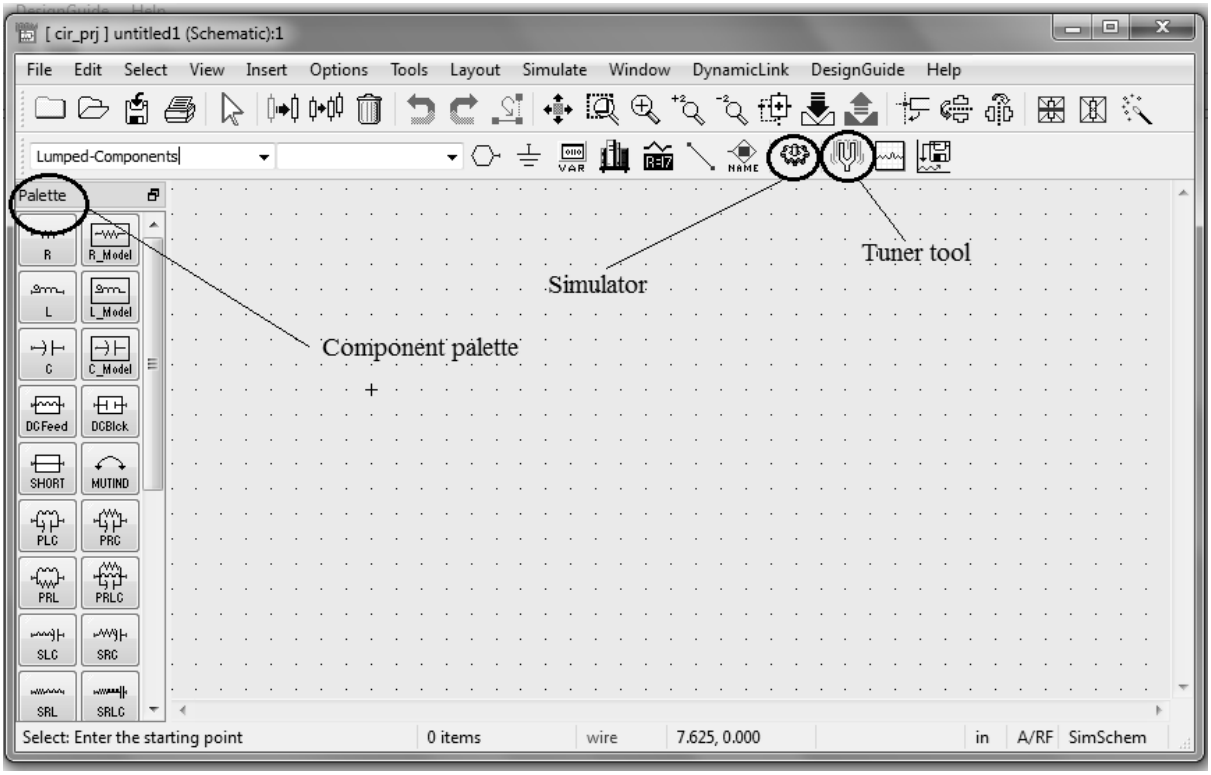

Fig.A.2: Schematic window in ADS

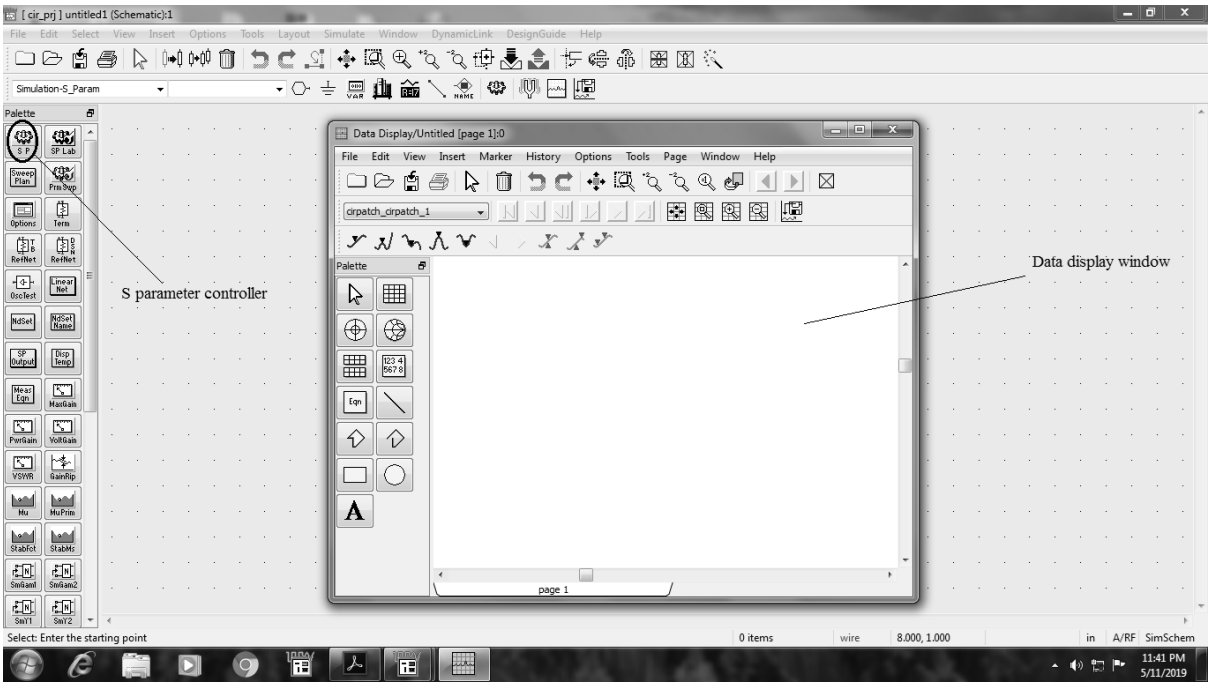

Fig.A.3: Data display window in ADS

The layout window is shown in Fig.A.4. In the layout, the electromagnetic simulations are performed by the momentum operator. First the substrate is defined by providing the basic parameters such as thickness, permittivity, loss tangent etc. as shown in the fig.

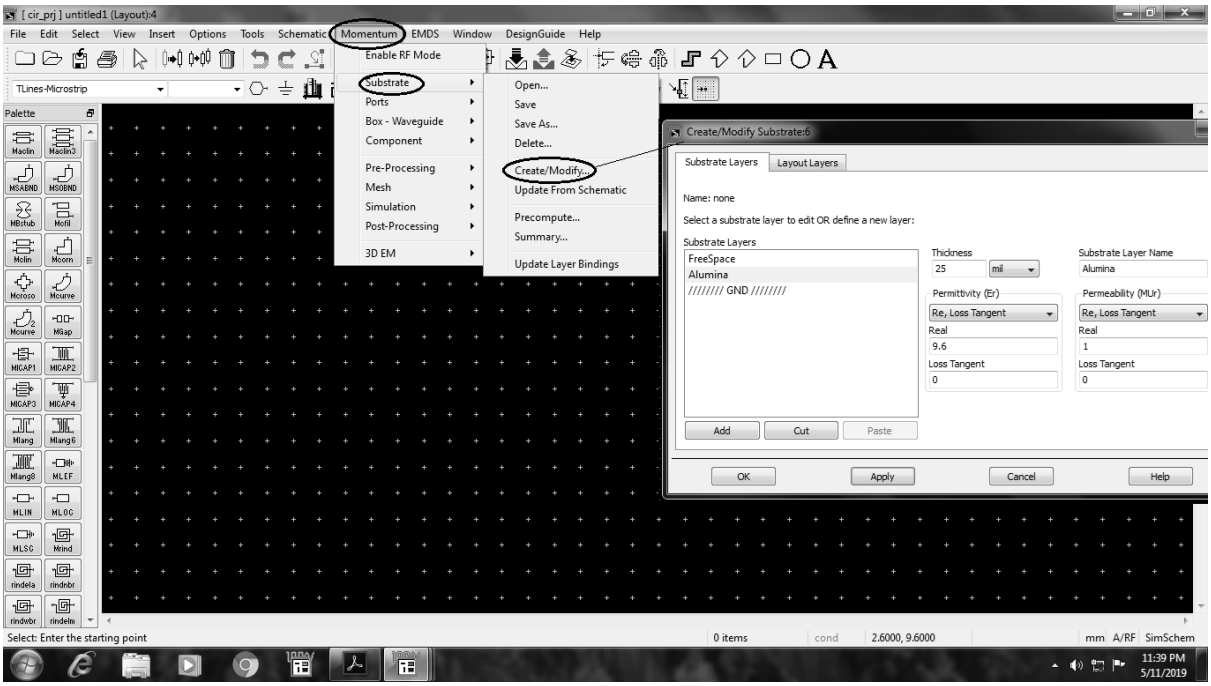

Fig.A.4: Layout window in ADS

The simulation window is ADS layout is shown in Fig.A.5. The start, stop and step frequency has to be provided for proper simulation. Results are displayed in the data display window.

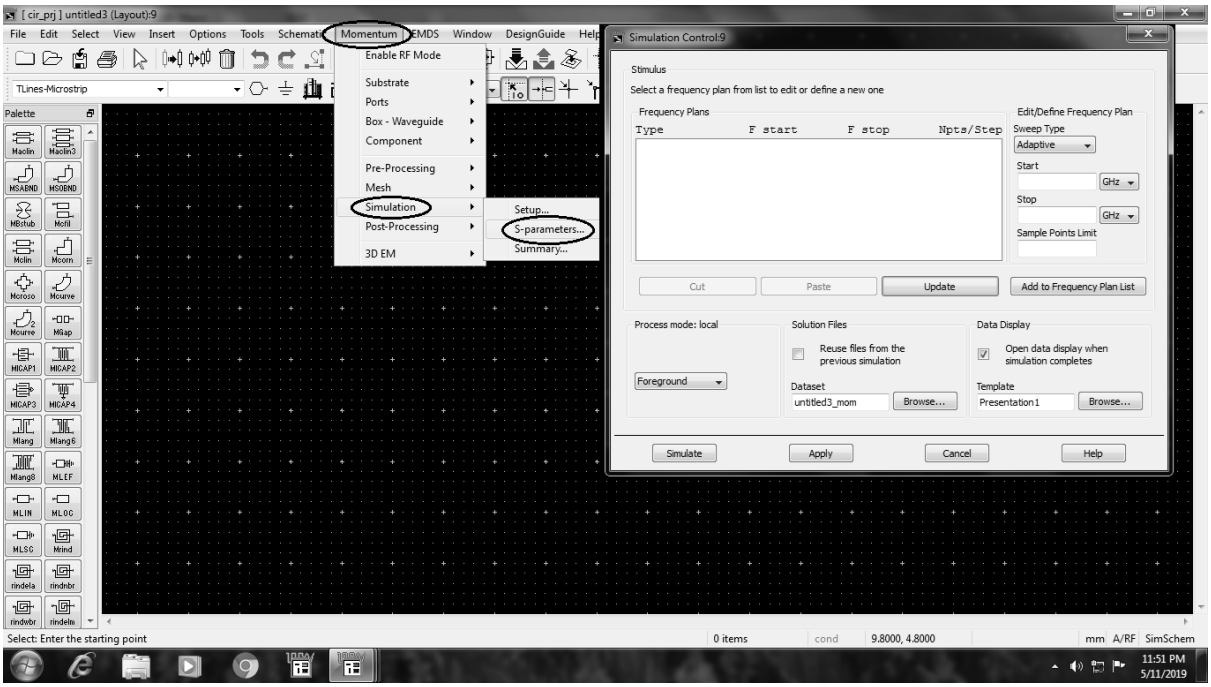

Fig.A.5: Simulation window in ADS

A.3 Introduction to IE3D

ZELAND IE3D has been used for the basic design of the rectangular patch and circular patch antennas. IE3D is based on MoM solutions of integral equation which has an excellent accuracy for frequency domain analysis. The version that has been used in this thesis is IE3D version 12. It offers EM simulations for structures with results ranging from S-parameters for simple designs and far-field plots for antennas.

A.4 Setup and working of IE3D

The antenna design and simulation is done in the Mgrid window. The Mgrid window is shown in Fig.A.6. In the Mgrid window, a new project is created of design and simulation. The basic parameters are defined at first as shown in Fig.A.7. The basic parameters include substrate definition, substrate height, dielectric constant and loss tangent.

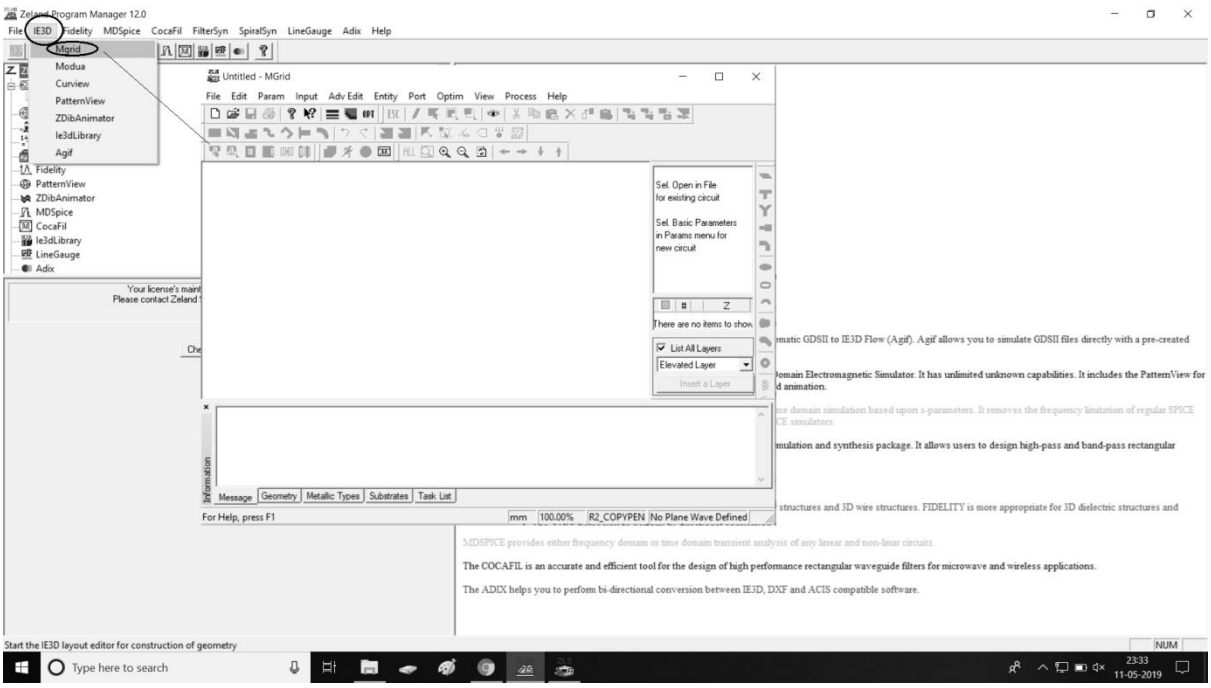

Fig.A.6: Mgrid window in IE3D

The antenna design window is shown in Fig.A.8. Various design options are also shown. Antenna of different geometrical shapes can be designed. The port options and simulation tool are also showed. The simulation setup is shown in Fig.A.9. The start, stop and step frequency should be carefully defined. There are options to view the S-parameters, current distribution and radiation pattern separately. For the radiation pattern the range of theta and phi should be carefully defined.

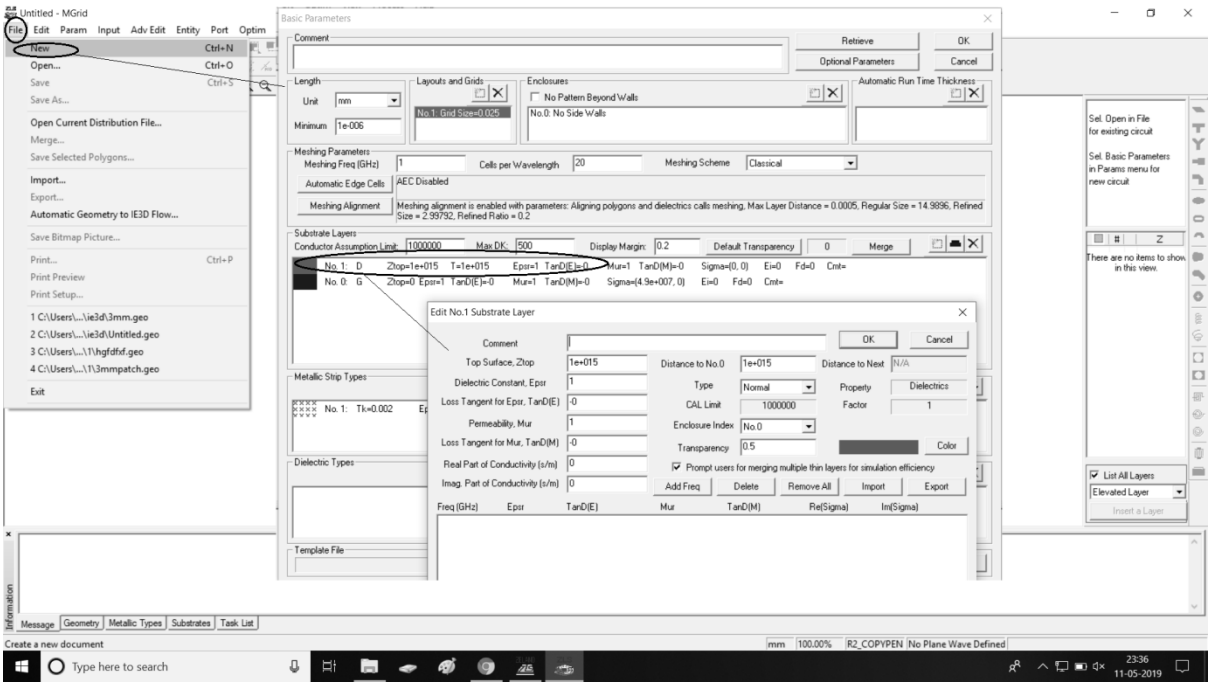

Fig.A.7: Parameter definition in IE3D

The data display window is shown in Fig.A.10. Here we can view the various parameters like S, Z and Y. We can view the magnitude, phase, real part and imaginary part of parameters like Z and Y. We can see the S parameter plot in dB. We can also see the Smith Chart if required.

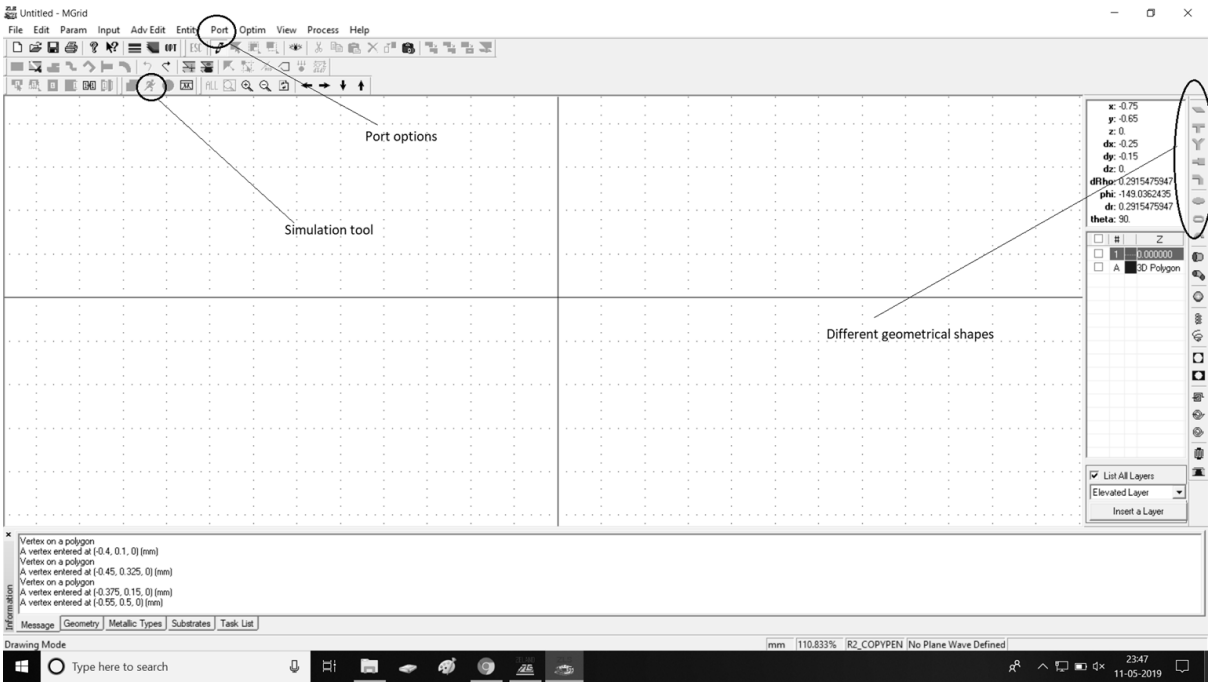

Fig.A.8: Mgrid window with various tools

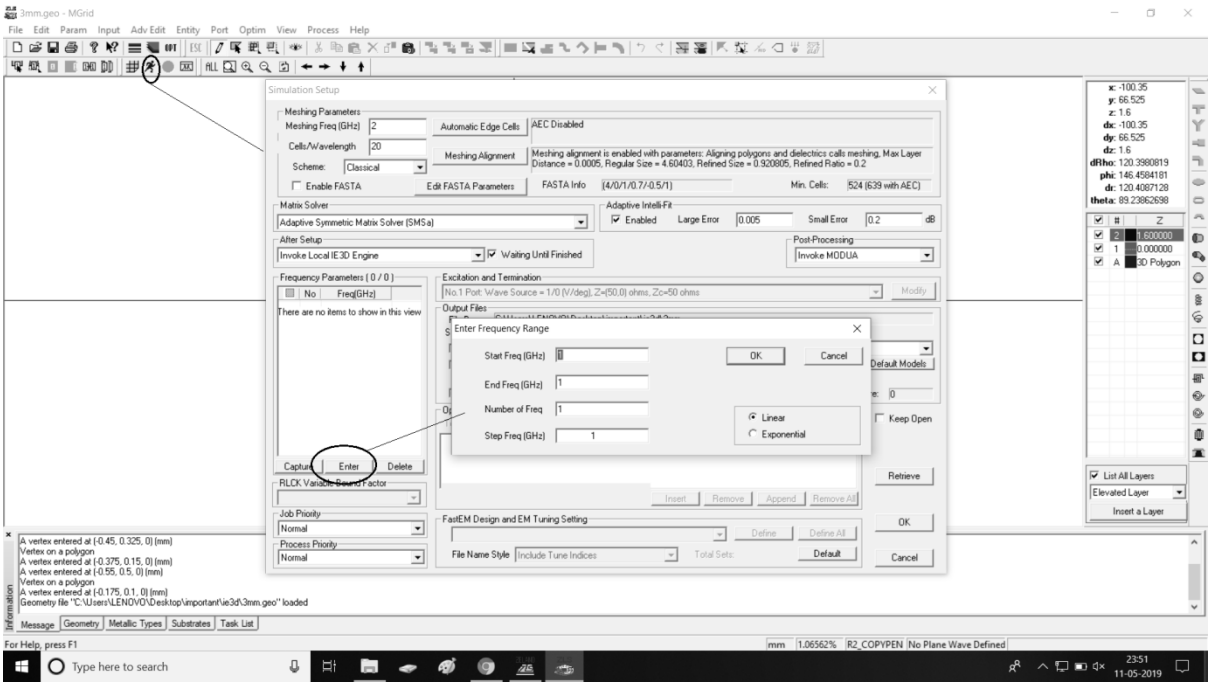

Fig.A.9: Simulation setup

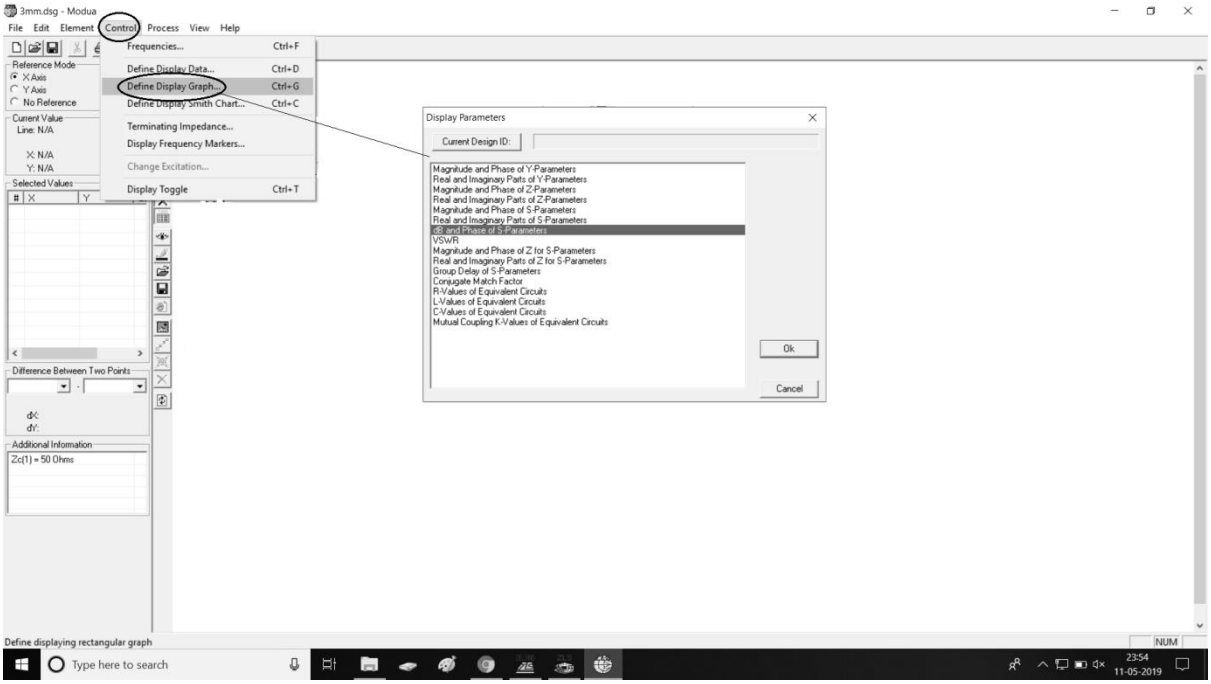

Fig.A.10: Data display window in IE3D

Appendix B

Component Data Sheets

NPN 6 GHz wideband transistor BFR93A

FEATURES

- High power gain
- Low noise figure
- Very low intermodulation distortion.

APPLICATIONS

- RF wideband amplifiers and oscillators.

DESCRIPTION

NPN wideband transistor in a plastic SOT23 package.
PNP complement: BFT93.

PINNING

PIN	DESCRIPTION
1	base
2	emitter
3	collector

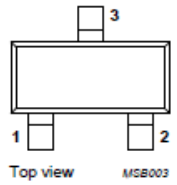

Marking code: R2p.

Fig.1 SOT23.

QUICK REFERENCE DATA

SYMBOL	PARAMETER	CONDITIONS	TYP.	MAX.	UNIT
V_{CBO}	collector-base voltage	open emitter	–	15	V
V_{CEO}	collector-emitter voltage	open base	–	12	V
I_C	collector current (DC)		–	35	mA
P_{tot}	total power dissipation	$T_s \leq 95$ °C	–	300	mW
C_{re}	feedback capacitance	$I_C = 0$; $V_{CE} = 5$ V; f = 1 MHz	0.6	–	pF
f_T	transition frequency	$I_C = 30$ mA; $V_{CE} = 5$ V; f = 500 MHz	6	–	GHz
G_{UM}	maximum unilateral power gain	$I_C = 30$ mA; $V_{CE} = 8$ V; f = 1 GHz; $T_{amb} = 25$ °C	13	–	dB
		$I_C = 30$ mA; $V_{CE} = 8$ V; f = 2 GHz; $T_{amb} = 25$ °C	7	–	dB
F	noise figure	$I_C = 5$ mA; $V_{CE} = 8$ V; f = 1 GHz; $\Gamma_s = \Gamma_{opt}$; $T_{amb} = 25$ °C	1.9	–	dB
V_O	output voltage	$d_{im} = -60$ dB; $I_C = 30$ mA; $V_{CE} = 8$ V; $R_L = 75\ \Omega$; $T_{amb} = 25$ °C; $f_p + f_q - f_r = 793.25$ MHz	425	–	mV

LIMITING VALUES

In accordance with the Absolute Maximum Rating System (IEC 134).

SYMBOL	PARAMETER	CONDITIONS	MIN.	MAX.	UNIT
V_{CBO}	collector-base voltage	open emitter	–	15	V
V_{CEO}	collector-emitter voltage	open base	–	12	V
V_{EBO}	emitter-base voltage	open collector	–	2	V
I_C	collector current (DC)		–	35	mA
P_{tot}	total power dissipation	$T_s \leq 95$ °C; note 1	–	300	mW
T_{stg}	storage temperature		–65	+150	°C
T_j	junction temperature		–	+175	°C

Note

1. T_s is the temperature at the soldering point of the collector pin.

THERMAL CHARACTERISTICS

SYMBOL	PARAMETER	CONDITIONS	VALUE	UNIT
$R_{th\ j\text{-}s}$	thermal resistance from junction to soldering point	$T_s \leq 95$ °C; note 1	260	K/W

Note

1. T_s is the temperature at the soldering point of the collector pin.

CHARACTERISTICS

T_j = 25 °C unless otherwise specified.

SYMBOL	PARAMETER	CONDITIONS	MIN.	TYP.	MAX.	UNIT
I_{CBO}	collector cut-off current	$I_E = 0$; $V_{CB} = 5$ V	–	–	50	nA
h_{FE}	DC current gain	$I_C = 30$ mA; $V_{CE} = 5$ V	40	90	–	
C_c	collector capacitance	$I_E = i_e = 0$; $V_{CB} = 5$ V; f = 1 MHz	–	0.7	–	pF
C_e	emitter capacitance	$I_C = i_c = 0$; $V_{EB} = 0.5$ V; f = 1 MHz	–	1.9	–	pF
C_{re}	feedback capacitance	$I_C = i_c = 0$; $V_{CE} = 5$ V; f = 1 MHz; $T_{amb} = 25$ °C	–	0.6	–	pF
f_T	transition frequency	$I_C = 30$ mA; $V_{CE} = 5$ V; f = 500 MHz	4.5	6	–	GHz
G_{UM}	maximum unilateral power gain (note 1)	$I_C = 30$ mA; $V_{CE} = 8$ V; f = 1 GHz; $T_{amb} = 25$ °C	–	13	–	dB
		$I_C = 30$ mA; $V_{CE} = 8$ V; f = 2 GHz; $T_{amb} = 25$ °C	–	7	–	dB
F	noise figure (note 2)	$I_C = 5$ mA; $V_{CE} = 8$ V; f = 1 GHz; $\Gamma_s = \Gamma_{opt}$; $T_{amb} = 25$ °C	–	1.9	–	dB
		$I_C = 5$ mA; $V_{CE} = 8$ V; f = 2 GHz; $\Gamma_s = \Gamma_{opt}$; $T_{amb} = 25$ °C	–	3	–	dB
V_O	output voltage	notes 2 and 3	–	425	–	mV
d_2	second order intermodulation distortion	notes 2 and 4	–	–50	–	dB

Notes

1. G_{UM} is the maximum unilateral power gain, assuming S_{12} is zero and $G_{UM} = 10 \log \frac{|S_{21}|^2}{(1-|S_{11}|^2)(1-|S_{22}|^2)}$ dB.
2. Measured on the same die in a SOT37 package (BFR91A).
3. d_{im} = –60 dB (DIN 45004B); $I_C = 30$ mA; $V_{CE} = 8$ V; $R_L = 75\ \Omega$; $T_{amb} = 25$ °C;
   $V_p = V_O$ at d_{im} = –60 dB; f_p = 795.25 MHz;
   $V_q = V_O$ –6 dB at f_q = 803.25 MHz;
   $V_r = V_O$ –6 dB at f_r = 805.25 MHz;
   measured at $f_p + f_q - f_r$ = 793.25 MHz.
4. $I_C = 30$ mA; $V_{CE} = 8$ V; $R_L = 75\ \Omega$; $T_{amb} = 25$ °C;
   V_p = 200 mV at f_p = 250 MHz;
   V_q = 200 mV at f_q = 560 MHz;
   measured at $f_p + f_q$ = 810 MHz.

High Q / Low ESR Multilayer SMD Ceramic Capacitor
0402, 0603 & 0805 Sizes, NP0 Dielectric, (MCHH)Series

multicomp

RoHS Compliant

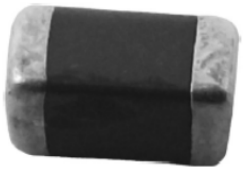

Description:

MLCC consists of a conducting material and electrodes. To manufacture a chip-type SMT and achieve miniaturization, high density and high efficiency, ceramic condensers are used. WTC HH series MLCC is used at high frequencies generally have a small temperature coefficient of capacitance, typical within the ±30ppm/°C required for NP0 (C0G) classification and have excellent conductivity internal electrode. Thus, WTC HH series MLCC will be with the feature of low ESR and high Q characteristics.

Features:

- High Q and low ESR performance at high frequency.
- Quality improvement of telephone calls for low power loss and better performance.

Applications:

- Mobile telecommunication: Mobile phone, WLAN
- RF module: Power amplifier, VCO
- Tuners

How To Order:

MCHH	15	N	100	G	500	C	T
	Size	**Dielectric**	**Capacitance**	**Tolerance**	**Rated Voltage**	**Termination**	**Packaging style**
Multicomp HH = High Q/ Low ESR	15 = 0402 (1005) 18 = 0603 (1608) 21 = 0805 (2012)	N = NP0 (C0G)	Two significant digits followed by no. of zeros. And R is in place of decimal point. eg.: R47 = 0.47pF 0R5 = 0.5pF 1R0 = 1.0pF 100 = 10 × 10^0 = 10pF	A = ±0.05pF B = ±0.1pF C = ±0.25pF D = ±0.5pF F = ±1% G = ±2% J = ±5%	Two significant digits followed by no. of zeros. And R is in place of decimal point. 160 = 16 V DC 250 = 25 V DC 500 = 50 V DC 101 = 100 V DC 201 = 200 V DC 251 = 250 V DC 501 = 500 V DC 631 = 630 V DC	L = Ag/Ni/Sn C = Cu/Ni/Sn	T = 7" reeled G = 13" reeled

Partial NP0 items are with Ag/Ni/Sn terminations, please ref to below product range of NPO dielectric for detail.

External Dimensions:

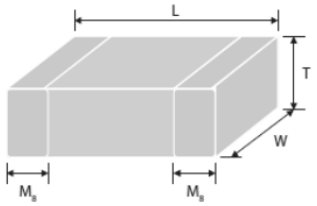

The outline of MLCC

Size Inch (mm)	L (mm)	W (mm)	T (mm)/Symbol		Remark	M_B (mm)
0402 (1005)	1 ±0.05	0.5 ±0.05	0.5 ±0.05	N	#	0.25 +0.05/-0.1
0603 (1608)	1.6 ±0.1	0.8 ±0.1	0.8 ±0.07	S	-	0.4 ±0.15
	1.6 +0.15/-0.1	0.8 +0.15/-0.1	0.8 +0.15/-0.1	X	-	
0805 (2012)	2 ±0.15	1.25 ±0.1	0.6 ±0.1	A	-	0.5 ±0.2
			0.8 ±0.1	B	-	
			1.25 ±0.1	D	#	

Reflow soldering only is recommended.

www.element14.com
www.farnell.com
www.newark.com

multicomp

General Electrical Data:

Dielectric	NP0
Size	0402, 0603, 0805
Capacitance*	0402: 0.5pF to 470pF** 0603: 0.5pF to 3300pF 0805: 0.5pF to 390pF
Capacitance tolerance	Cap ≤ 5pF#1: A (±0.05pF), B (±0.1pF), C (±0.25pF) 5pF < Cap < 10pF: C (±0.25pF), D (±0.5pF) Cap ≥ 10pF: F (±1%), G (±2%), J (±5%)
Rated voltage (WVDC)	16V, 25V, 50V, 100V, 200V, 250V, 500V, 630V
Q*	Cap < 30pF: Q ≥400 +20C Cap ≥ 30pF: Q ≥1,000
Insulation resistance at Ur	≥10GΩ or RxC ≥100Ω -F whichever is smaller.
Operating temperature	-55°C to +125°C
Capacitance change	±30ppm
Termination	Ni/Sn (lead-free termination)

#1: NP0, 0.1pF product only provide B tolerance
* Measured at the conditions of 25°C ambient temperature and 30% to 70% related humidity.
Apply 1 ±0.2Vrms, 1MHz ±10% for Cap ≤ 1,000pF and 1 ±0.2Vrms, 1kHz ±10% for Cap>1,000pF.
** 0402, Capacitance <0.5pF: On request.

Packaging Dimension And Quantity:

Size	Thickness (mm)/Symbol		Paper tape		Plastic tape	
			7" reel	13" reel	7" reel	13" reel
0402	0.5 ±0.05	N	10k	50k	-	-
0603	0.8 ±0.07	S	4k	15k	-	-
	0.8 +0.15/-0.1	X			-	-
0805	0.6 ±0.1	A	4k	15k	-	-
	0.8 ±0.1	B			-	-
	1.25 ±0.1	D	-	-	3k	10k

Unit : pieces

Type CRG Series

Key Features

- Thick film resistors with a high power to size ratio, ideally suited to industrial and general purpose use. A range from 1 ohm to 10M and tolerances of 1% and 5%. Also including zero ohm links.
- Suitable for most applications, including high frequency operation, owing to the short lead structure and low capacitance.
- Seven Package Sizes
- Terminal finish: Matte Sn

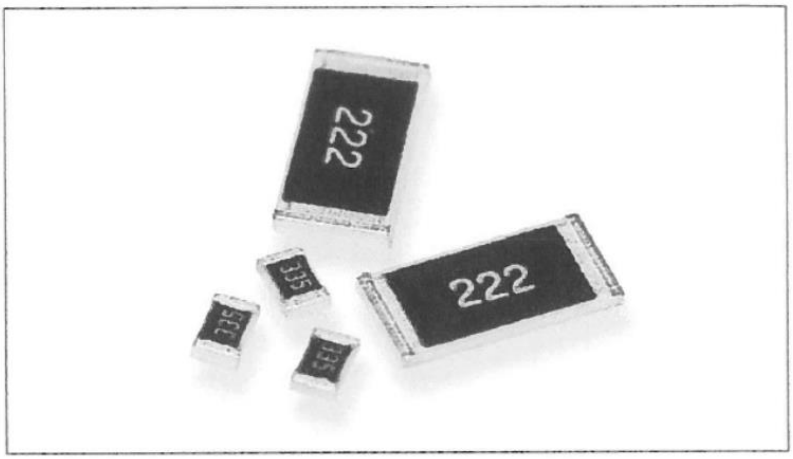

Precious metal terminations are screen printed onto a ceramic base and fired. The resistive element is screen printed and fired and the passivation layer added. Each resistor is trimmed to tolerance by laser. The pre-scribed tile is broken into strips, the end plating is fired on and the strips broken into individual components. Final termination is made by electroplating.

Characteristics – Electrical

		0201			0402			0603				0805			
Rated Power @ 70 °C (W)		0.05			0.063			0.1				0.125			
Resistance Range	Min	10	1	11	10	1	11	1	101	1	11	1	101	1	11
(Ohms)	Max	1M0	10	1M0	2M0	10	3M3	100	1M0	10	10M	100	1M0	10	10M
Tolerance (%)		1	5	5	1	5	5	1	1	5	5	1	1	5	5
Code letter		F	J	J	F	J	J	F	F	J	J	F	F	J	J
Selection Series		E24 E96	E24	E24	E24 E96	E24	E24	E24	E24 E96	E24	E24	E24	E24 E96	E24	E24
Temp. Coefficient (ppm/°C)		±200	±400	±200	±100	±400	±200	±200	±100	±200	±200	±200	±100	±400	±200

		1206				2010				2512			
Rated Power @ 70 °C (W)		0.25				0.5				1			
Resistance Range	Min	1	101	1	11	1	101	1	11	1	101	1	11
Ohms	Max	100	1M0	10	10M	100	1M0	10	10M	100	1M0	10	10M
Tolerance (%)		1	1	5	5	1	1	5	5	1	1	5	5
Code letter		F	F	J	J	F	F	J	J	F	F	J	J
Selection Series		E24	E24 E96	E24	E24	E24	E24 E96	E24	E24	E24	E24 E96	E24	E24
Temp. Coefficient (ppm/°C)		±200	±100	±400	±200	±200	±100	±400	±200	±200	±100	±400	±200

	0201	0402	0603	0805	1206	2010	2512
Working Voltage (V)	25	50	50	150	200	200	200
Max. Overload Voltage (V)	50	100	100	300	400	400	400
Operating Temp. Range (°C)	-55 to +125						
Climatic Category (°C)	55/125/56						
Insulation Resistance Dry Min (Mohms)	1000						
Stability (%)	3						
Zerohm (A) Current Max	0.5	1	1	2	2	2	2
Resistance Max	<50 mOhm			<50 mOhm			

Type CRG Series

Dimensions

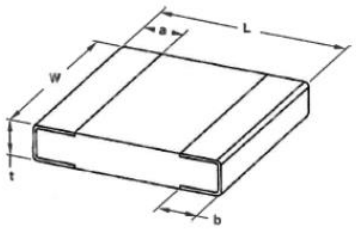

Style	L	W	t	a	b
0201	0.6 ±0.03	0.3 ±0.03	0.23 ±0.03	0.10 ±0.05	0.15 ±0.05
0402	1.0 ±0.1	0.5 ±0.05	0.35 ±0.05	0.2 ±0.1	0.25 ±0.1
0603	1.6 ±0.1	0.8 ±0.15	0.45 ±0.1	0.3 ±0.2	0.3 ±0.1
0805	2.0 ±0.15	1.25 ±0.15	0.55 ±0.1	0.4 ±0.2	0.4 ±0.2
1206	3.1 ±0.15	1.55 ±0.15	0.55 ±0.1	0.45 ±0.2	0.45 ±0.2
2010	5.0 ±0.1	2.5 ±0.15	0.55 ±0.1	0.6 ±0.25	0.5 ±0.2
2512	6.35 ±0.1	3.2 ±0.15	0.55 ±0.1	0.6 ±0.25	0.5 ±0.2

Marking Codes - Case Sizes 0805 to 2512

IEC 4 Digit Marking

Resistance	100Ω	2.2KΩ	10KΩ	49.9KΩ	100KΩ
Marking Code	1000	2201	1002	4992	1003

Case Sizes 0603

E24 3 Digit Marking - Example: 101=100Ω 102=1KΩ

E24	10	11	12	13	15	16	18	20	22	24	27	30
	33	36	39	43	47	51	56	62	68	75	82	91

E96 3 Digit Marking - Examples: 14C=13K7Ω, 13C=13K3Ω, 68B=4K99Ω, 68X=49.9Ω

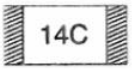

0603 E96 Marking Code Table

Code	E96	Code	E96	Code	E96	Code	E96
01	100	25	178	49	316	73	562
02	102	26	182	50	324	74	576
03	105	27	187	51	332	75	590
04	107	28	191	52	340	76	604
05	110	29	196	53	348	77	619
06	113	30	200	54	357	78	634
07	115	31	205	55	365	79	649
08	118	32	210	56	374	80	665
09	121	33	215	57	383	81	681
10	124	34	221	58	392	82	698
11	127	35	226	59	402	83	715
12	130	36	232	60	412	84	732
13	133	37	237	61	422	85	750
14	137	38	243	62	432	86	768
15	140	39	249	63	442	87	787
16	143	40	255	64	453	88	806
17	147	41	261	65	464	89	825
18	150	42	267	66	475	90	845
19	154	43	274	67	487	91	866
20	158	44	280	68	499	92	887
21	162	45	287	69	511	93	909
22	165	46	294	70	523	94	931
23	169	47	301	71	536	95	953
24	174	48	309	72	549	96	976

Code	A	B	C	D	E	F	G	H	X	Y	Z
Multiplier	10^9	10^7	10^8	10^3	10^4	10^5	10^6	10^7	10^{-1}	10^{-2}	10^{-3}

Dimensions are in millimeters and inches unless otherwise specified. Values in brackets are standard equivalents.

Dimensions are shown for reference purposes only. Specifications subject to change.

For email, phone or live chat, go to: te.com/help

Bibliography

[1] N. Carrara, "The Detection of Microwaves," *Proceedings of the Institute of Radio Engineers*, vol. 20, no. 10, pp. 1615-1625, 1932.

[2] Duixian Liu, Hisamatsu Nakano,Thomas Zwick Zhi Ning Chen, "Handbook of Antenna Technologies," *Springer Reference*.

[3] L. J. Chu, "Physical Limitations of Omni-Directional Antennas," *J. App. Phys.*, vol. 19, pp. 1163-1175, Dec. 1948.

[4] Dudley SM, "Practical issues for spectrum management with cognitive radio," *IEEE Proc*, pp. 249-250, 2014.

[5] Morishita H Fujimoto K, "Modern small antennas," *Cambridge University Press, Cambridge*, p. 8, 2013.

[6] H. A. Wheeler, "Fundamental Limitations of Small Antennas," *Proc. IRE*, vol. 35, pp. 1479-1484, Dec. 1947.

[7] Rumsey, "Highlights of antenna history," *IEEE Antennas and Propagation Society*, p. 8, Dec. 1981.

[8] Fujimoto K, "Integrated antenna system," *Encyclopedia of RF and microwave engineering*, pp. 2113–2147, 2005.

[9] and R. L. Wallace J. G. Linvill, "Negative Impedance Converters Employing Transistors," *U.S. Patent*, Dec. 1955.

[10] Pilwerbetsky A Stuart HR, "Electrically small antenna elements using negative permittivity resonator," *IEEE Trans Antennas Propag*, vol. 54, pp. 1644–1653, 2006.

[11] C. C. Chen, K. Fujimoto J. L. Volakis, "Small Antennas : Miniaturization Techniques & Applications," *1st edition, Mc-Graw Hil*, 2010.

[12] R. F. Harrington, "Time-Harmonic Electromagnetic Fields," *Wiley-IEEE Press*, 2001.

[13] O. Staub, "Electrically Small Antennas," *Ph.D. Dissertation, Ecole Polytechnique Federale de Lausanne*, 2001.

[14] J. S. McLean, "A Re-Examination of the Fundamental Limits on the Radiation," *IEEE Trans. Antennas Propag.*, vol. 44, no. 6, pp. 672-676, May 1996.

[15] P. Jarmuszewski, and Y. Q W. Geyi, "The Foster reactance theorem for antennas and radiation Q," *IEEE Trans. Antennas Propag.*, vol. 48, no. 3, pp. 401-408, Mar. 2000.

[16] R. F. Harrington, "Effect of Antenna Size on Gain, Bandwidth and Efficiency," *Journal of Research of the National Bureau of Standards - D. Radio Propagation*, vol. 64, p. 12, June 1959.

[17] R. E. Collin and S. Rothschild, "Evaluation of Antenna Q," *IEEE Transactions on Antennas*, vol. 12, pp. 23-27, 1964.

[18] R. C. Hansen, "“Fundamental limitations in antennas," *Proc. IEEE*, vol. 69, pp. 170-182, Feb. 1981.

[19] J. G. Linvill, "Transistor Negative-Impedance Converters," *Proceedings of the IRE*, vol. 41, pp. 725-729, 1953.

[20] A. D. Harris and G. A. Myers, "An Investigation Of Broadband Miniature Antennas Techical Report," *Naval Postgraduate School*, Sept. 1968.

[21] A. K. Perry, "Broadband antenna systems realized from active circuit conjugate impedance matching," *M.S. Thesis, Naval Postgraduate School, Monterey, CA*, Sept. 1973.

[22] John L. Volakis Stavros Koulouridis, "Non-Foster Circuits for Small Broadband Antennas," *IEEE*, 2009.

[23] S. Koulouridis and J. Volakis, "Minimization of flare dipole via shape optimization and matching circuits," *in Proc. IEEE Antennas Propagat. Int. Symp. Hawaii, USA*, pp. 4785-4788, June 2007.

[24] J. T Aberle, "Two-Port Representation of an Antenna with Application to NonFoster Matching Networks," *IEEE Trans. on Antennas and Propagation*, vol. 1, no. 56, pp. 1218-1222, May 2008.

[25] S. E. Sussman-Fort and R. M. Rudish, "Non-Foster Impedance Matching of Electrically-Small Antennas," *Antennas and Propagation, IEEE Transactions*, vol. 57, pp. 2230-2241, 2009.

[26] R. M. Rudish and S. E. Sussman-Fort, "Non-Foster Impedance Matching Improves S/N of Wideband Electrically Small VHF Antennas and Arrays," *Pro-ceedings of the 2nd IASTED international conference on Antennas, Radar, and Wave Propagation*, pp. 19-21, Jul. 2005.

[27] S. E. Sussman-Fort and R. M. Rudish, "Progress in use of non-Foster impedances to match electrically-small antennas and arrays," *the Antenna Applicat. Symp.,Allerton Park*, pp. 21-23, Sept. 2005.

[28] S. E. Sussman-Fort and R. M. Rudish, "Non-Foster Impedance Matching for Transmit Applications," *2006 IEEE Int. Workshop on Antenna Technol.: Small Antennas and Novel Metamater.*, March 2006.

[29] S. E. Sussman-Fort, "Matching network design using non-Foster impedances," *Int. J. RF Microw. Comput.-Aided Eng*, vol. 16, no. 2, pp. 135-142, March 2006.

[30] S. E. Sussman-Fort and R. M. Rudish, "Non-Foster impedance matching of a lossy, electrically-small antenna over an extended frequency range," *the Antenna Applicat. Symp., Allerton Park, IL*, pp. 220-240, Sept 2007.

[31] S. E. Sussman-Fort and R. M. Rudish, "Non-Foster impedance matching of electrically-small antennas to transmitters," *he Antenna Applicat. Symp. Allerton Park, IL*, pp. 326-342, Sept 2008.

[32] Khalid Z. Rajab, Max Munoz and Yang Hao Yifeng Fan, "Electrically Small Half-Loop Antenna Design with Non foter matching network," *6th European Conference on Antennas and Propagation (EUCAP)*, 2011.

[33] Keum Su Song, "Non-Foster Impedance Matching and Loading Networks for Electrically Small Antennas," *PHD DISSERTATION*, 2011.

[34] P.Gardner and P.S. Hall O.O. Tade, "Negative Impedance Converters for Broadband Antenna Matching," *Proceedings of the 42nd European Microwave Conference*, Oct. 2012.

[35] Minu M. Jacob, "Broadband Non-Foster Matching of an Electrically Small Loop Antenna," *IEEE*, 2012.

[36] Seyyed Hamzeh Hashemi Homayoon Oraizi, "Design of a non foster impedance matching network for electrically small antennas," *IEEE*, no. 978-1-4673-5820-0/, 2013.

[37] Yunsu Kang, and Kangwook Kim Hyemin Yang, "An Application of the Negative Impedance Converter to Resistively Loaded Vee Dipole Antenna Matching," *IEEE*, 2014.

[38] K. Kim and W. R. Scott, "“Design and realization of a discretely loaded resistive vee dipole for ground-penetrating radars," *Radio Scien.*, vol. 39, pp. 1-9, jul. 2004.

[39] and Tan-Huat Chio Yizhu Shen, "Matching Electrically Small Antenna Using Non-Foster Circuit in the FM-Band," *The 8th European Conference on Antennas and Propagation*, 2014.

[40] W. Dyab, T. K. Sarkar,M. Salazar-Palma M. N. Abdallah, "Electrically Small Antennas Design Challenges," *AP-S*, 2015.

[41] H. Bode, "Network Analysis and Feedback Amplifier Design," *New Yorkk,Van Nostrand*, p. 367, 1947.

[42] R. M. Fano, "Theoretical Limitations on the Broadband Matching of Arbitrary Impedances," *J. Franklin Inst*, vol. 249, pp. 57-83,139-155, Jan, Feb 1950.

[43] Bair Buyantuev, Viacheslav Turgaliev, Dmitry Kholodnyak Nikolay Ivanov, "Non-Foster Broadband Matching Networks for Electrically-small Antennas," *Loughborough Antennas & Propagation Conference (LAPC)*, 2016.

[44] Mohamed Manoufali and Amin Abbosh, "Non-Foster Impedance Matching of an Electrically Small Loop Antenna for Biomedical Telemetry," *Proceedings of 2017 Asia Pacific Microwave Conference*, 2017.

[45] Dmitry Kholodnyak Bair Buyantuev, "Applications of Non-Foster Elements to Design Advanced RF And Microwave Devices," *IEEE conf.*, 2018.

[46] V. Turgaliev and D. Kholodnyak N. Ivanov, "Performance improvement of an electrically-small loop antenna matched with non-Foster negative inductance," *Proc. 2017 IEEE MTT-S Int. Microwave Symp., Honolulu, HI, USA*, pp. 348-351, Jun. 2017.

[47] B. Delacressonniere and J. Gautier S. Kolev, "Using a negative capacitance to increase the tuning range of a varactor diode in MMIC technology," *IEEE Trans. Microwave Theory Tech*, vol. 49, no. 12, pp. 2425-2430, 2001.

[48] A. Antoniou, "Floating negative-impedance converters," *IEEE Trans. Circuit Theory*, vol. 19, no. 2, pp. 209-212, 1972.

[49] K.N. Salama and U. Cam S. Kilinc, "Realization of fully controllable negative inductance with single operational transresistance amplifier," *Circuits, Systems and Signal Processing*, vol. 25, no. 1, pp. 47-57, 2006.

[50] A. Lahiri and M. Gupta, "Realizations of grounded negative capacitance using CFOAs," *Circuits, Systems, and Signal Processing*, vol. 30, no. 1, pp. 143-155, 2011.

[51] Y. Shen and T.-H. Chio, "Limitation of negative impedance converter using operational amplifier for matching electrically small antenna," *Proc. 2013 IEEE AP-S Int. Symp., Orlando, FL, USA*, pp. 1962-1963, July 2013.

[52] T. Kaneko and Y. Horii, "Influence of transistor packages and circuit dimensions for accurate design of negative impedance converters," *Proc. 2013 Asia-Pacific Microwave Conf., Seoul, Korea*, pp. 1194-1196, Nov. 2013.

[53] J.M.C. Covington III, J.W. Shehan, T.P. Weldon, and R.S.Adams S. Kshatri, "Capacitance and bandwidth tradeoffs in a cross-coupled CMOS negative capacitor," *Proc. IEEE SoutheastCon, Jacksonville, FL, USA*, pp. 1-4, Apr. 2013.

[54] K.L. Smith, J.W. Shehan, V.S. Kshatri, T.P.Weldon, and R.S. Adams J.M.C. Covington III, "Measurement of a CMOS negative inductor for wideband non-Foster metamaterials," *Proc. IEEE SoutheastCon Lexington, KY, USA*, pp. 1-4, March 2014.

[55] J.M.C. Covington III, J.W. Shehan, T.P. Weldon, and R.S.Adams S. Kshatri, "Compensation of frequency dependent parasitic resistance in a CMOS Linvill negative inductor," *Proc. IEEE SoutheastCon, Lexington, KY, USA*, pp. 1-4, March 2014.

[56] H. Mirzaei and G.V. Eleftheriades, "Squint-free leaky-wave radiation with non-Foster artificial transmission lines," *Proc. 5th Int. Congress Advanced Electromagnetic Materials in Microwaves and Optics,Barcelona, Spain*, pp. 24-26, Sep 2011.

[57] H. Mirzaei and G.V. Eleftheriades, "An active artificial transmission line for squint-free series-fed antenna array applications lines," *Proc. 41st Eur. Microwave Conf., Manchester, UK*, pp. 503-506, Oct. 2011.

[58] S. Hrabar, D. Segovia-Vargas, and A. Kiricenko E. Ugarte-Munoz, "Stability of non-Foster reactive elements for use in active metamaterials and antennas," *IEEE Trans. Antennas Propag*, vol. 60, no. 7, pp. 3490-3494, 2012.

[59] V. Turgaliev, A. Rusakov, K. Zemlyakov, and I.Vendik D. Kholodnyak, "A frequency independent phase inverting all-pass network suitable for a design of ultra-wideband 180° phase

shifters," *Proc. 41st Eur. Microwave Conf., Manchester, UK*, pp. 643-646., 2011.

[60] V. Turgaliev, D. Kholodnyak, and N. Ivanov E. Vorobev, "Active tunable inductor using non-Foster element," *Proc. 2017 IEEE Conf.Russian Young Researchers in Electrical and Electronic Engin St. Petersburg and Moscow, Russia*, pp. 346-349, Feb 2017.

[61] Vicente Gonzalez-Posadas, Angel Parra-Cerrada, Alvaro Blanco-Campo,Eduardo Ugarte-Muñoz, Daniel Segovia-Vargas Jose Luis Jimenez-Martin, "Full Conditions for the Stability Analysis of Negative Impedance Converters," *6th European Conference on Antennas and Propagation (EUCAP)*, pp. 135-138, 2011.

[62] Brownlie, "On the Stability Properties of a Negative Impedance Converter," *Circuit Theory, IEEE Transactions*, vol. 13, no. 1, pp. 98-99, March 1966.

[63] Volker Wienstroer and Rainer Kronberger Christian Stedler, "Noise Performance of an Antenna Matching Network with Negative-Impedance Converter (NIC)," *The 8th European Conference on Antennas and Propagation (EuCAP 2014)*, pp. 2709-2713, 2014.

[64] and Hao Xin Qi Tang, "Stability analysis and parasitic effects of negative impedance converter circuits," *IEEE trans.*, 2015.

[65] and W. Struble A. Platzker, "Rigorous determination of the stability of linear N-node circuits from network determinants and the appropriate role of the stability factor K of their reduced two-ports," *Integ. Nonlinear Microwave & Millimeterwave Circuits*, pp. 93-97, Oct 1994.

[66] R. M. Foster, "A reactance theorem," *Bell System Technical Journa*, vol. 3, no. 2, pp. 259–267, 1924.

[67] J. T. Aberle, "Two-Port Representation of an Antenna With Application to Non-Foster Matching Networks," *IEEE Transactions*, vol. 56, pp. 1218-1222, 2008.

[68] Negative impedance converter. Wikipedia.

[69] Minu Mariam Jacob, "Non-Foster Circuits for High Performance Antennas: Advantages and Practical Limitations," 2016.

[70] J. T. Aberle and R. Lopesinger-Romak, "Antennas with Non-Foster Matching Networks," *Morgan & Claypool Publishers, San Rafael, CA*, 2007.

[71] B. R. Long, "Analysis of stable negative impedance loaded dipole and canonical chiral elements with application to novel active media," *Ph.D. Dissertation, The*, 2001.

[72] J. Choma and W. K. Chen, "Feedback Networks: Theory and Circuit Applications," *World Scientific Publishing Co. Pte. Ltd.*, 2007.

[73] A. I. Larky, "Negative-Impedance Converter Design," *Ph.D. Dissertation, Stanford*, Oct. 1956.

[74] Oluwabunmi O. Tade, "NEGATIVE IMPEDANCE CONVERTERS FOR ANTENNA

MATCHING," *Phd Dissertation,University of Birmingham, Edgbaston*.

[75] Fu Tian Wong, "Practical issues of using NIC circuits as an antenna matching element," *M.E. Thesis*, 2011.

[76] G. A. Deschamps, "Microstrip Microwave Antennas," *Proc. 3rd USAF Symposium on*, 1953.

[77] R. E. Munson, "Single Slot Cavity Antennas Assembly," *US Patent*, January 1973.

[78] R. E. Munson, "Conformal Microstrip Antennas and Microstrip Phased Arrays," *IEEE Transactions on Antennas and Propagation*, vol. 22, 1974.

[79] J. Q. Howell, "Microstrip Antennas," *IEEE Transactions on Antennas and Propagation*, vol. 23, 1975.

[80] S. A. Long, M. R. Allerding, and M. D. Walton L. C. Shen, "Resonant Frequency of a Circular Disc Printed-Circuit Antenna," *IEEE Trans. Antennas Propagation*, vol. 25, no. 4, pp. 595–596, July 1977.

[81] A. G. Derneryd, "Analysis of the Microstrip Disk Antenna Element," *IEEE Trans. Antennas Propagation*, vol. 27, no. 4, pp. 660–664, September 1979.

[82] S. A. Long and M. D.Walton, "A Dual-Frequency Stacked Circular-Disc Antenna," *IEEE Trans. Antennas Propagat.*, vol. 27, no. 2, pp. 270–273, March 1979.

[83] F. Zavosh and J. T. Aberle, "Infinite Phased Arrays of Cavity-Backed Patches," vol. 42, no. 3, pp. 390–398, March 1994.

[84] J. T. Aberle and D. M. Pozar, "Analysis of Infinite Arrays of One- and Two-Probe-Fed Circular Patches," *IEEE Trans. Antennas Propagat.*, vol. 38, no. 4, pp. 421–432, April 1990.

[85] C. A. Balanis, "Advanced Engineering Electromagnetics," *Second Edition, JohnWiley & Sons, New York*, 2012.

[86] J. T. Aberle and F. Zavosh, "Analysis of Probe-Fed Circular Microstrip Patches Backed by Circular Cavities," *Electromagnetics*, vol. 14, pp. 239–258, 1994.

[87] F. Zavosh and J. T. Aberle, "Infinite Phased Arrays of Cavity-Backed Patches," *IEEE Trans.*, vol. 42, no. 3, pp. 390–398, March 1994.

[88] S. B. De Assis Fonseca and A. J. Giarola, "Microstrip Disk Antennas, Part I: Efficiency of Space Wave Launching," *IEEE Trans. Antennas Propagat.*, vol. 32, no. 6, pp. 561–567, June 1984.

[89] S. B. De Assis Fonseca and A. J. Giarola, "Microstrip Disk Antennas, Part II: The Problem of Surface Wave Radiation by Dielectric Truncation," *IEEE Trans. Antennas Propagat.*, vol. 32, no. 6, pp. 568–573, June 1984.

[90] C. A. Balanis, "Antenna Theory: A Review," *Proceedings of the IEEE*, vol. Vol. 80, January

1992.

[91] D. M. Pozar, "Microwave Engineering," *3rd edition, Wiley*, 2004.

[92] and Hao Xin Qi Tang, "Stability analysis and parasitic effects of negative impedance ," *converter circuits*, 2015.